

115P

FACILITY FORM 608

N 64 28936

(ACCESSION NUMBER)

115

(PAGES)

CR 58248

(NASA CR OR TMX OR AD NUMBER)

(THRU)

1

(CODE)

08

(CATEGORY)

INVESTIGATION AND ANALYSIS

OF THE INFLUENCE OF PERTURBING FORCES

ON TRACKING OF ORBITAL VEHICLES

4103-6011-RU-000

JUNE 28, 1964

OTS PRICE

XEROX

\$

960ph

MICROFILM

\$

PREPARED FOR

GEORGE C. MARSHALL SPACE FLIGHT CENTER

UNDER CONTRACT NUMBER NAS8-11073

TRW SPACE TECHNOLOGY LABORATORIES

THOMPSON RAMO WOOLDRIDGE INC.

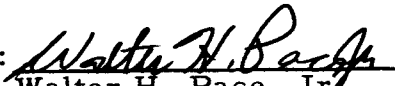
INVESTIGATION AND ANALYSIS
OF THE INFLUENCE OF PERTURBING FORCES
ON TRACKING OF ORBITAL VEHICLES

Prepared for
George C. Marshall Space Flight Center
Under Contract Number NAS 8-11073


4103-6011-RU-000

June 28, 1964

Approved by:


Walter H. Pace, Jr.
Project Manager

Approved by:


E. M. Boughton
Assistant Director
for Projects
Mission Analysis and
Simulation Laboratory

TRW SPACE TECHNOLOGY LABORATORIES
Thompson Ramo Wooldridge, Inc.
One Space Park, Redondo Beach, California

ACKNOWLEDGEMENTS

The following personnel were among those contributing to this study:

E. M. Boughton

T. H. S. Brown

M. P. Francis

B. Hamermesh

F. J. Lombard

T. A. Magness

W. H. Pace, Jr.

CONTENTS

	<u>Page</u>
1. INTRODUCTION	1-1
2. EFFECTS OF THRUST PERTURBATIONS	2-1
2.1 Effects of Continuous Low Thrust on Earth Orbits	2-1
2.2 Effects of Intermittent Venting on Earth Orbits	2-37
2.3 Use of Venting Thrusts for Control of Earth Orbits	2-62
2.4 Effects of Continuous Low Thrust on Translunar Trajectories	2-64
2.5 Effects of Intermittent Venting on Translunar Trajectories	2-65
3. EFFECTS OF NATURAL PERTURBATIONS	3-1
3.1 Nominal Values	3-2
3.2 Analytic Approximations	3-4
3.3 Computer Simulation	3-14
3.4 Recommended Models	3-23
4. CONCLUSIONS	4-1
APPENDIX.	A-1
REFERENCES	R-1

1. INTRODUCTION

This volume contains the results of a study done by TRW Space Technology Laboratories for the George C. Marshall Space Flight Center under National Aeronautics and Space Administration Contract Number NAS8-11073. The purpose of the study was to determine the effects of various perturbing forces on the earth parking orbit and translunar phases of a lunar mission.

The perturbations studied have been divided into thrust perturbations and natural perturbations. The thrust perturbations include gas leakage and venting, while the natural perturbations include gravitational models, solar radiation pressure, and atmospheric drag. Thrust perturbations are discussed in Section 2 and natural perturbations are discussed in Section 3. The effects of both the entire force and the uncertainty in the force are considered. Special emphasis was placed on the effects of venting or gas leakage thrusts on earth orbits. The total effects, tracking effects, and uncertainty effects of these thrusts are all included.

2. EFFECTS OF THRUST PERTURBATIONS

This section is concerned with the effects of venting and gas leakage on earth orbits and translunar trajectories. Two general types of thrust are considered: continuous thrust and intermittent thrust. Gas leakage is normally a continuous thrust, but venting may be either intermittent or a combination of intermittent and continuous. The intermittent venting case is covered explicitly in the results, and the combined effects can be obtained by summing the separate effects, since the assumption of linearity is valid in the usual range of effects.

For earth orbits, the total effects, tracking effects, and uncertainty effects are presented for both continuous and intermittent thrusts. In addition, a discussion of the use of venting to control the orbit is included.

For translunar trajectories the total effects and uncertainty effects are presented.

2.1 EFFECT OF CONTINUOUS LOW THRUST ON EARTH ORBITS

The effect of a continuous low thrust on earth orbits can be divided into three types: (1) total effects, (2) tracking effects, and (3) uncertainty effects. The total effects are simply the changes in vehicle coordinates that result from the application of a continuous low thrust. The tracking effects are the errors in prediction of the vehicle coordinates from tracking data caused by the thrust, and are usually smaller than the total effects. The uncertainty effects are the errors resulting from taking into account an erroneous estimate of the thrust in predicting the vehicle coordinates.

These three effects are discussed in Sections 2.1.1, 2.1.2, and 2.1.3.

2.1.1 Total Effects

Two methods of determining the total effects of continuous low thrust on earth orbits have been used. Most of the results presented were obtained from an integrating trajectory program, since this allowed the generation of radar data to be used in the calculation of tracking effects. Analytic expressions and sample results are also presented, however, since they allow a simpler method of calculation as long as the system is linear.

Integrated. The STL N-stage integrating trajectory program was used to calculate the differences between the coordinates of a thrusting vehicle and a non-thrusting vehicle with the same initial conditions. This program yields the coordinates of both vehicles relative to the earth, and of one vehicle relative to the other at a prescribed set of times. The coordinate system used for the relative positions is centered at the non-thrusting vehicle and is illustrated in Figure 2.1.1-1. The u direction is radial, the v direction is horizontal in the direction of motion, and the w direction is out-of-plane.

A nominally-circular orbit with a 200 kilometer altitude was chosen as the basis for determining the effects of low thrust. This orbit is equatorial, with its initial position on the x -axis and its initial velocity in the y direction, where the xyz coordinates form the usual earth-centered inertial system with x toward the vernal equinox and z toward the north pole. Thus the z direction and the w direction coincide.

The thrusting vehicle was given an acceleration of $5(10^{-5})g$ in each of the u , v , w , x , and y directions separately. The results of these fixed thrusts are presented in Figures 2.1.1-2 through 2.1.1-8.

The curves present the same results in two different forms for easy comparisons. First, all components of the position change caused by each thrust are shown in Figures 2.1.1-2 through 2.1.1-6. These figures show the u , v , and w effects of thrusting in each of the five directions, and show the relative sizes of the effects.

In Figures 2.1.1-7 and 2.1.1-8 comparisons between the effects of the five thrusts are made in terms of their effects in the radial and downrange directions. No comparison in the crossrange direction is made, because only crossrange thrust gives a crossrange effect.

For the particular thrust level and orbit used, the following conclusions can be drawn from the curves:

1. The only significant effect of out-of-plane thrust is in the out-of-plane direction (Figure 2.1.1-4)
2. The only significant effects of in-plane thrusts are in-plane (Figures 2.1.1-2, 2.1.1-3, 2.1.1-5, and 2.1.1-6)

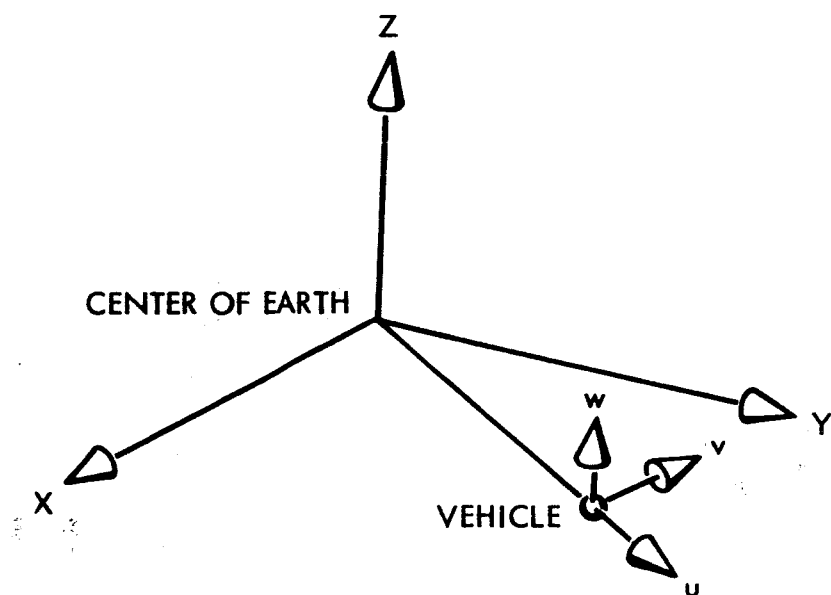


Figure 2.1.1-1. Definition of Orbit-plane Coordinate System

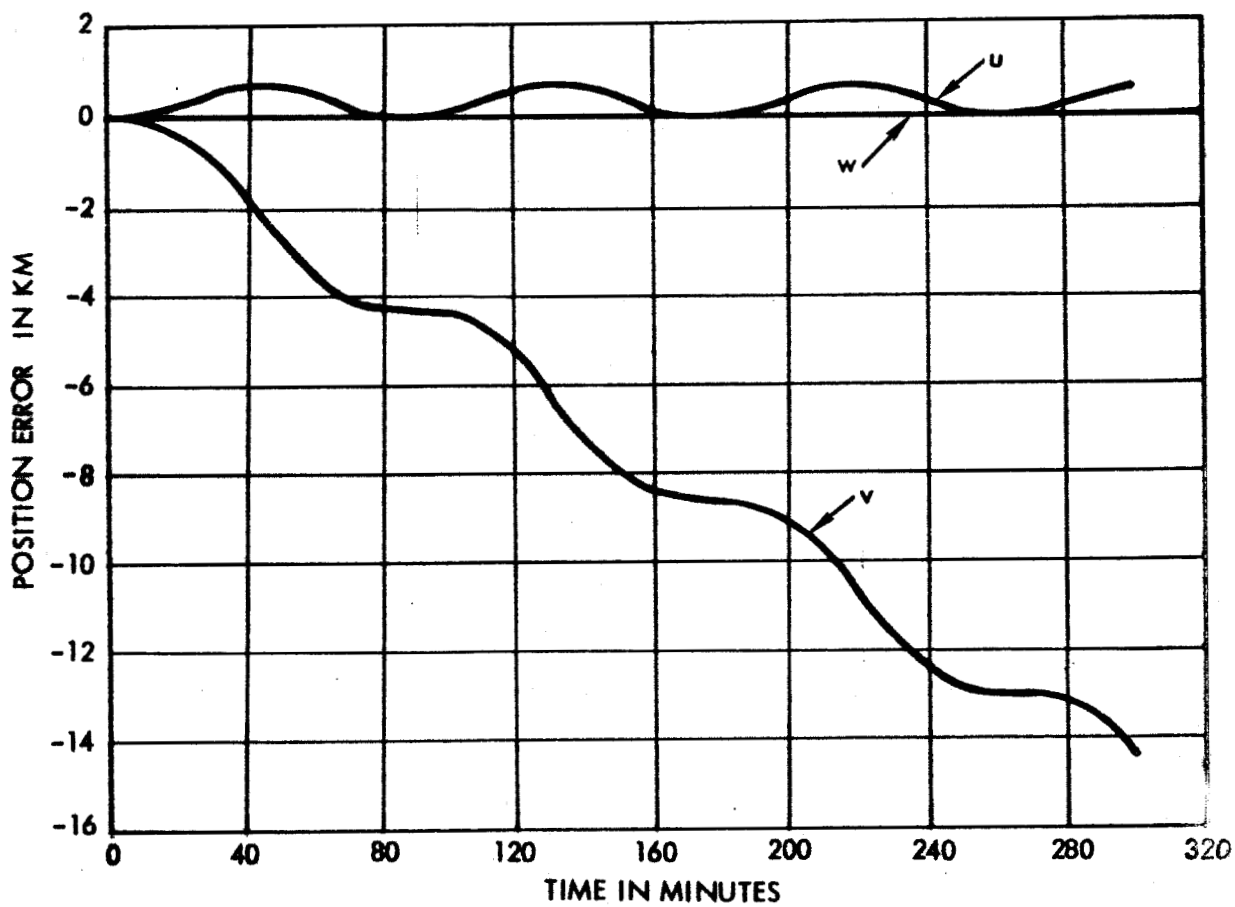


Figure 2.1.1-2. uvw Effects of u Thrust, $5(10^{-5})g$ Continuous, 200 km Circular Orbit Integrated

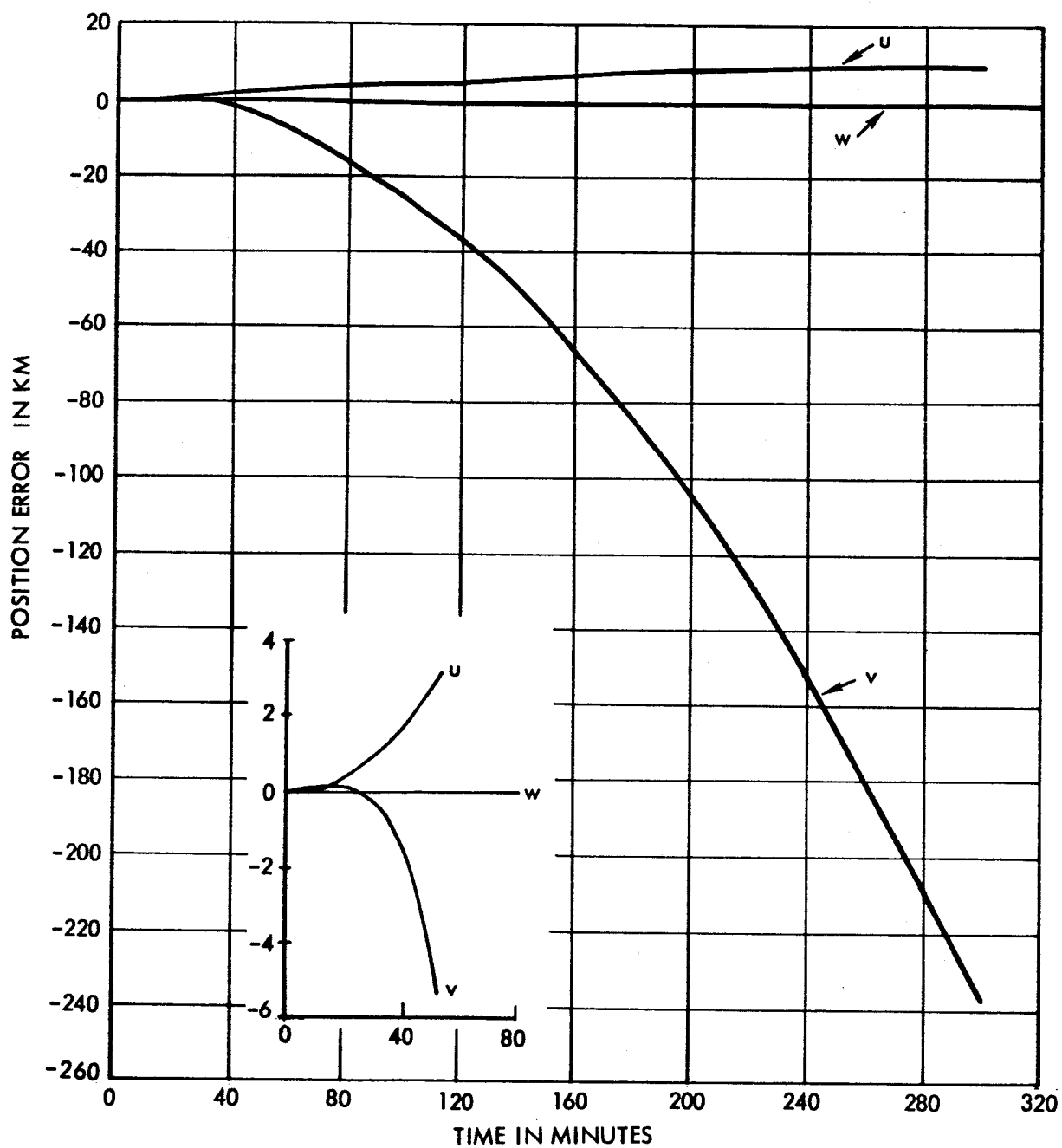


Figure 2.1.1-3. uvw Effects of v Thrust, $5(10^{-5})g$ Continuous, 200 km Circular Orbit Integrated

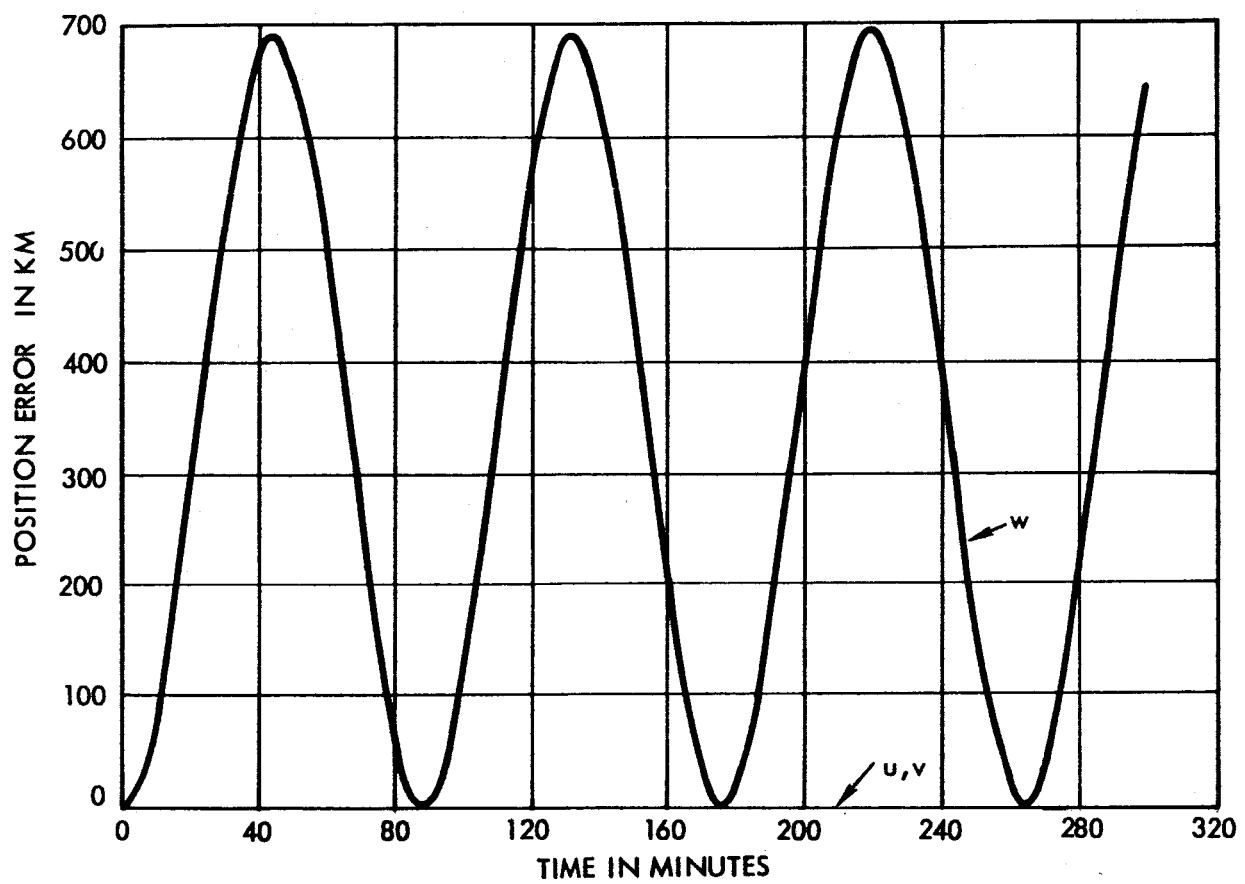


Figure 2.1.1-4. uvw Effects of w Thrust, $5(10^{-5})g$ Continuous, 200 km Circular Orbit Integrated

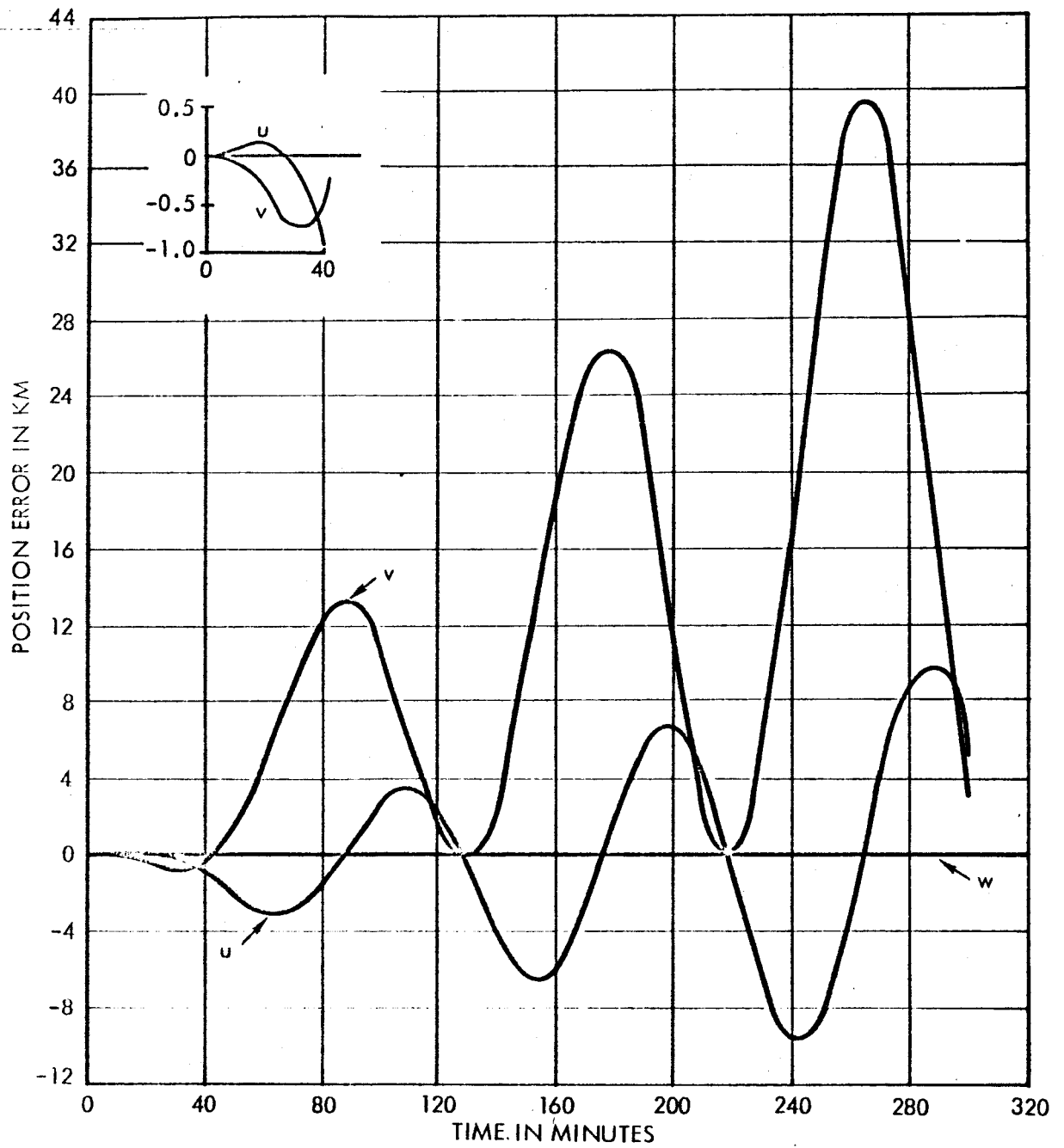


Figure 2.1.1-5 uvw Effects of x Thrust, $5(10^{-5})g$ Continuous, 200 km Circular Orbit Integrated

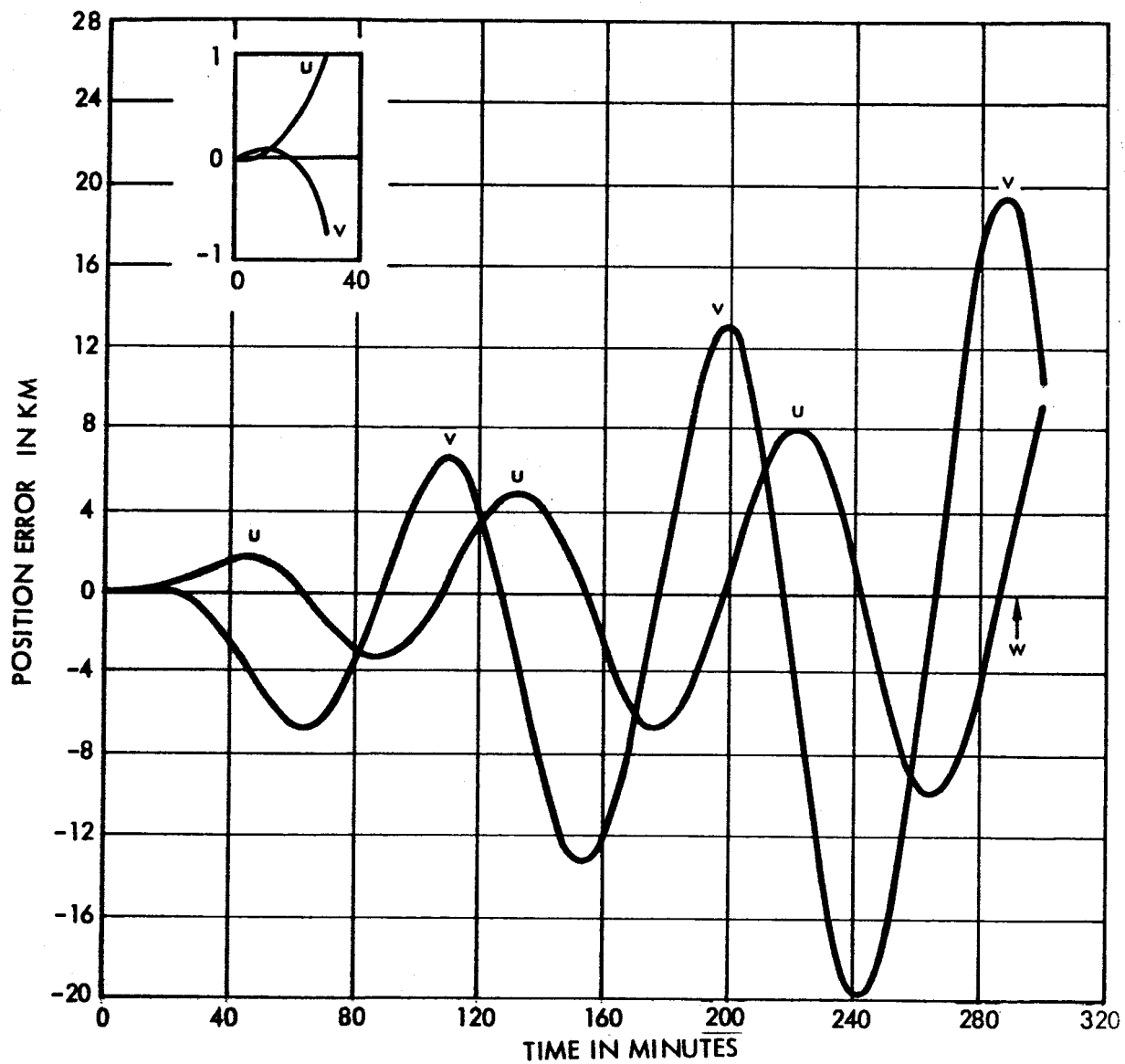


Figure 2.1.1-6. vw Effects of y Thrust, $5(10^{-5})g$ Continuous, 200 km Circular Orbit Integrated

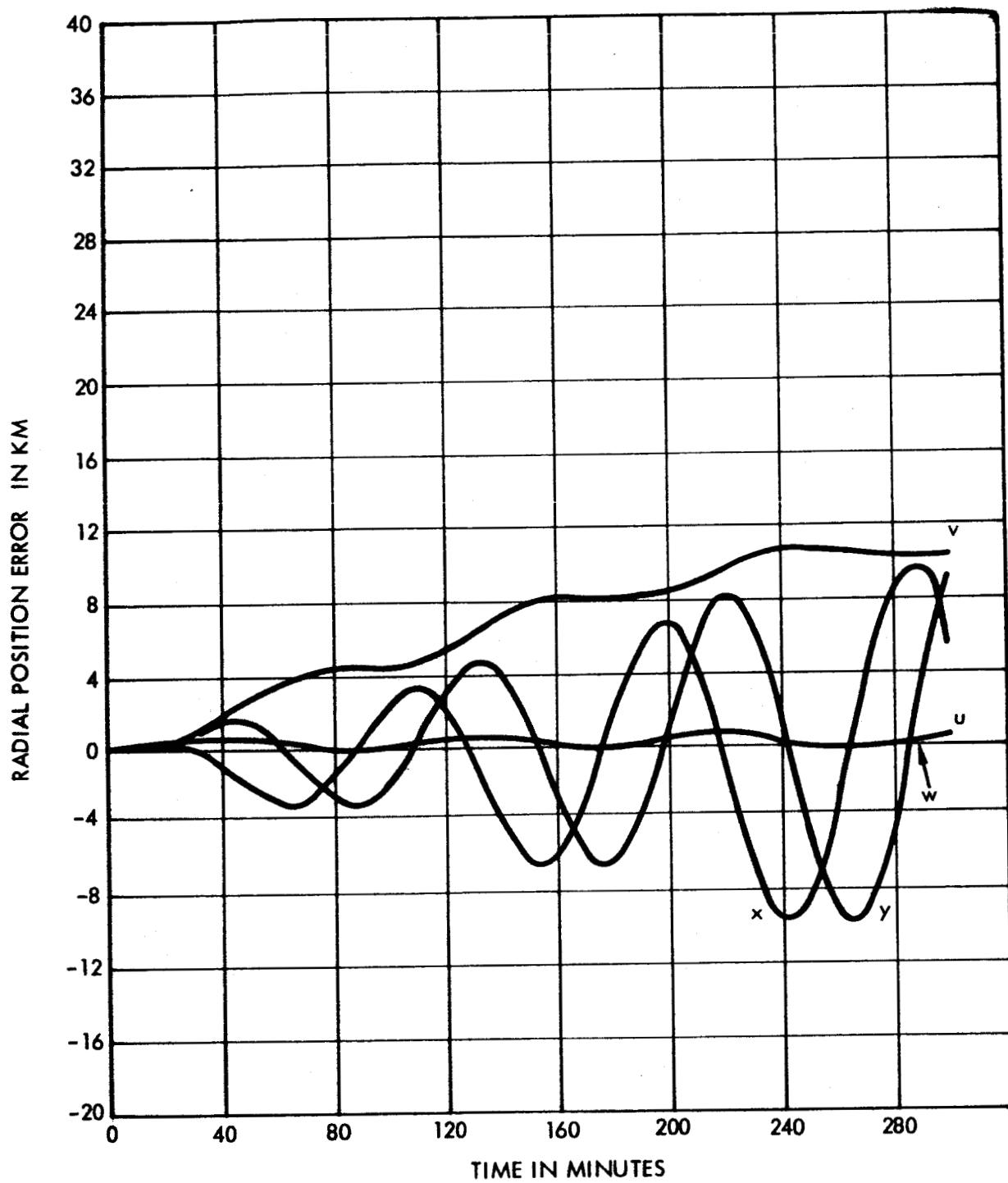


Figure 2.1.1-7. u Effects of u, v, w, x, y Thrusts, $5(10^{-5})g$ Continuous, 200 km Circular Orbit Integrated

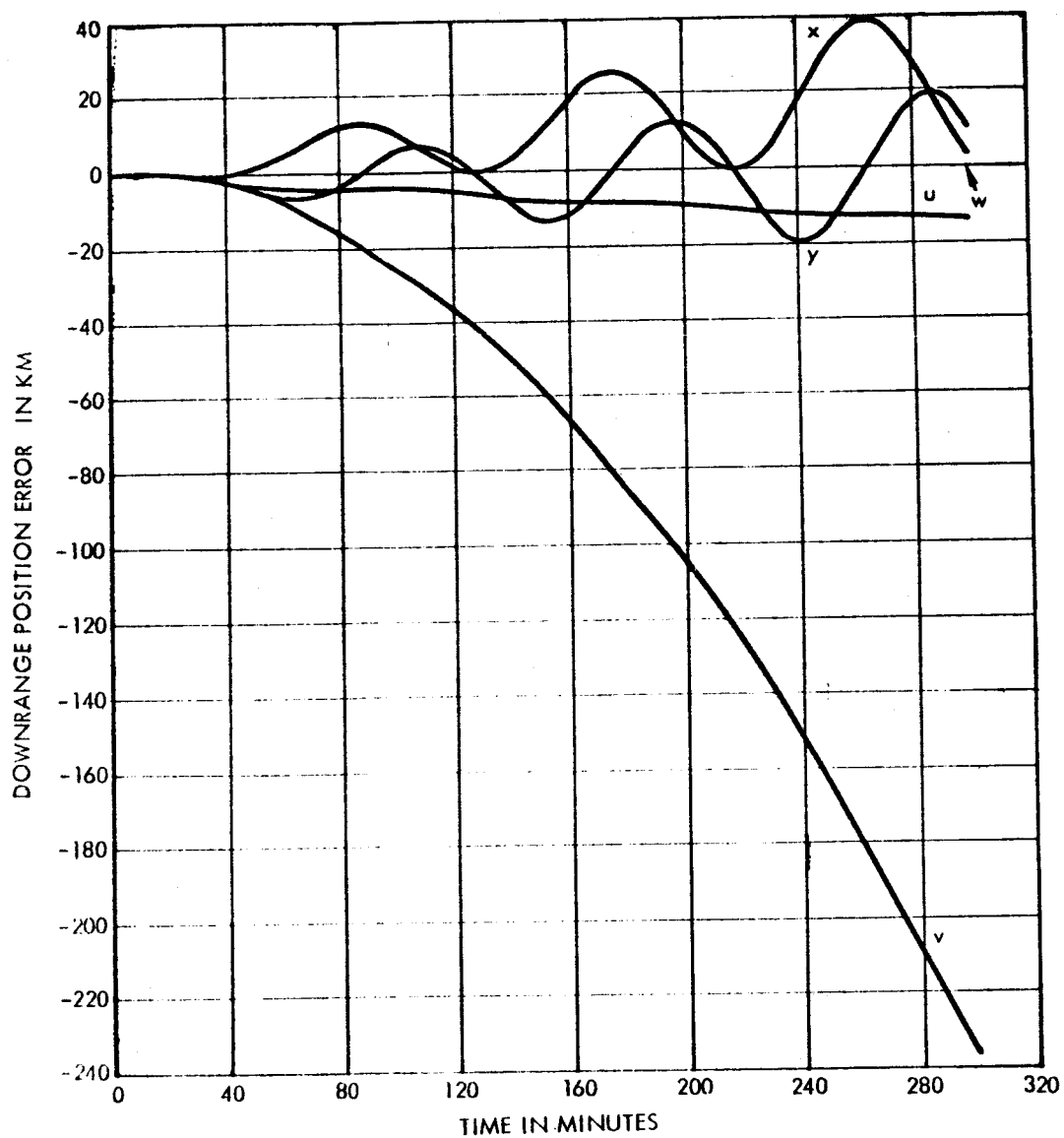


Figure 2.1.1-8. d Effect of u, v, w, x, y Thrusts, $5(10^{-5})g$ Continuous, 200 km Circular Orbit Integrated

3. The downrange effect of an in-plane thrust is larger than the radial effect after about half an orbit. (Figures 2.1.1-2, 2.1.1-3, 2.1.1-5, and 2.1.1-6)
4. Downrange thrust gives the largest effects of any thrust in both the radial and downrange directions (Figures 2.1.1-8 and 2.1.1-8)

Analytic. The analytic expressions derived for the effects of continuous low thrust are based on linear perturbations of a nominally circular orbit. The coordinate system used is the uvw system introduced earlier. In this coordinate system, the differential equations are the following:

$$\ddot{u} - 3\omega^2 u - 2\omega \dot{v} = a_u$$

$$2\omega \dot{u} + \ddot{v} = a_v$$

$$\ddot{w} + \omega^2 w = a_w$$

where

$$\omega = \text{angular frequency, } \omega = \frac{2\pi}{P}$$

$$P = \text{orbital period}$$

$$a_u, a_v, a_w = \text{acceleration in the } u, v, w \text{ directions}$$

$$u_o, \dot{u}_o = \text{the initial position and velocity conditions: } u(t), \dot{u}(t) \text{ evaluated at } t = 0$$

Note that the differential equations are linear with constant coefficients. The coordinates are proportional to the driving force and superposition may be used to add separate solutions.

The solution for u, v , and w may therefore be written in matrix form as

$$\begin{bmatrix} u \\ v \\ w \end{bmatrix} = A \begin{bmatrix} u_o \\ v_o \\ w_o \end{bmatrix} + B \begin{bmatrix} \dot{u}_o \\ \dot{v}_o \\ \dot{w}_o \end{bmatrix} + C \begin{bmatrix} a_u \\ a_v \\ a_w \end{bmatrix}$$

for constant accelerations. The coefficients A, B, and C can be found by usual methods to be

$$A = \begin{bmatrix} 4 - 3\cos \omega t & 0 & 0 \\ -6(\omega t - \sin \omega t) & 1 & 0 \\ 0 & 0 & \cos \omega t \end{bmatrix}$$

$$B = \frac{1}{\epsilon} \begin{bmatrix} \sin \omega t & 2(1 - \cos \omega t) & 0 \\ -2(1 - \cos \omega t) & -3\omega t + 4\sin \omega t & 0 \\ 0 & 0 & \sin \omega t \end{bmatrix}$$

$$C = \frac{1}{\epsilon^2} \begin{bmatrix} 1 - \cos \omega t & 2(\omega t - \sin \omega t) & 0 \\ -2(\omega t - \sin \omega t) & -\frac{3}{2}(\omega t)^2 + 4(1 - \cos \omega t) & 0 \\ 0 & 0 & 1 - \cos \omega t \end{bmatrix}$$

Several important features of the C matrix should be noted:

- 1) The w motion is independent of whatever is occurring in the u and v directions.
- 2) The u motion with $a_v = 0$ is the negative of the v motion with $a_u = 0$. This means that the downrange effect of a radial thrust is the same as the radial effect of a downrange thrust, except for the matter of sign.
- 3) The crossrange motion w is the same as the u motion due to an acceleration in the u direction. This together with the previous observation means that the entire motion can be defined with only three graphs. All five combinations of coordinates and thrust are plotted in Figures 2.1.1-9 through 2.1.1-13, but as can be seen in the graphs, two of the five are redundant.

The altitude of the nominal circular orbit affects the position deviation caused by a low thrust through ω . The amplitude of the effect is inversely proportional to ω^2 and the speed of the effect is directly proportional to ω . The effects of changing the altitude from 200 km to 700 km are shown in Figures 2.1.1-9 through 2.1.1-13. Notice that the downrange effect of downrange thrust

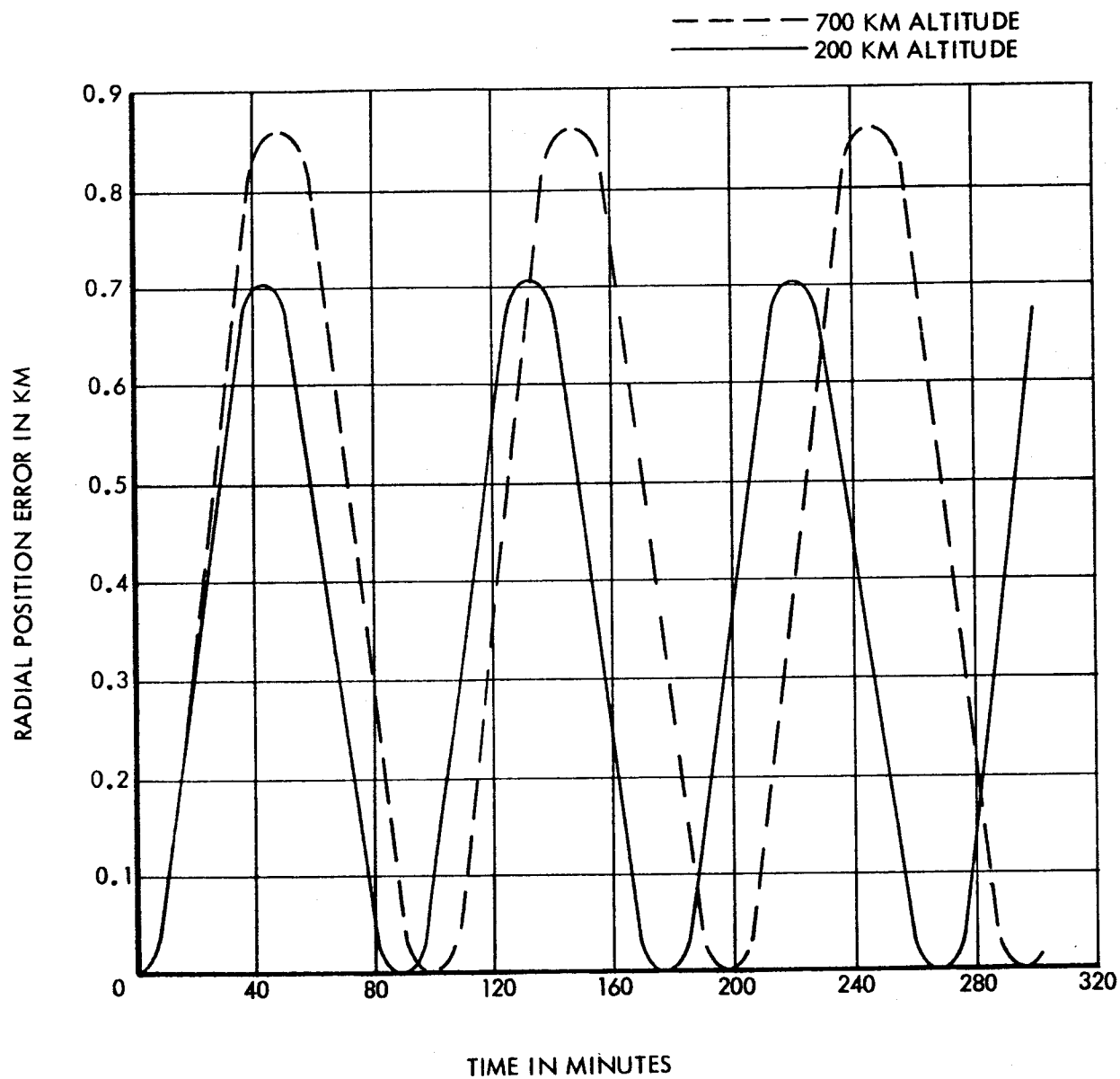


Figure 2.1.1-9. u Effect of u Thrust, $5(10^{-5})g$ Continuous, 200 km and 700 km Circular Orbits, Analytic

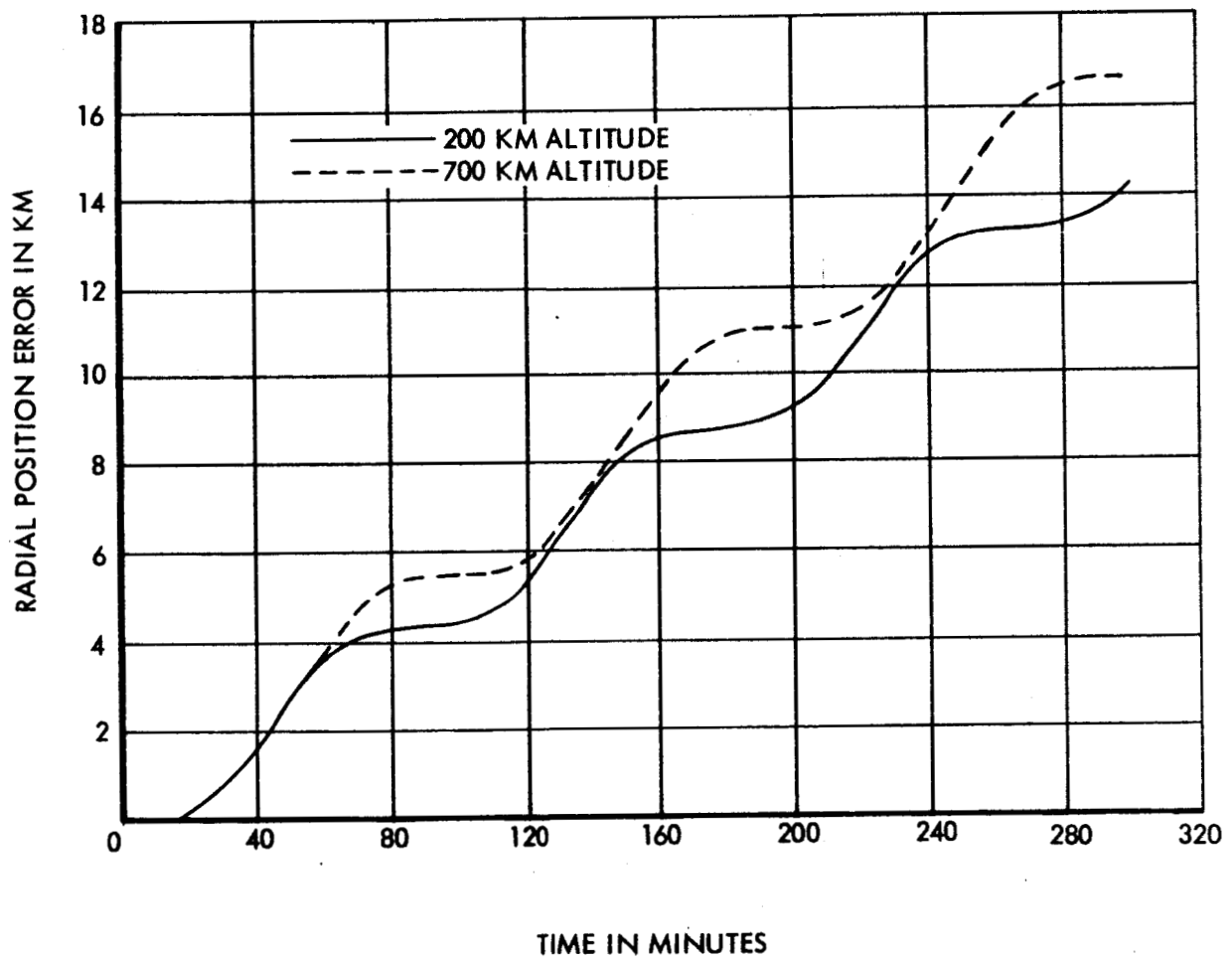


Figure 2.1.1-10. u Effect of v Thrust, $5(10^{-5})g$ Continuous, 200 km and 700 km Circular Orbits, Analytic

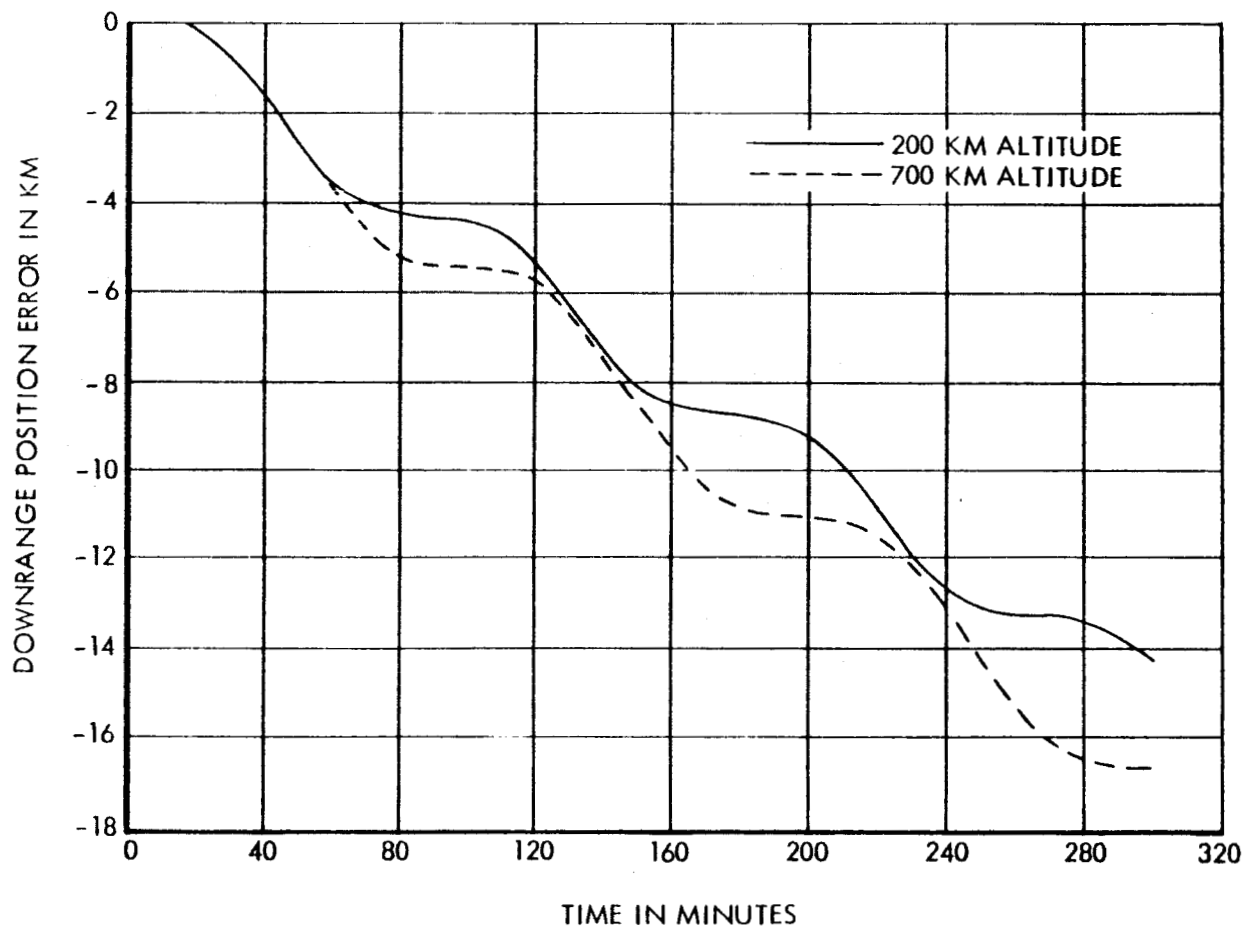


Figure 2.1.1-11. v Effect of u Thrust, $5(10^{-5})g$ Continuous, 200 km and 700 km Circular Orbits, Analytic

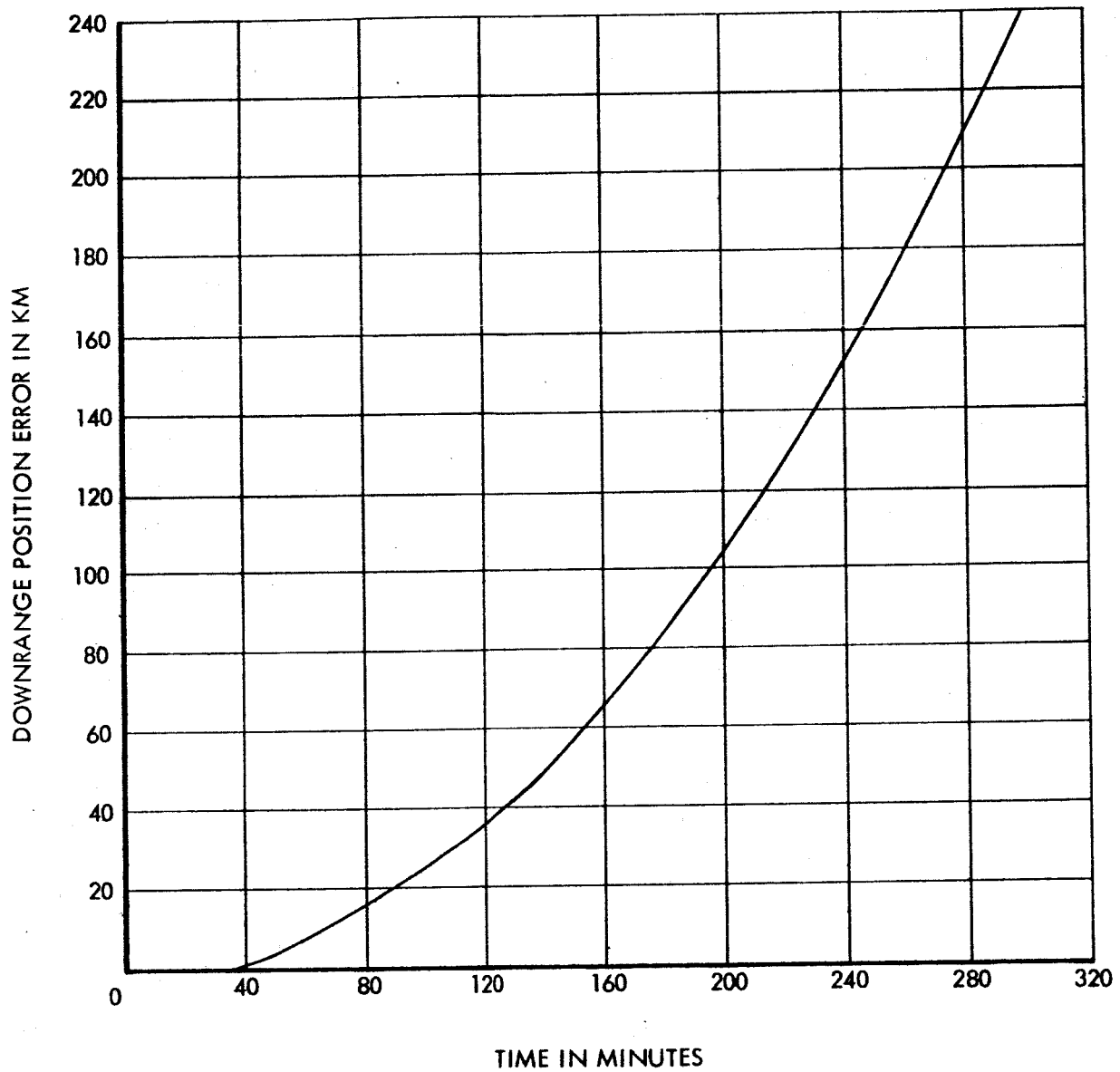


Figure 2.1.1-12. v Effect of v Thrust, $5(10^{-5})g$ Continuous, 200 km and 700 km Circular Orbits, Analytic

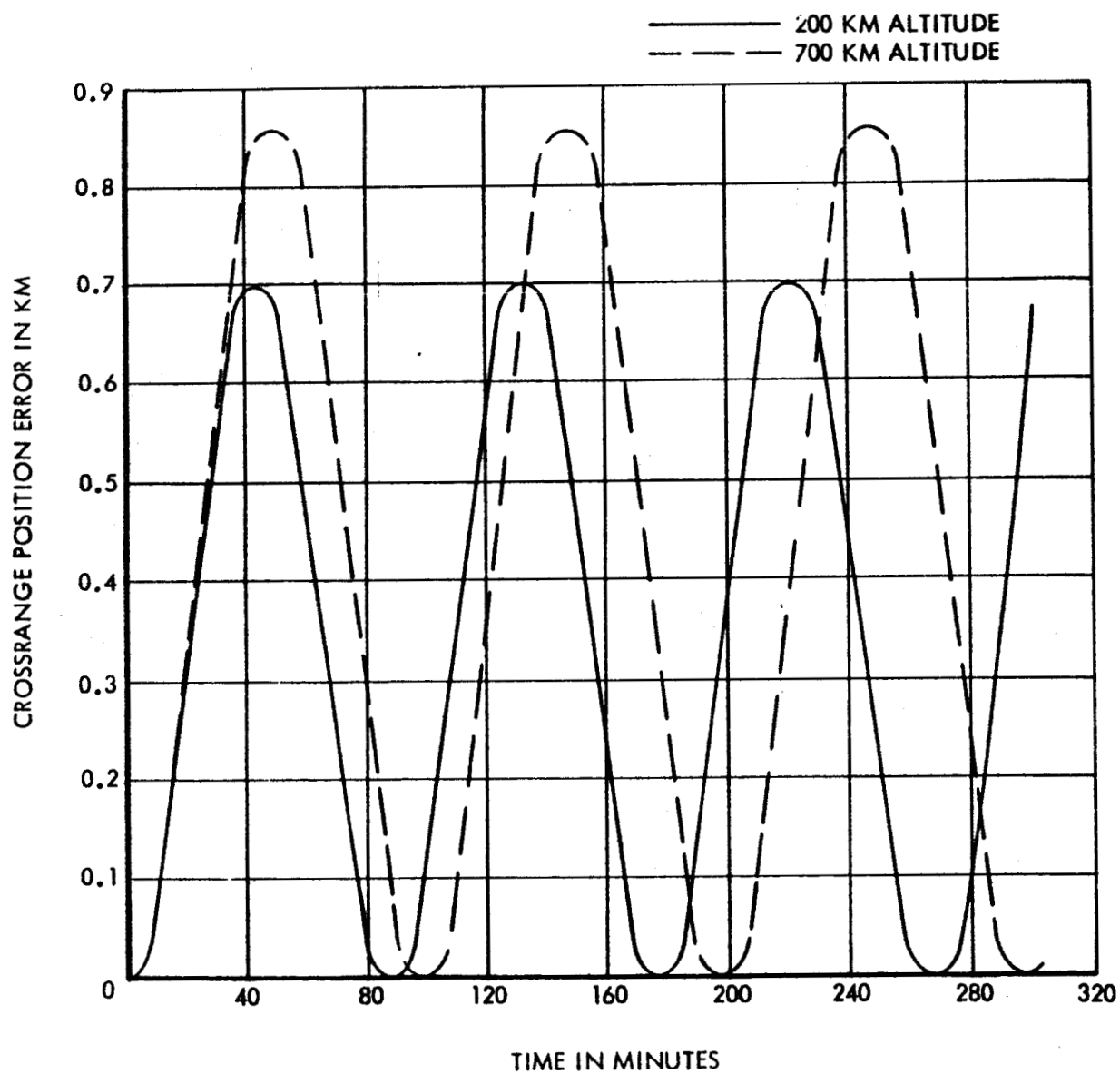


Figure 2.1.1-13. w Effect of w Thrust, $5(10^{-5})g$ Continuous, 200 km and 700 km Circular Orbits, Analytic

is essentially independent of altitude. This is a result of the fact that the dominant term is $(1/\omega^2)(\omega t)^2$ or simply t^2 .

The analytic formulation depends on the orbit being nearly circular. The approximations involve setting $\cos e = 1$ and $\sin e = e$, where e is the eccentricity of the orbit. For elliptical orbits in the range of 150 to 700 km altitude, e is less than about 0.05, and the approximation is certainly good enough for results that are to be presented graphically. The only restriction is that ω should be calculated from the period of the nominal orbit, whether it is circular or not.

In most cases the analytic results agree closely with the integrated results. In the radial effect of downrange thrust, however, a discrepancy was noticed. The integrated effect was lower than the analytic effect after one revolution. Therefore, the thrust was reduced to $5(10^{-6})g$ in the integration and the results were multiplied by ten and plotted for comparison with the original curve. (See Figure 2.1.11-14). For the lower thrust the results agree closely with the analytic results.

The u, v, w coordinate system used to express the position effects of low thrust is a rotating system located at the nominal position of the vehicle without thrust. Therefore, two velocity vectors may be of interest. The first is the rate of change of the u, v , and w coordinates of the thrusting vehicle, and is obtained by differentiating the coordinates with respect to time. The resulting equation for this velocity with initial conditions and fixed thrust is

$$\begin{bmatrix} \dot{u} \\ \dot{v} \\ \dot{w} \end{bmatrix} = \frac{dA}{dt} \begin{bmatrix} u_o \\ v_o \\ w_o \end{bmatrix} + \frac{dB}{dt} \begin{bmatrix} \dot{u}_o \\ \dot{v}_o \\ \dot{w}_o \end{bmatrix} + \frac{dC}{dt} \begin{bmatrix} a_u \\ a_v \\ a_w \end{bmatrix}$$

where

$$\frac{dA}{dt} = \omega \begin{bmatrix} 3\sin \omega t & 0 & 0 \\ -6(1 - \cos \omega t) & 0 & 0 \\ 0 & 0 & -\sin \omega t \end{bmatrix}$$

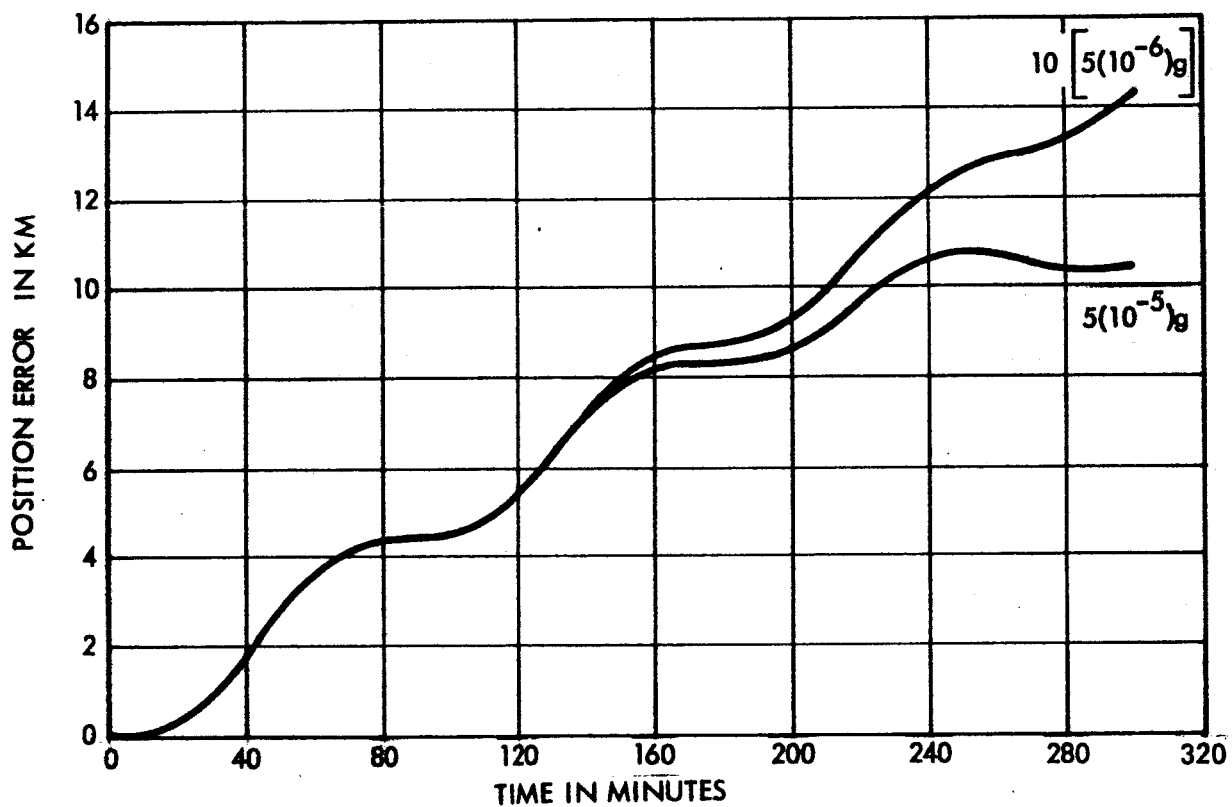


Figure 2.1.1-14. Linearity Study, u Effects of v Thrusts, 200 km Circular Orbit Integrated

$$\frac{dB}{dt} = \begin{bmatrix} \cos \omega t & 2\sin \omega t & 0 \\ -2\sin \omega t & -3 + 4\cos \omega t & 0 \\ 0 & 0 & \cos \omega t \end{bmatrix}$$

$$\frac{dC}{dt} = \frac{1}{\omega} \begin{bmatrix} \sin \omega t & 2(1 - \cos \omega t) & 0 \\ -2(1 - \cos \omega t) & -3\omega t + 4\sin \omega t & 0 \\ 0 & 0 & \sin \omega t \end{bmatrix}$$

The other velocity vector of interest is the difference between the inertial velocity of the thrusting vehicle and the inertial velocity of the nominal vehicle. Even though this is an inertial velocity vector, its components in the rotating u, v, w coordinate system can be obtained from

$$\begin{bmatrix} V_u \\ V_v \\ V_w \end{bmatrix} = \begin{bmatrix} \dot{u} \\ \dot{v} \\ \dot{w} \end{bmatrix} + \Omega \begin{bmatrix} u \\ v \\ w \end{bmatrix}$$

where

$$\begin{bmatrix} V_u \\ V_v \\ V_w \end{bmatrix} = \begin{matrix} \text{the components in the } u, v, w \text{ coordinate systems of} \\ \text{the inertial velocity difference} \end{matrix}$$

$$\Omega = \begin{bmatrix} 0 & -\omega & 0 \\ \omega & 0 & 0 \\ 0 & 0 & 0 \end{bmatrix}$$

The second term results from the fact that the u, v, w system is rotating. That is, the inertial velocity difference is not zero when $\dot{u} = \dot{v} = \dot{w} = 0$ unless $u = v = w = 0$ also.

Substitution yields

$$\begin{bmatrix} V_u \\ V_v \\ V_w \end{bmatrix} = \left[\frac{dA}{dt} + \Omega A \right] \begin{bmatrix} u_o \\ v_o \\ w_o \end{bmatrix} + \left[\frac{dB}{dt} + \Omega B \right] \begin{bmatrix} \dot{u}_o \\ \dot{v}_o \\ \dot{w}_o \end{bmatrix} + \left[\frac{dC}{dt} + \Omega C \right] \begin{bmatrix} a_u \\ a_v \\ a_w \end{bmatrix}$$

or, more concisely,

$$\begin{bmatrix} V_u \\ V_v \\ V_w \end{bmatrix} = D \begin{bmatrix} u_o \\ v_o \\ w_o \end{bmatrix} + E \begin{bmatrix} \dot{u}_o \\ \dot{v}_o \\ \dot{w}_o \end{bmatrix} + F \begin{bmatrix} a_u \\ a_v \\ a_w \end{bmatrix}$$

where the accelerations are still assumed constant,

By straightforward manipulation, the coefficients obtained are

$$D = \omega \begin{bmatrix} 6\omega t - 3\sin \omega t & -1 & 0 \\ -2 + 3\cos \omega t & 0 & 0 \\ 0 & 0 & -\sin \omega t \end{bmatrix}$$

$$E = \begin{bmatrix} 2 - \cos \omega t & 3\omega t - 2\sin \omega t & 0 \\ -\sin \omega t & -1 + 2\cos \omega t & 0 \\ 0 & 0 & \cos \omega t \end{bmatrix}$$

$$F = \frac{1}{\omega} \begin{bmatrix} 2\omega t - \sin \omega t & -2 + \frac{3}{2}(\omega t)^2 + 2\cos \omega t & 0 \\ -1 + \cos \omega t & -\omega t + 2\sin \omega t & 0 \\ 0 & 0 & \sin \omega t \end{bmatrix}$$

The largest effects of continuous thrust are produced when the thrust is in the downrange direction. Then the downrange position and the radial velocity have large secular effects which are simply related to each other. The secular term in downrange position is $-\left(3/2\right)t^2 a_v$ and the secular term in radial velocity is $\left(3/2\right)\omega t^2 a_v$. In order to obtain the secular radial velocity effect from the secular downrange position effect it is only necessary to multiply by $-\omega$. The value of ω varies from 1/845 for a 200 km orbit to 1/941 for a 700 km orbit (with time measured in seconds). As a convenient rule of thumb, therefore, it can be said that radial velocity error can be obtained from downrange position error by reversing the sign and dividing by 900. Figure 2.1.1-15 shows the components of inertial velocity effect of downrange thrust obtained from the integrating trajectory program. Comparison with Figure 2.1.1-3 shows the similarity between position and velocity errors.

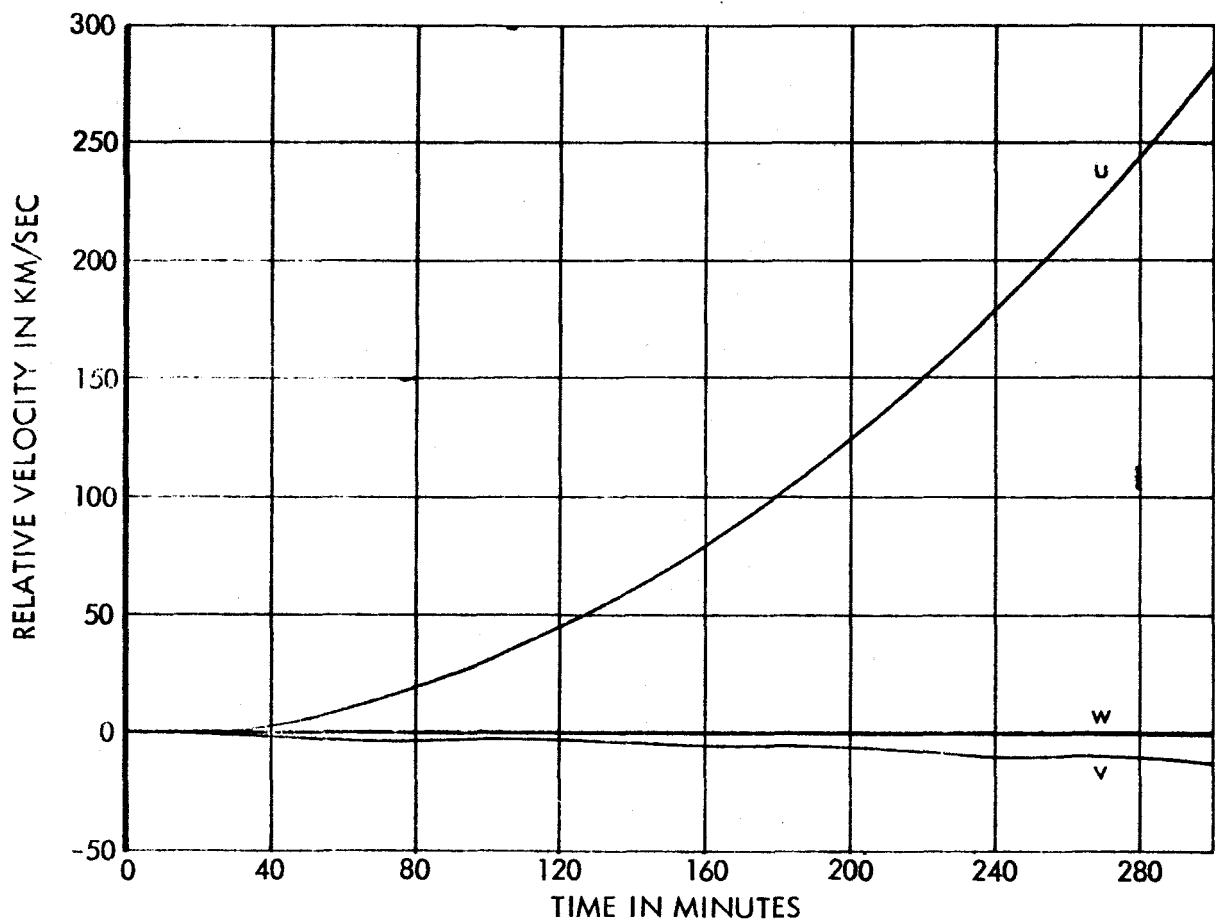


Figure 2.1.1-15. Orbit-plane Components of Inertial Velocity Error from $5(10^{-5})g$ Continuous Downrange Thrust and 200 km Circular Orbit

2.1.2 Tracking Effects

The effects of continuous low thrusts on the tracking of earth orbits were determined by doing actual fits to noise-free tracking data generated by the perturbed trajectories, and then comparing the resulting estimated orbits with the actual orbits. The observations were generated by the STL N-stage trajectory program and were processed by the STL General Tracking Program to obtain the initial conditions of the non-thrusting orbits which best fit the data in a least-squares sense. The N-stage program was then used to calculate the differences between the original thrusting orbits and the orbits resulting from the initial conditions found by the General Tracking Program.

The orbit used was nominally circular at an altitude of 200 kilometers with zero inclination and was perturbed by an acceleration of $5(10^{-5})g$ in various directions. Observations were made by three tracking stations located at one degree north latitude and 15, 135, and 255 degrees east longitude. Range, azimuth, and elevation observations were taken every ten seconds during the period of visibility of the vehicle to each station. The one-sigma uncertainties were assumed to be 10 meters, 0.015 degrees, and 0.015 degrees in range, azimuth, and elevation, respectively.

In addition to the parameters associated with the total effects of low thrust, the number of tracking passes affects the tracking effects. Therefore the results for each thrust are shown for several different numbers of passes.

The curves present the tracking errors in two different forms. First, the position errors are plotted as functions of time over the entire 300-minute period considered. The results for different numbers of passes are shown on separate sheets. This presentation was chosen to show clearly the error involved in both predicting the orbit after the last data point and in extrapolating the prediction into the interval before the fit could be made. In the second form the effect of varying the number of passes on the accuracy at any time is shown by plotting on one sheet the prediction errors caused by various numbers of passes with time measured from the acquisition of the last data point.

Figures 2.1.2-1 through 2.1.2-3 show the u , v , and w position effects of u , v , and w thrusts on the prediction of the orbit from three tracking passes. The visibility periods are indicated by the blocks near the time axis. From these curves it can be seen that downrange thrust gives the largest in-plane tracking effects, just as it gives the largest in-plane total effects. It can also be seen that in-plane thrusts give an out-of-plane tracking error even though they cause no out-of-plane perturbation of the orbit. This is a result of using tracking data from stations out of the orbit plane.

Since downrange thrust gives the largest tracking effects, it was chosen for more detailed study with the results shown in Figures 2.1.2-4 through 2.1.2-9. In these figures the error in the prediction of the vehicle position is presented with the number of tracking passes as a parameter. In addition, these curves show the differences between the tracking estimate of the orbit and the actual orbit during the period covered by tracking data.

As might be expected, the error during the tracking interval is smaller than the error after the interval, because the fitting procedure has no information about errors where there are no observations. As more passes are used, the fit during the tracking interval has more error, since the actual thrusting orbit is approximated by a non-thrusting orbit in the tracking program. For short periods the approximation can be quite good, but for longer periods the errors become noticeable.

If the prediction error is plotted as a function of time after the last observation as in Figure 2.1.2-10, it can be seen that the best prediction occurs when only the last radar pass is used in the fit. Since the model used in the fit is incorrect (that is, thrust is not considered), the best prediction is obtained by using the latest information.

Attempts to solve for a negative drag coefficient to simulate solving for a downrange thrust have not given good results. In some cases convergence could not be obtained. On the other hand, when convergence was obtained, the standard deviation of the drag coefficient obtained corresponded to an acceleration larger than the $5(10^{-5})g$ used in this study. The results therefore indicate

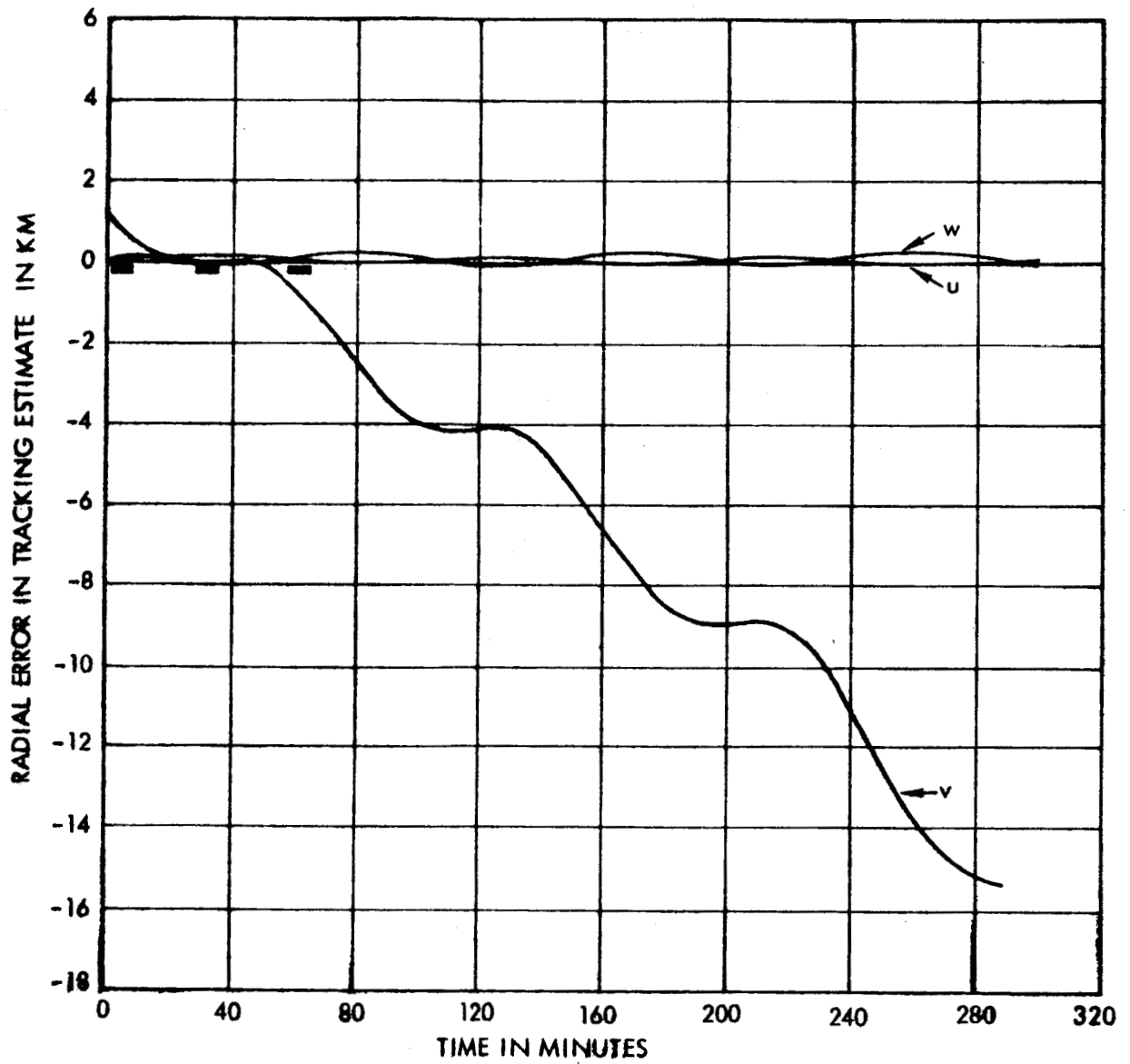


Figure 2.1.2-1. u Effects of u, v, w Thrusts, $5(10^{-5})g$ Continuous, 200 km Circular Orbit, 3 Passes (1 Revolution)

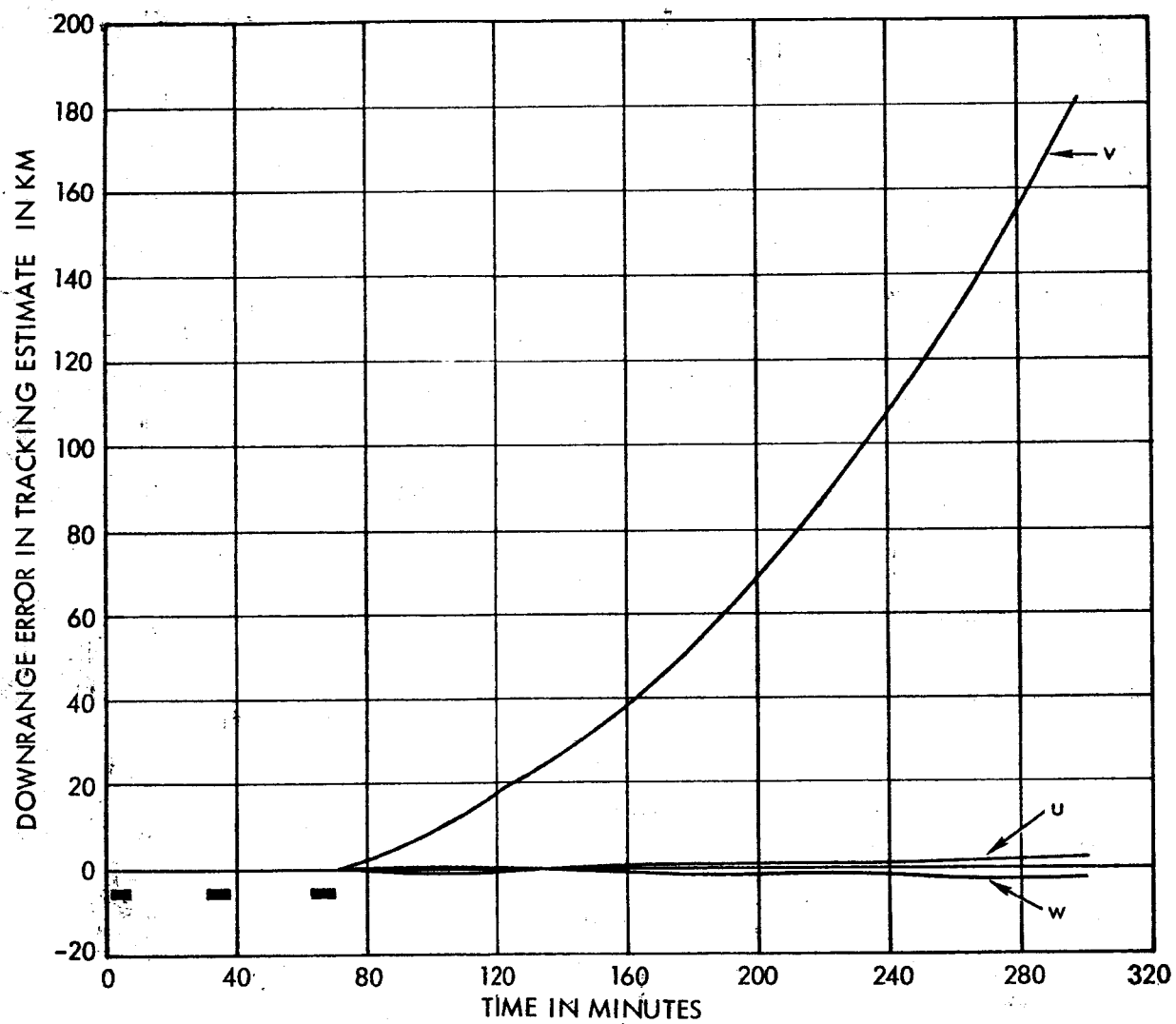


Figure 2.1.2-2. v Effects of u, v, w Thrusts, $5(10^{-5})g$ Continuous, 200 km Circular Orbit, 3 Passes (1 Revolution)

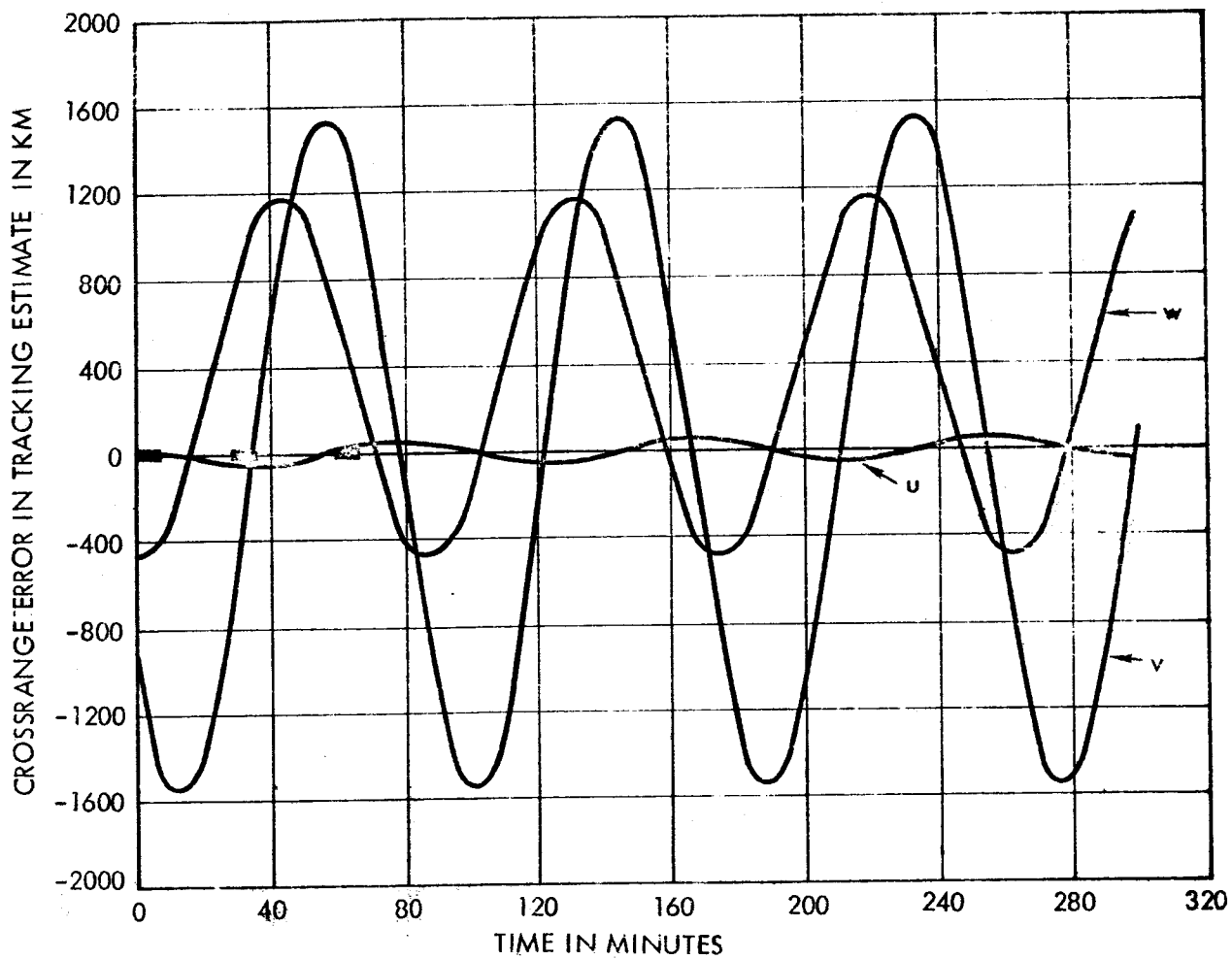


Figure 2.1.2-3. w Effect of u, v, w Thrusts, $5(10^{-5})g$ Continuous, 200 km Circular Orbit, Results by Integration, 3 Passes (1 Revolution)

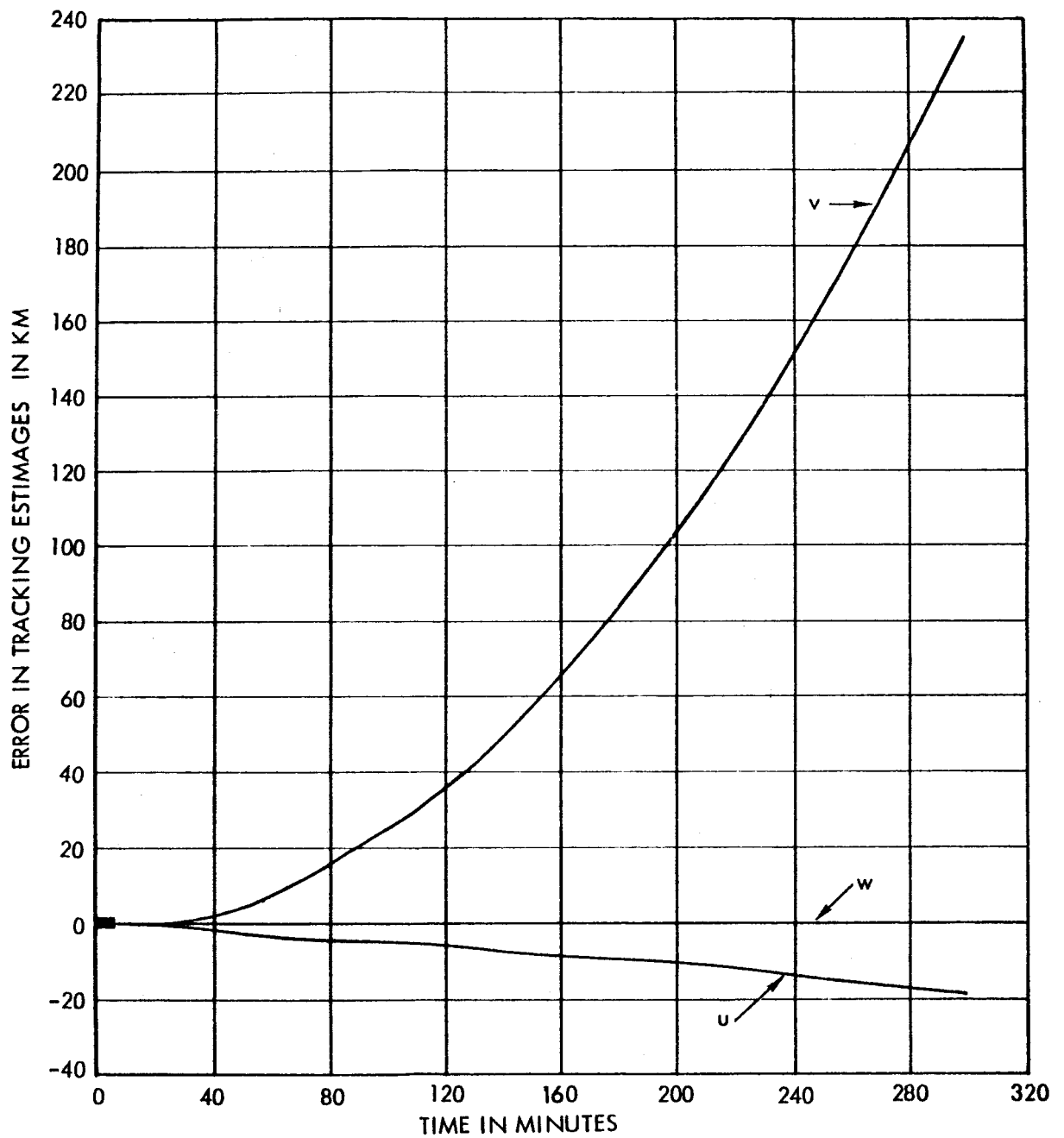


Figure 2.1.2-4. u, v, w Tracking Effects of v Thrust: $5(10^{-5})g$
Continuous, 200 km Orbit (Circular), 1 Pass

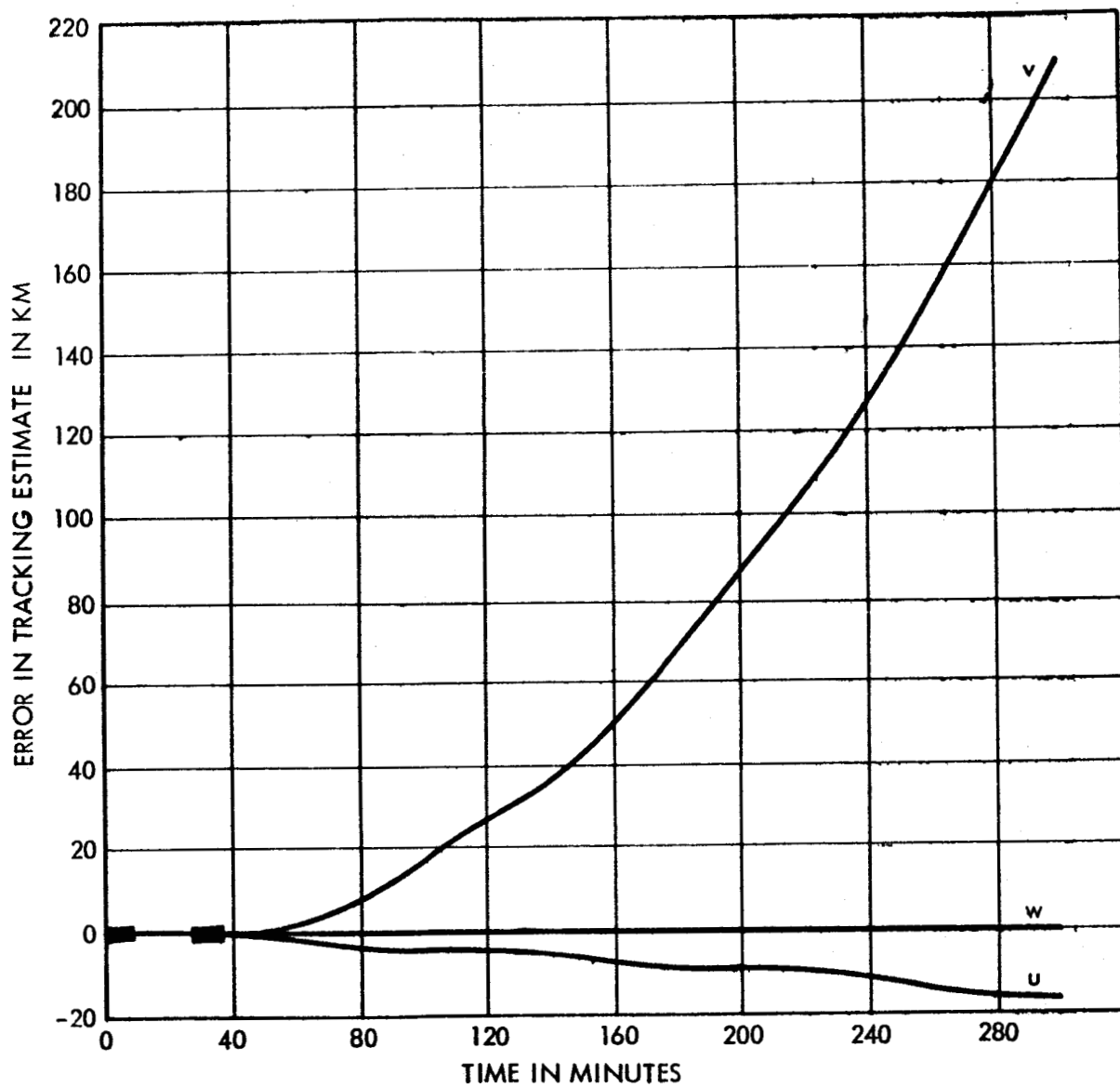


Figure 2.1.2-5. u, v, w Tracking Effect of v Thrust, $5(10^{-5})g$
Continuous, 200 km Circular Orbit, 2 Passes

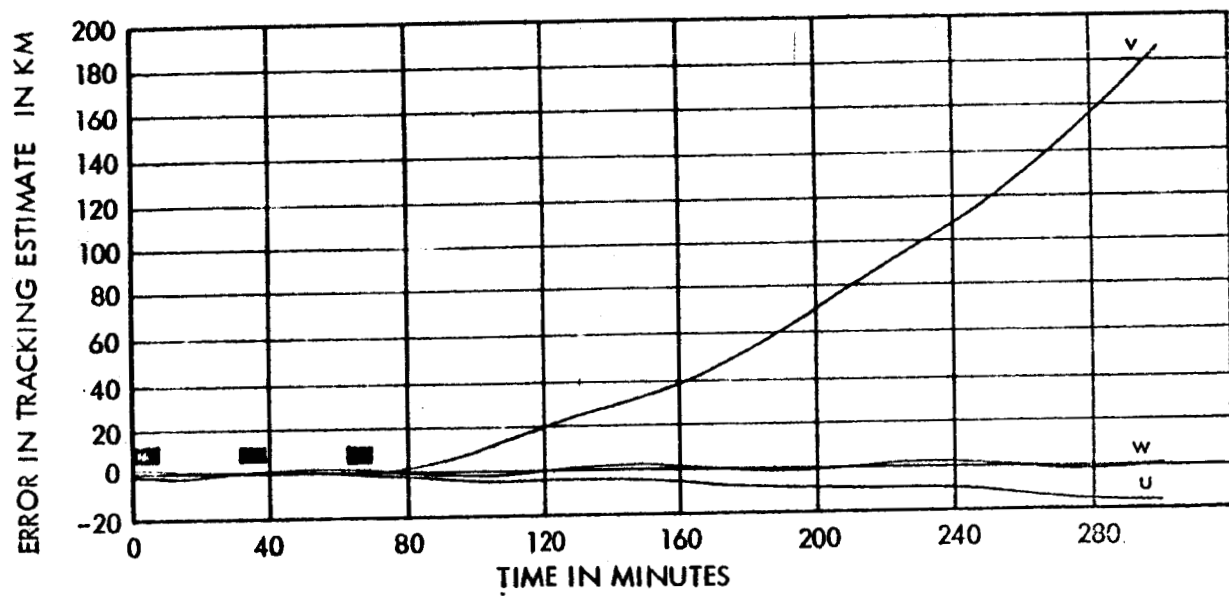


Figure 2.1.2-6. u, v, w Tracking Effects of v Thrust, $5(10^{-5})g$
Continuous, 200 km Circular, 3 Passes

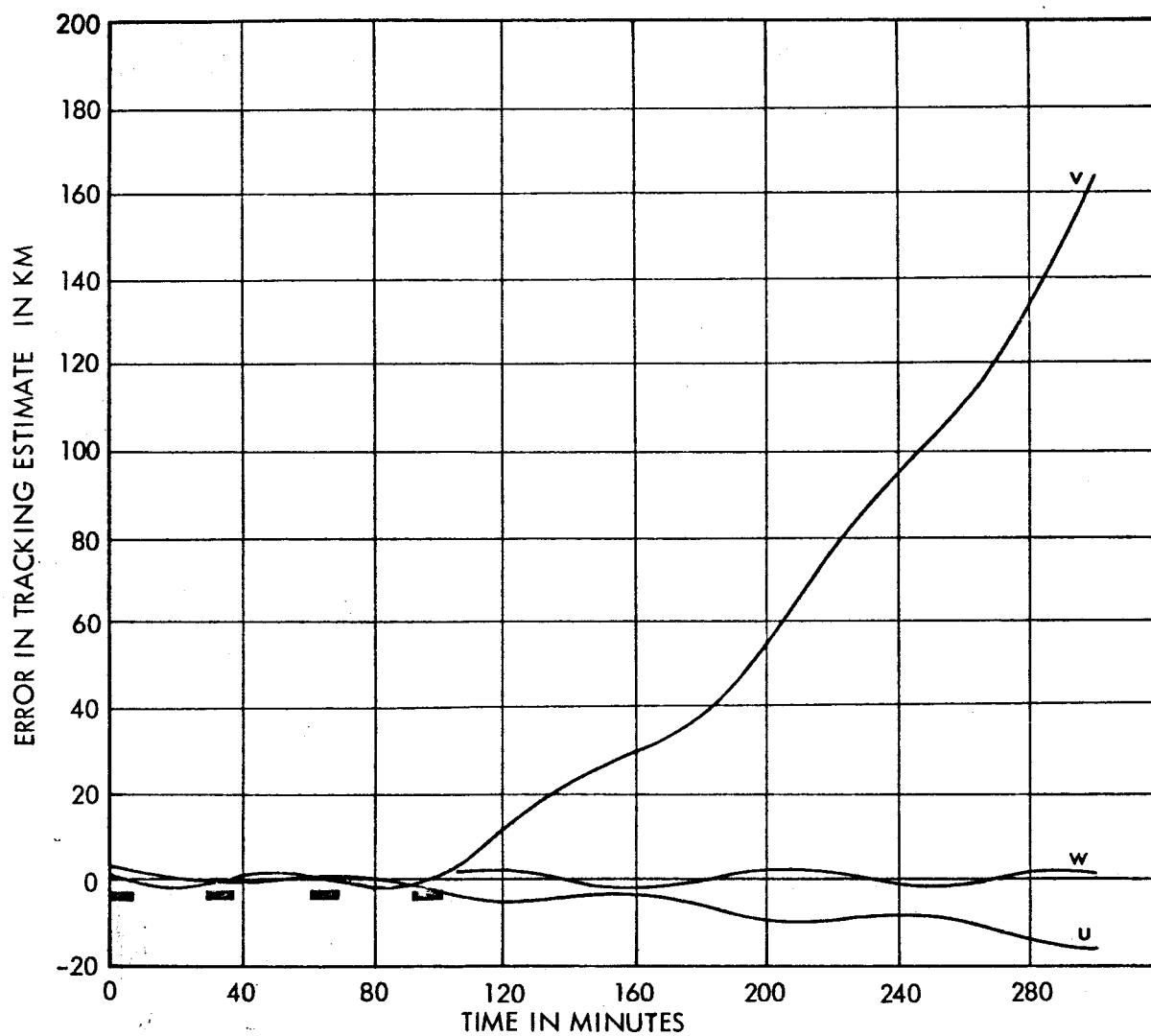


Figure 2.1.2-7. u, v, w Tracking Effects of v Thrust, $5(10^{-5})g$
Continuous, 200 km Circular Orbit, 4 Passes

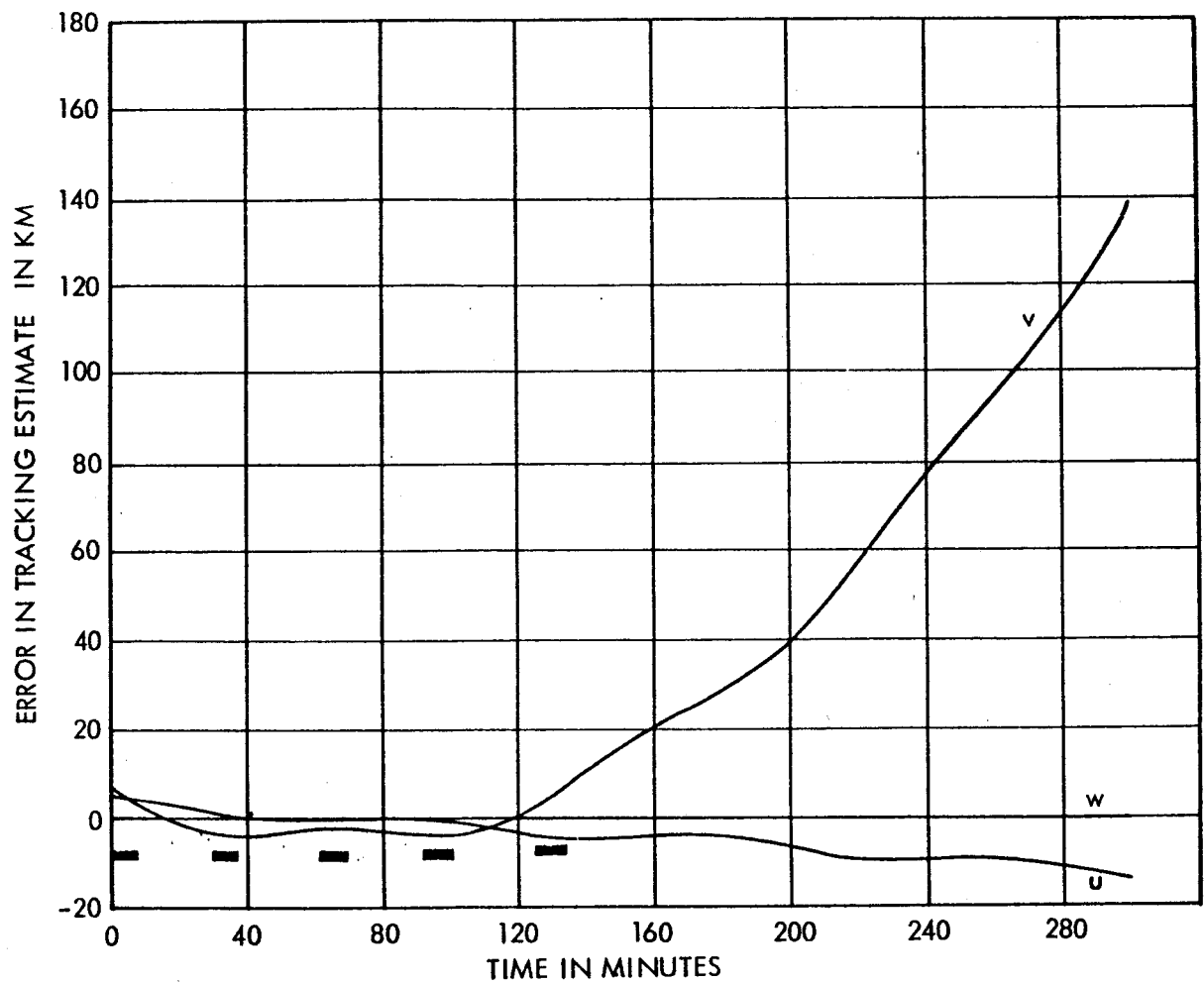


Figure 2.1.2-8. u, v, w Tracking Effects of Downrange Thrust (10^{-5})g Continuous, 200 km Circular Orbits, 5 Passes

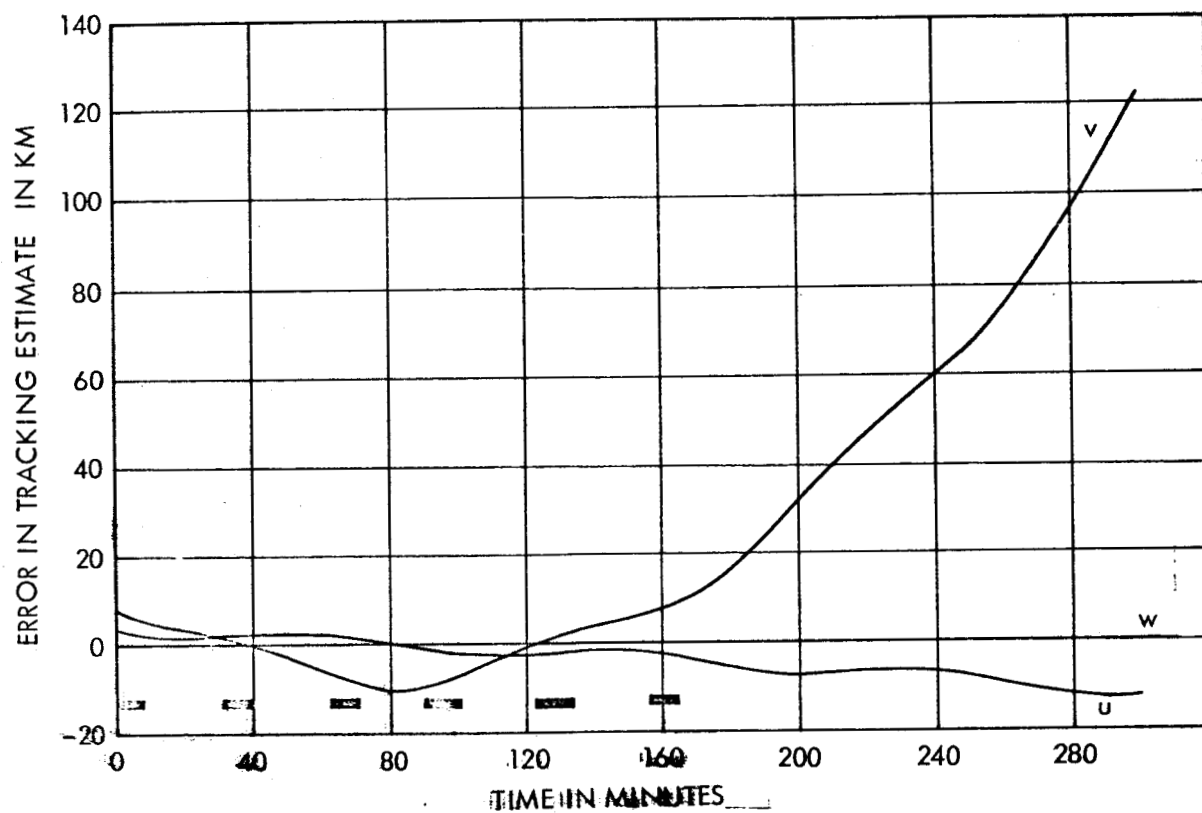


Figure 2.1.2-9. u, v, w Tracking Effects of v Thrust, $5(10^{-5})g$
Continuous, 200 km Circular Orbit, 6 Passes

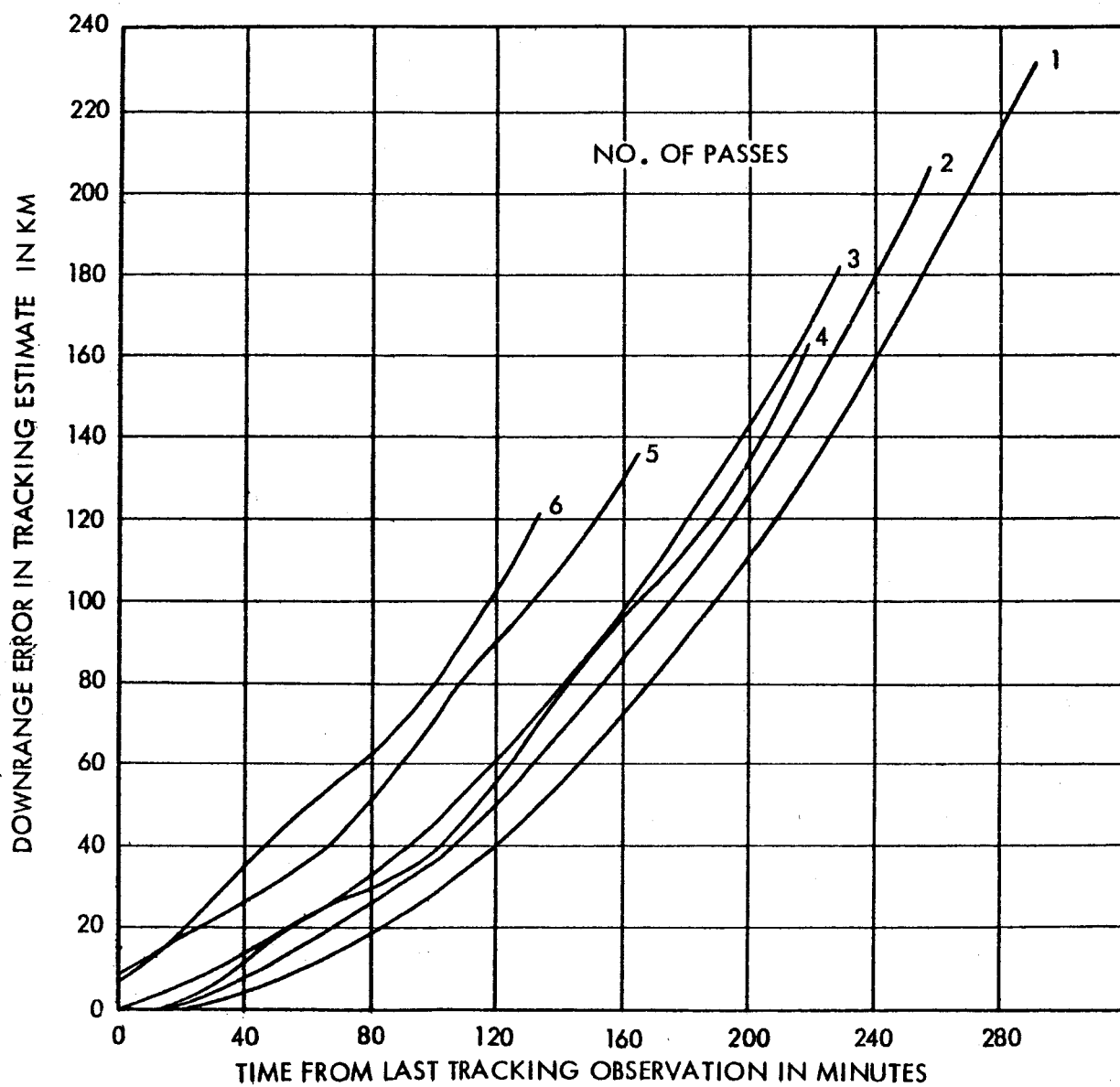


Figure 2.1.2-10. Tracking Prediction Error from $5(10^{-5})g$ Downrange Thrust

that it is not worthwhile to solve for a negative drag coefficient to determine a low downrange thrust.

With a more accurate model of the thrust in the tracking program, it should be possible to solve for the thrust, since the differences between the fit and the actual orbit are large enough to see on the graphs. The accuracy and convergence of the solution then should improve with more data. Verification of this is currently impossible, however, because the necessary programming is beyond the scope of this contract. This should be a profitable area for further study.

2.1.3 Uncertainty Effects of Low Thrust

A random low thrust may result from gas leakage, from uncertainties in continuous venting, or from a combination of the two. In any case the uncertain thrust is assumed to be fixed both in magnitude and direction relative to the body axes for any one mission. Different missions have different magnitudes and directions, however. The effects can be analyzed, therefore, with the analytic expressions already developed for the position and velocity errors resulting from a fixed thrust.

Since the random thrust is assumed to be small enough for linearity to exist, errors in position and velocity can be calculated from the acceleration errors from the following equations:

$$\begin{bmatrix} \delta u \\ \delta v \\ \delta w \end{bmatrix} = C \begin{bmatrix} \delta a_u \\ \delta a_v \\ \delta a_w \end{bmatrix}$$

$$\begin{bmatrix} \delta V_u \\ \delta V_v \\ \delta V_w \end{bmatrix} = F \begin{bmatrix} \delta a_u \\ \delta a_v \\ \delta a_w \end{bmatrix}$$

That is, the equations for the effects of thrust errors are of exactly the same form as the equations for the total thrust effects, since all effects are assumed to be in the linear region.

If the errors in accelerations are assumed to be Gaussian so that they are defined statistically by a covariance matrix, then the covariance matrix of position and velocity is given by

$$\Lambda = \begin{bmatrix} C \\ F \end{bmatrix} \Lambda_A \begin{bmatrix} C^T & F^T \end{bmatrix}$$

Covariance matrices of position and velocity may also be calculated separately if only one or the other is desired from

$$\Lambda_R = C \Lambda_A C^T$$

$$\Lambda_V = F \Lambda_A F^T$$

where

Λ = the (6 x 6) covariance matrix of position and velocity

Λ_A = the (3 x 3) covariance matrix of acceleration

Λ_R = the (3 x 3) covariance matrix of position

Λ_V = the (3 x 3) covariance matrix of velocity

If only components of position and velocity are of interest, both methods will give the same results, but the covariance matrix of some function of both position and velocity is calculated the full 6 x 6 covariance matrix should be used in order to account for the correlation between position and velocity.

2.2 EFFECTS OF INTERMITTENT VENTING ON EARTH ORBITS

The effects of intermittent venting can be divided into total effects, tracking effects and uncertainty effects just as for continuous low thrust. These effects are discussed in Sections 2.2.1, 2.2.2, 2.2.3, respectively.

2.2.1 Total Effects

Both an integrating trajectory program and analytical methods were used to investigate the total effects of intermittent venting, just as for continuous low thrust. The results are, therefore, divided into Integrated and Analytic sections.

Integrated. Since the range between maximum and minimum spacing of venting pulses is quite wide, it is very difficult to make meaningful statistical statements about the uncertainties in the effects. Instead, the effects of venting at minimum, mean, and maximum intervals have been obtained in order to establish the range of the variation. Since only extreme conditions were included in the venting information supplied by MSFC, it was necessary to postulate a model in order to calculate an "average" venting case.

The following table gives the results of two extreme cases of hydrogen agitation.

	<u>Interval</u>	<u>Duration</u>	<u>Velocity</u>
Complete Stagnation	15-20 min	0.75 min	1.1 ft/sec
Complete Agitation	80 min	3.0 min	4.8 ft/sec

From the values given above it appears that the velocity addition and the duration of venting are proportional to the interval between ventings. Therefore, for the deterministic model these are assumed to be given by

$$V = \frac{4.8}{80} T \quad \text{and} \quad \tau = \frac{3.0}{80} T$$

where

V = the velocity added by the venting in ft/sec

τ = the duration of the venting in minutes

T = the interval between ventings in minutes

for $T = 20$ min, from the formulas $V = 1.25$ ft/sec and $\tau = 0.75$ min. These values are sufficiently close to the ones tabulated above.

According to this model the average acceleration is the same for all intervals and is $0.0267 \text{ ft/sec}^2 = 0.000828 \text{ g}$.

If the limits of the interval between ventings are assumed to be 3σ values of a Gaussian distribution, then

$$\mu_T = 50 \text{ min} \quad \text{and} \quad \sigma_T = 10 \text{ min}$$

The corresponding durations and velocities can be calculated from the deterministic model if the interval is assumed to be the dominant random variable.

Regardless of the frequency or duration of venting, an ullage firing occurs immediately before each venting. The ullage firing has the following characteristics:

Duration	30 sec
Velocity addition	1.1 ft/sec
Average acceleration	$0.0367 \text{ ft/sec}^2 = 0.00114 \text{ g}$

The total effects of intermittent venting are presented in a set of curves having the same pattern as those presented for continuous thrust. The important points to be noted are:

- 1) The intermittent thrust causes more pronounced short period effects than the continuous thrust.
- 2) The short period effects are quite sensitive to the frequency of venting. (Figure 2.2.1-7.)

- 3) The entire effect of 20 minute period venting is not significantly different from the continuous thrust case. (Figures 2.2.1-7 and 2.1.1-2.)
- 4) The sensitivity of long period effects to venting period, T , is slight. (Figures 2.2.1-6 and 2.2.1-7.)
- 5) Correlation with first order theory is excellent. (Figures 2.2.1-2 and 2.2.1-11.)

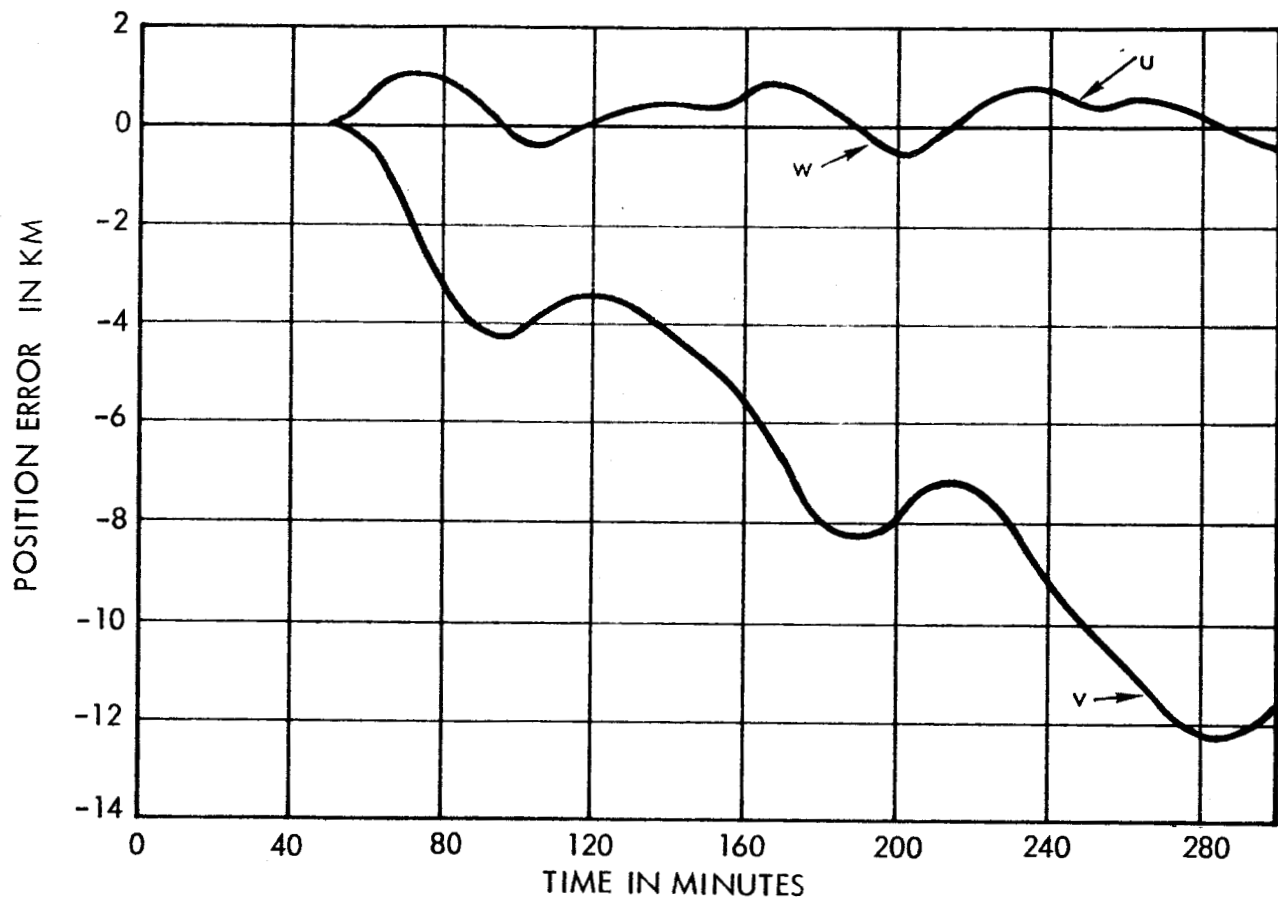


Figure 2.2.1-1. u, v, w Effects of u Thrust, 50-Minute Periodic
200 km Circular Orbit Integrated

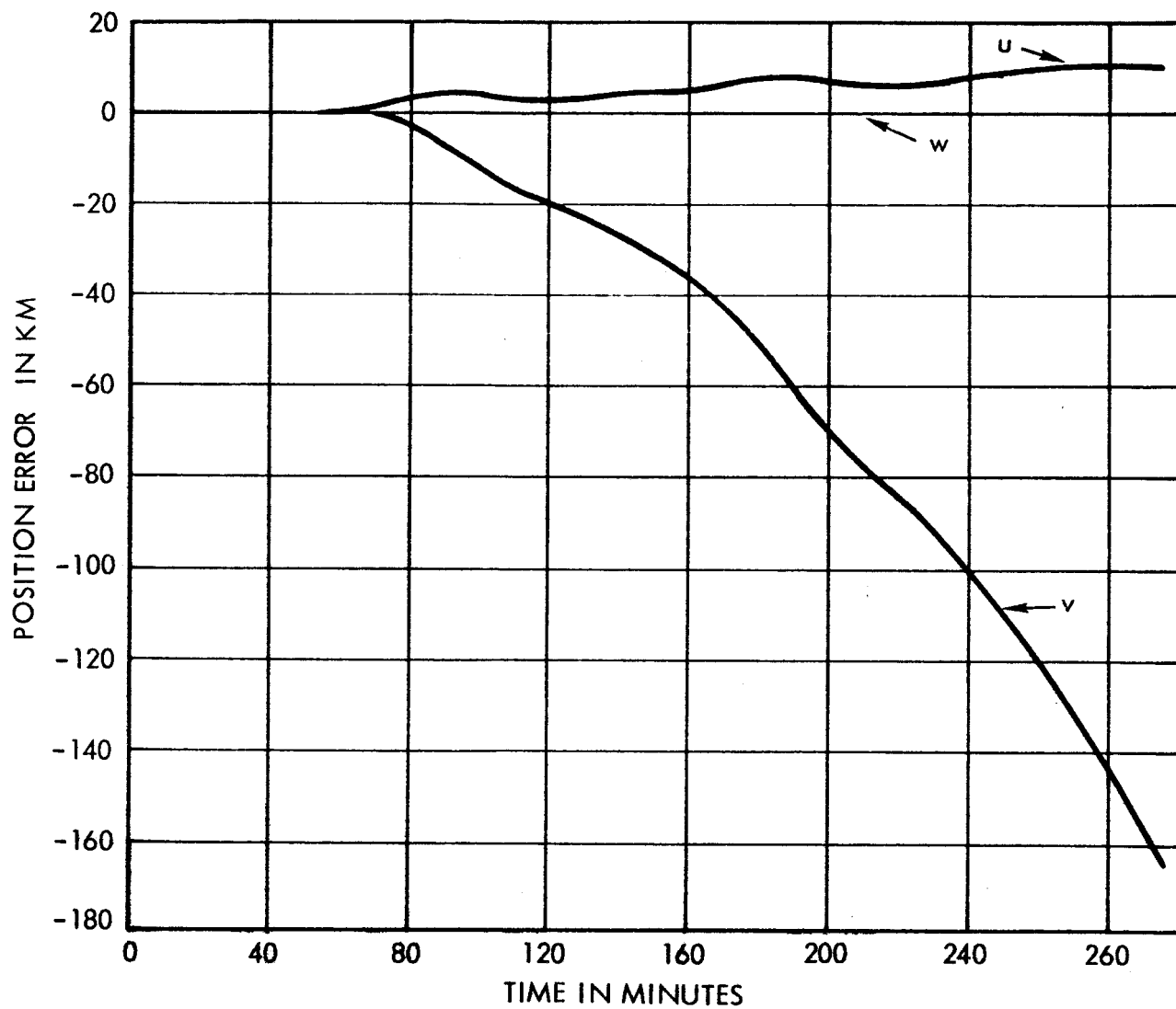


Figure 2.2.1-2. u, v, w Effects of v Thrust, 50-Minute Periodic, 200 km Circular Orbit Integrated

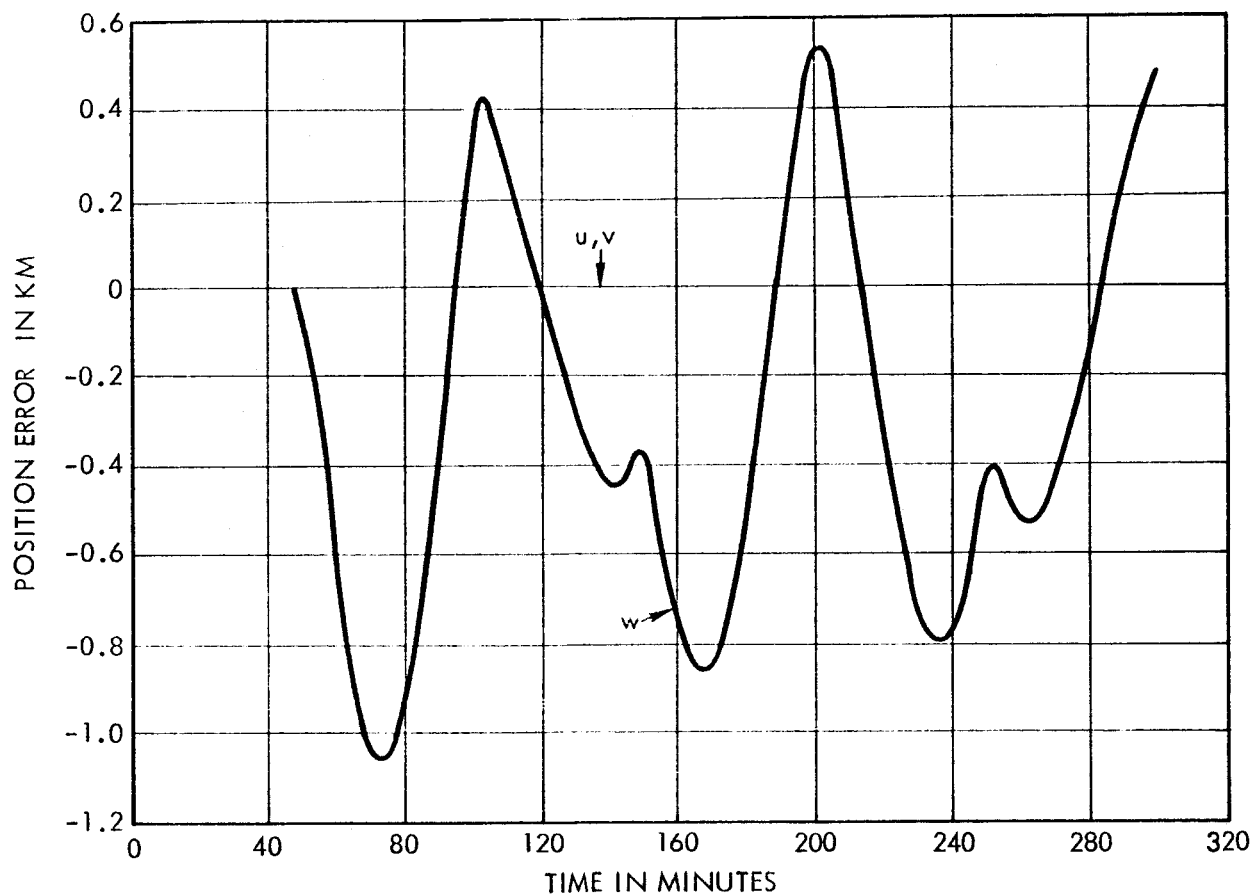


Figure 2.2.1-3. u, v, w Effects of w Thrust, 50-Minute Periodic, 200 km Circular Orbit

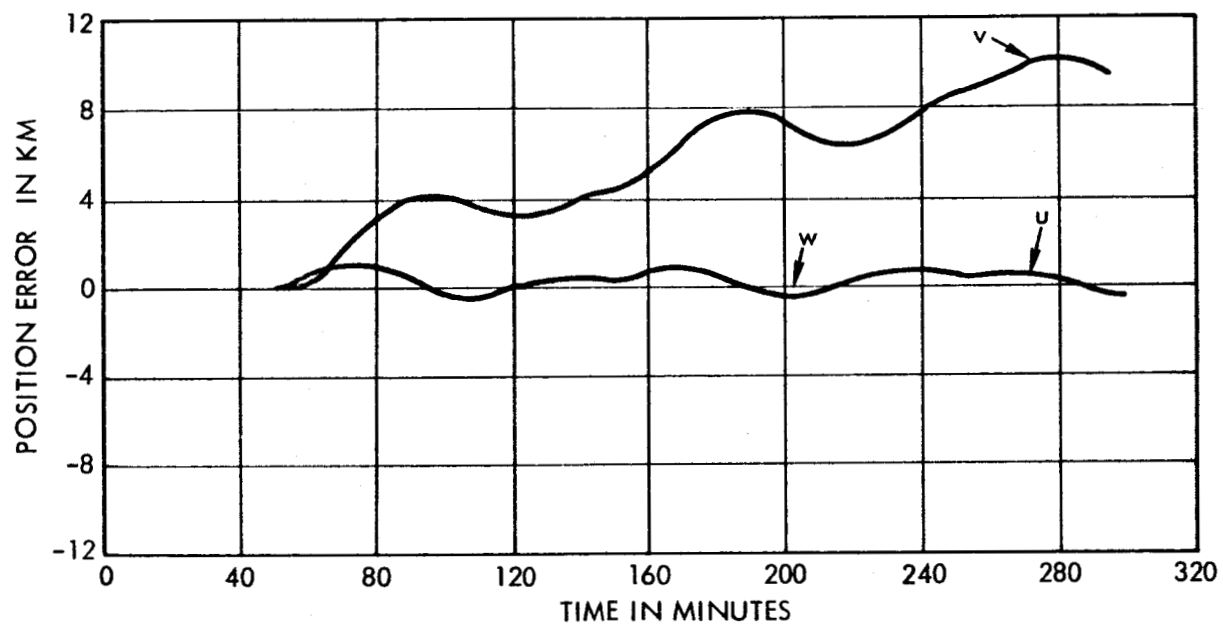


Figure 2.2.1-4. u Effect of u, v, w Thrusts, 50-Minute Periodic, 200 km Circular Orbit Integrated

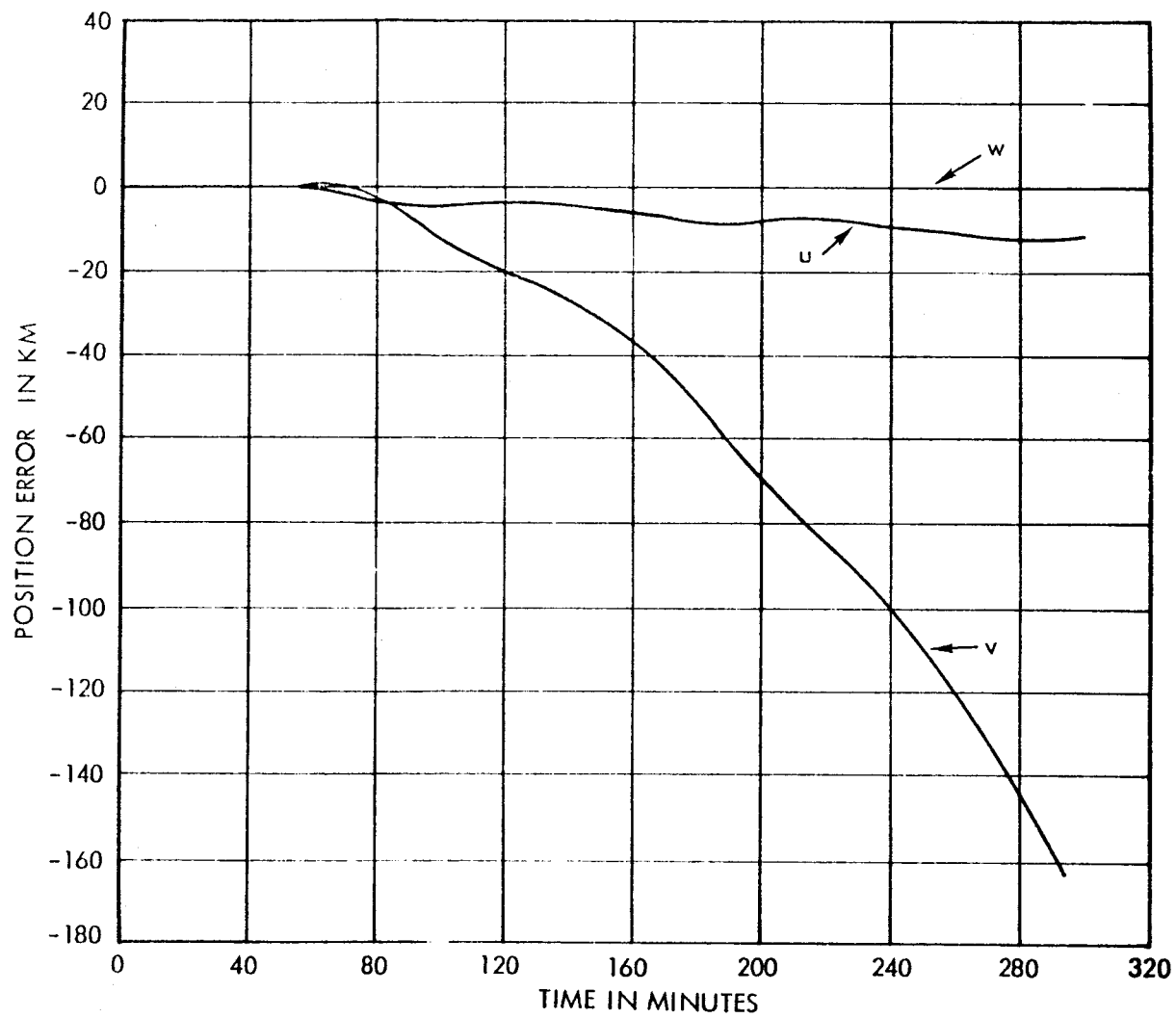


Figure 2.2.1-5. v Effect of u, v, w Thrusts, 50-Minute Periodic, 200 km Circular Orbit Integrated

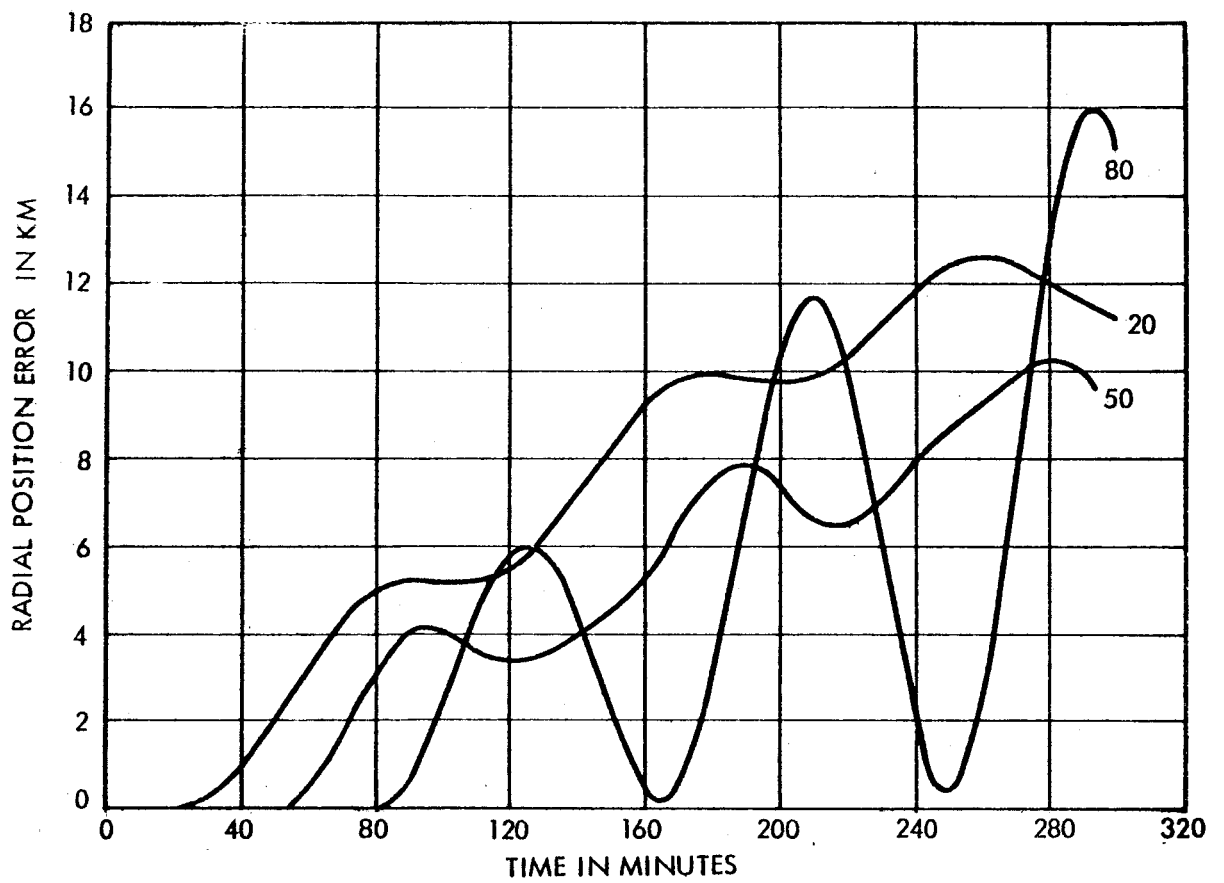


Figure 2.2.1-6. u Effect of v Thrusts, 20-, 50-, 80-Minute Periodic, 200 km Circular Orbits

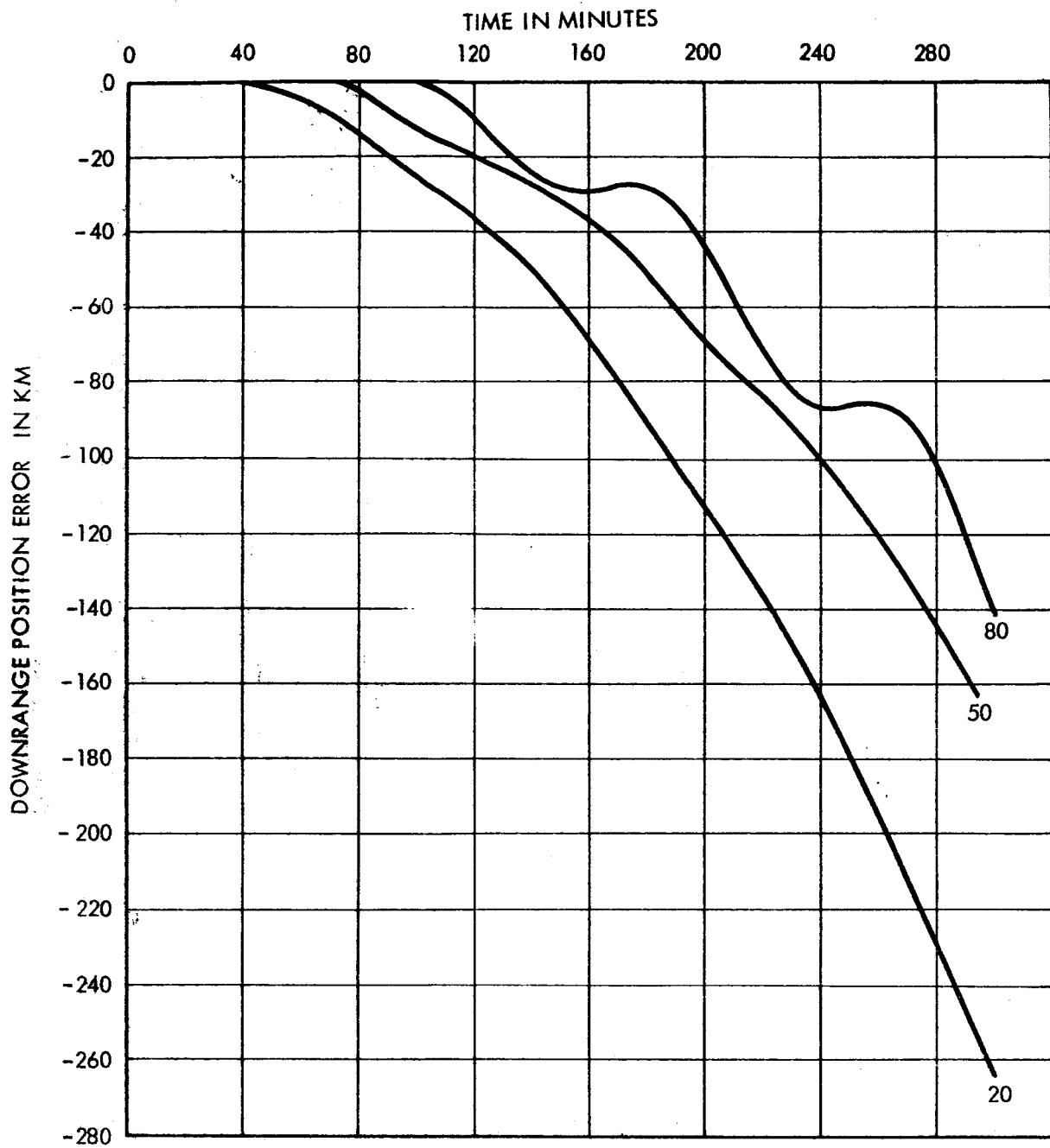


Figure 2.2.1-7. ν Effect of ν Thrusts, 20-, 50-, 80-Minute Periodic, 2 km Circular Orbits

Analytic. The effects of intermittent venting can be approximated by considering the sum of the effects of a series of velocity impulses. The response to each impulse can be calculated from the equations given previously with the velocity components as initial conditions. Thus, for an impulse at time $t = 0$ the position effect is given by

$$\begin{bmatrix} u \\ v \\ w \end{bmatrix} = B \begin{bmatrix} \dot{u}_0 \\ \dot{v}_0 \\ \dot{w}_0 \end{bmatrix}$$

A more accurate formulation which takes into account the length of the acceleration pulse can be obtained by adding the effects of a fixed acceleration applied at $t = 0$ and its negative applied at $t = \tau$, where τ is the length of the pulse.

Thus

$$\begin{bmatrix} u(t) \\ v(t) \\ w(t) \end{bmatrix} = C(t) \begin{bmatrix} a_u \\ a_v \\ a_w \end{bmatrix} + C(t - \tau) \begin{bmatrix} a_u \\ a_v \\ a_w \end{bmatrix}; \quad t > \tau$$

or

$$\begin{bmatrix} u(t) \\ v(t) \\ w(t) \end{bmatrix} = [C(t) - C(t - \tau)] \begin{bmatrix} a_u \\ a_v \\ a_w \end{bmatrix}; \quad t > \tau$$

Performing the indicated subtraction yields the fact that

$$C(t) - C(t - \tau) \doteq \tau B(t - \frac{\tau}{2})$$

under the assumption that

$$\frac{2 \sin \frac{\omega \tau}{2}}{\omega \tau} \doteq 1$$

Only the periodic terms in B are in error if the above assumption is false, and the amplitudes of the actual periodic terms will always be less than or equal to the ones given in B. Therefore, the response to a venting pulse of length τ for $t > \tau$ can be safely approximated by an impulse occurring at $t = \tau/2$ if

$$\begin{bmatrix} \dot{u}(\frac{\tau}{2}) \\ \dot{v}(\frac{\tau}{2}) \\ \dot{w}(\frac{\tau}{2}) \end{bmatrix} = \tau \begin{bmatrix} a_u \\ a_v \\ a_w \end{bmatrix}$$

or

$$\begin{bmatrix} u(t) \\ v(t) \\ w(t) \end{bmatrix} \doteq B(t - \frac{\tau}{2}) \begin{bmatrix} \tau a_u \\ \tau a_v \\ \tau a_w \end{bmatrix} ; t > \tau$$

The effects of several venting pulses can be obtained by adding the separate effects with the appropriate shifts in time axes. When this done it becomes apparent that the periodic portions of response depend strongly on the interval between the pulses. For example, pulsing once per orbit causes the periodic terms to increase at a maximum rate, while pulsing twice per orbit alternately introduces and cancels periodic terms (assuming all pulses are in the same direction in orbit-plane coordinates).

2.2.2 Tracking Effects

The effects of intermittent venting on the prediction of earth orbits from tracking data were analyzed with the same procedure and tracking model used for continuous thrusts, and the results are presented in a similar manner.

The results of tracking a vehicle which vents at 50-minute intervals are shown in Figures 2.2.2-1 through 2.2.2-8 for various numbers of radar passes. Figure 2.2.2-9 summarizes the prediction error in the downrange direction. Just as for continuous thrust, the prediction error increases as more radar passes are used. It is best, therefore, to use only the latest pass as long as the random errors associated with it are small enough.

Since both the continuous thrust and the intermittent thrust results indicate that the best procedure is to use the last radar pass only, because of the systematic error effect, the effects of random data noise for one pass have been calculated and are presented in Figure 2.2.2-10. The curves show that the random effect is much less than the systematic effect for the particular tracking system used, and therefore, that the last pass only should be used for best results.

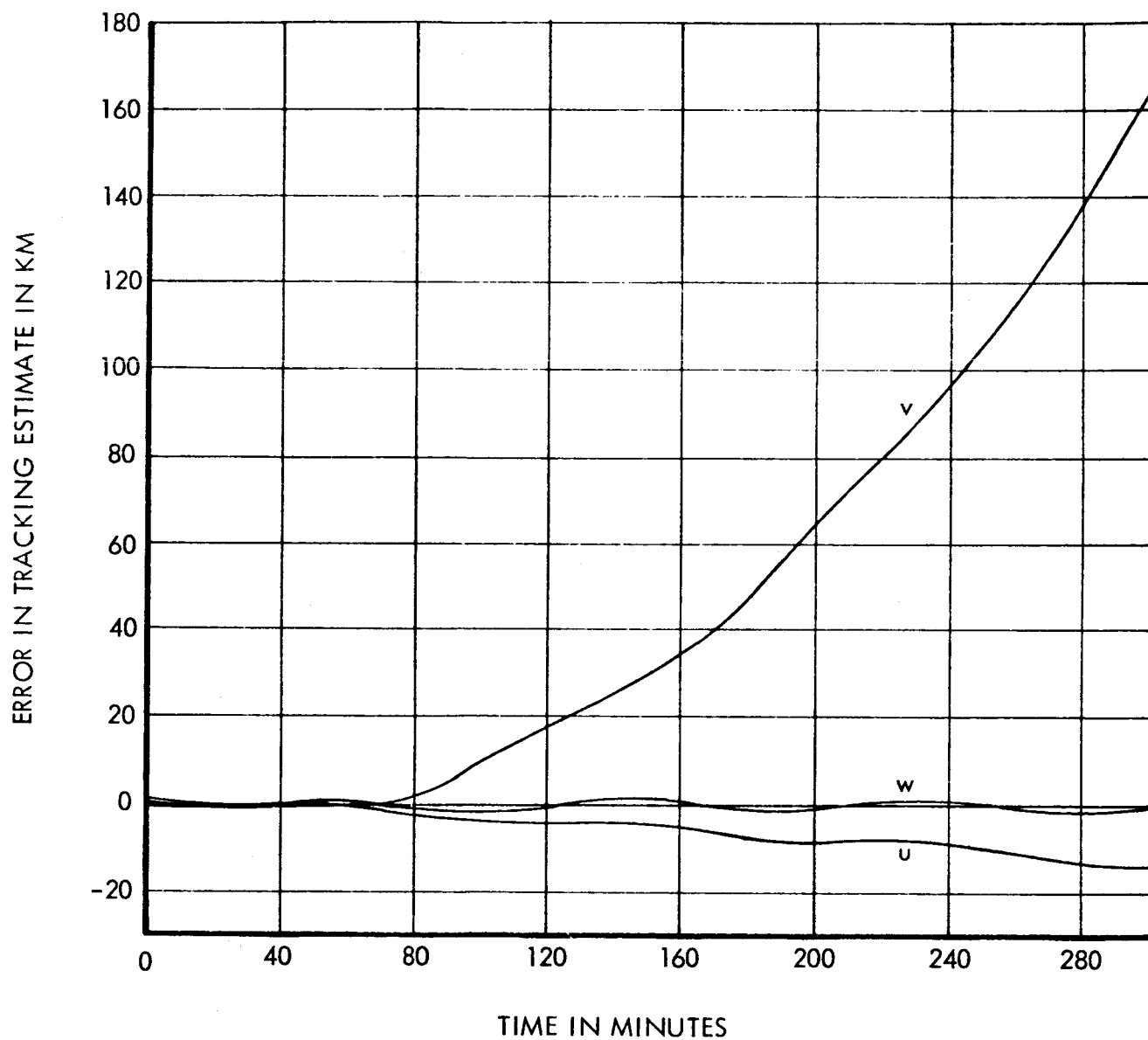


Figure 2.2.2-1. u, v, w Tracking Effect of v Thrust, 50-Minute Periodic, 200 km Circular Orbit, 3 Passes

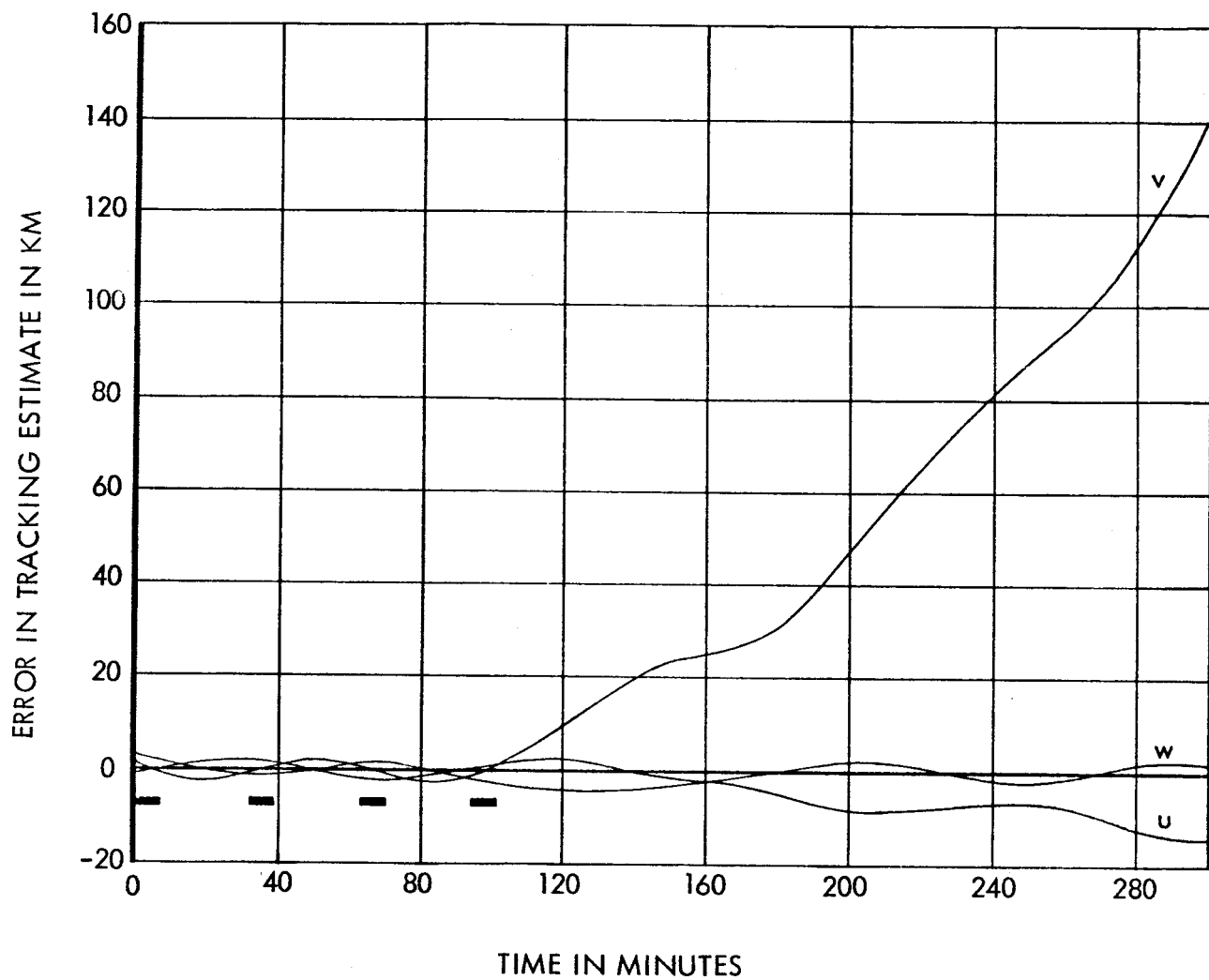


Figure 2.2.2-2. u, v, w Tracking Effects of v Thrust, 50-Minute Periodic, 200 km Circular Orbit, 4 Passes

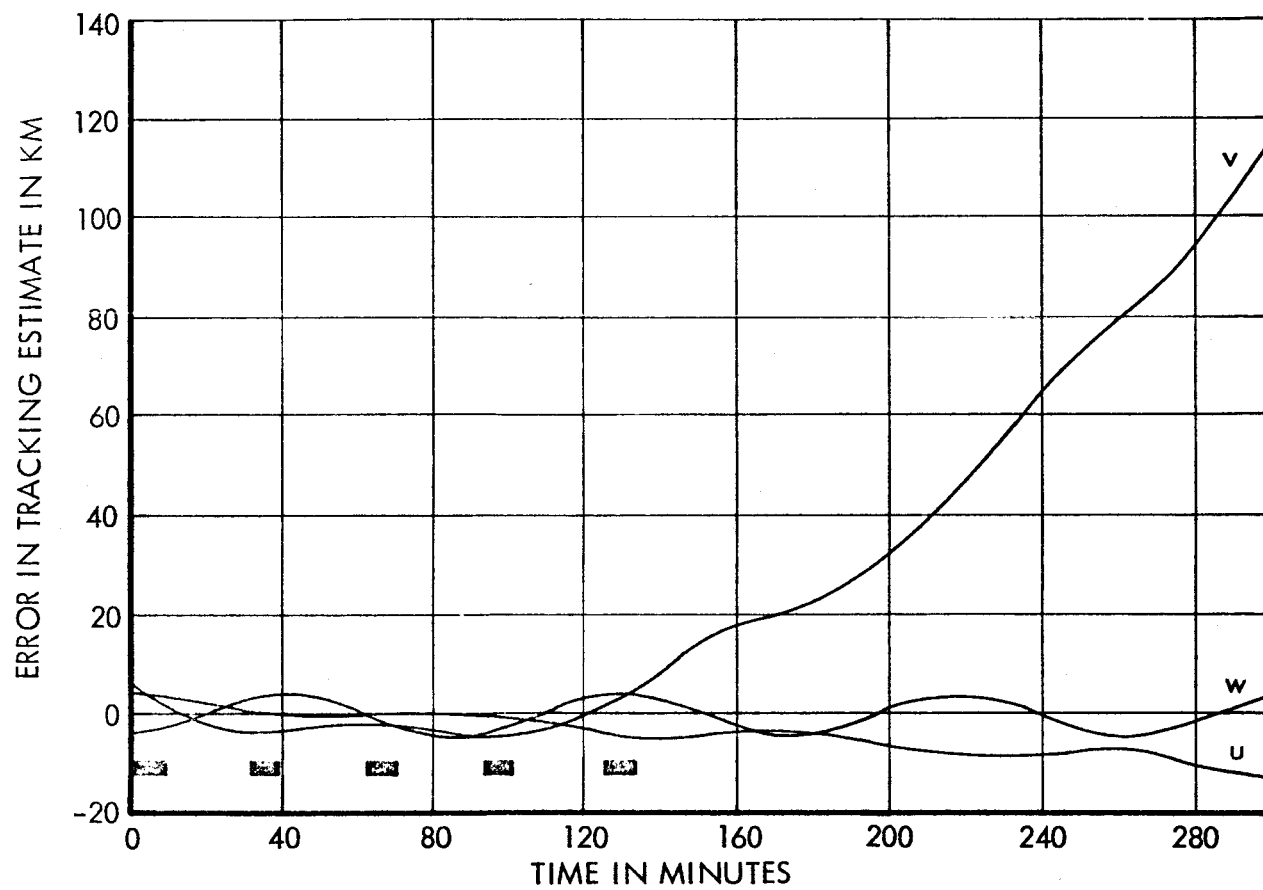


Figure 2.2.2-3. u, v, w Tracking Effect of v Thrust, 50-Minute Periodic, 200 km Circular Orbit, 5 Passes

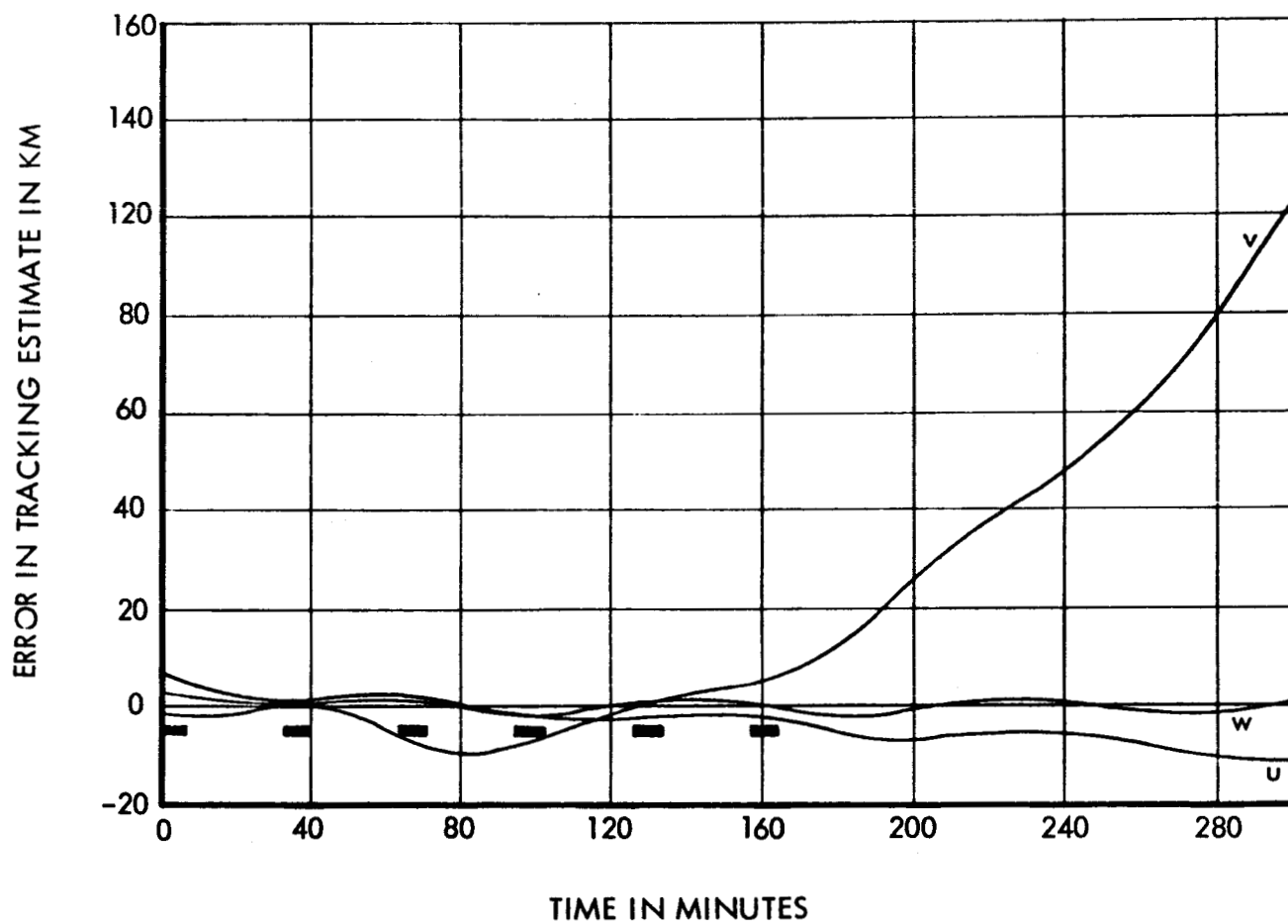


Figure 2.2.2-4. u, v, w Tracking Effects of v Thrusts, 50-Minute Periodic, 200 km Circular Orbit, 6 Passes

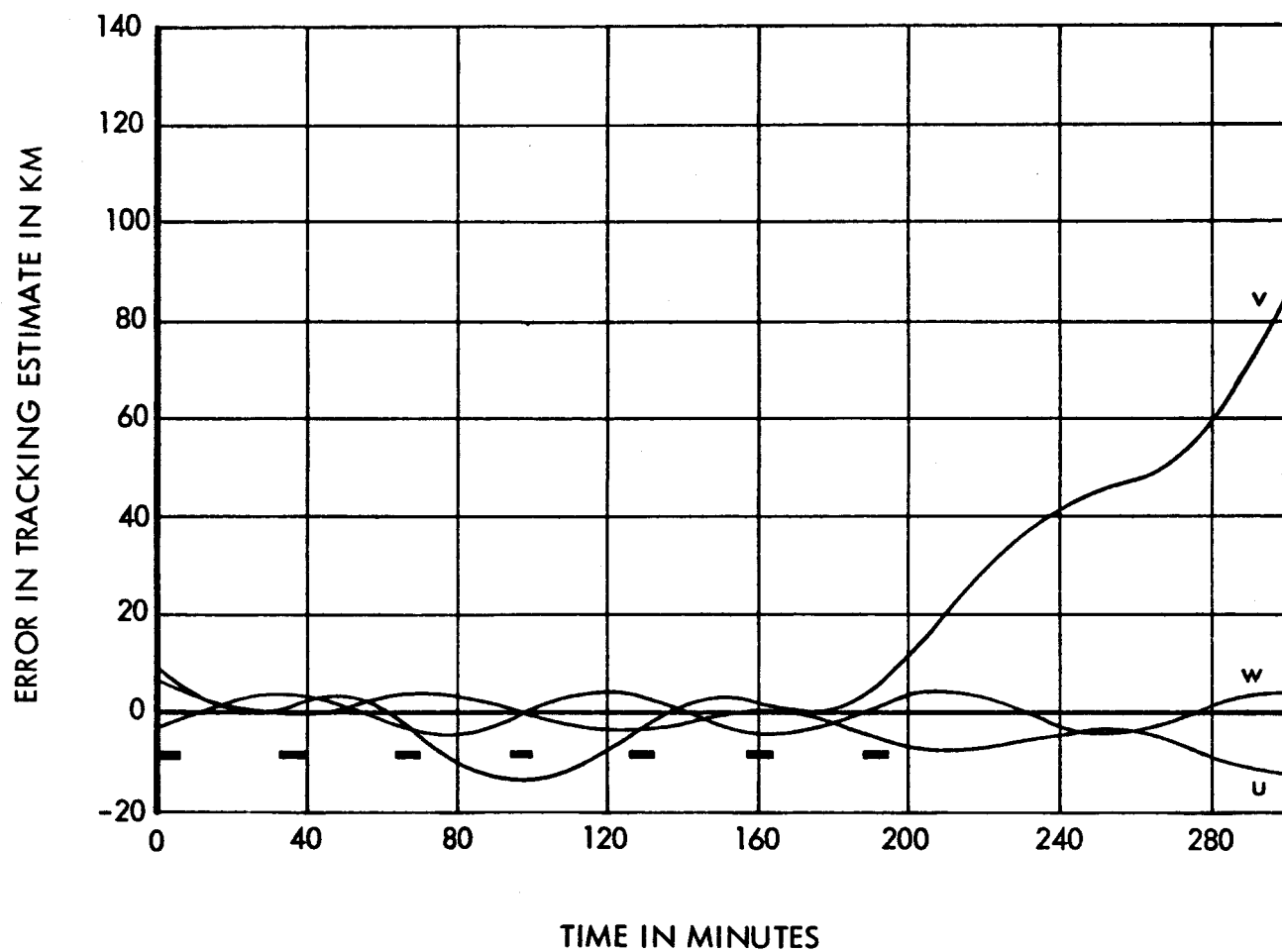


Figure 2.2.2-5. u, v, w Tracking Effect of v Thrust, 50-Minute Periodic, 200 km Circular Orbit, 7 Passes

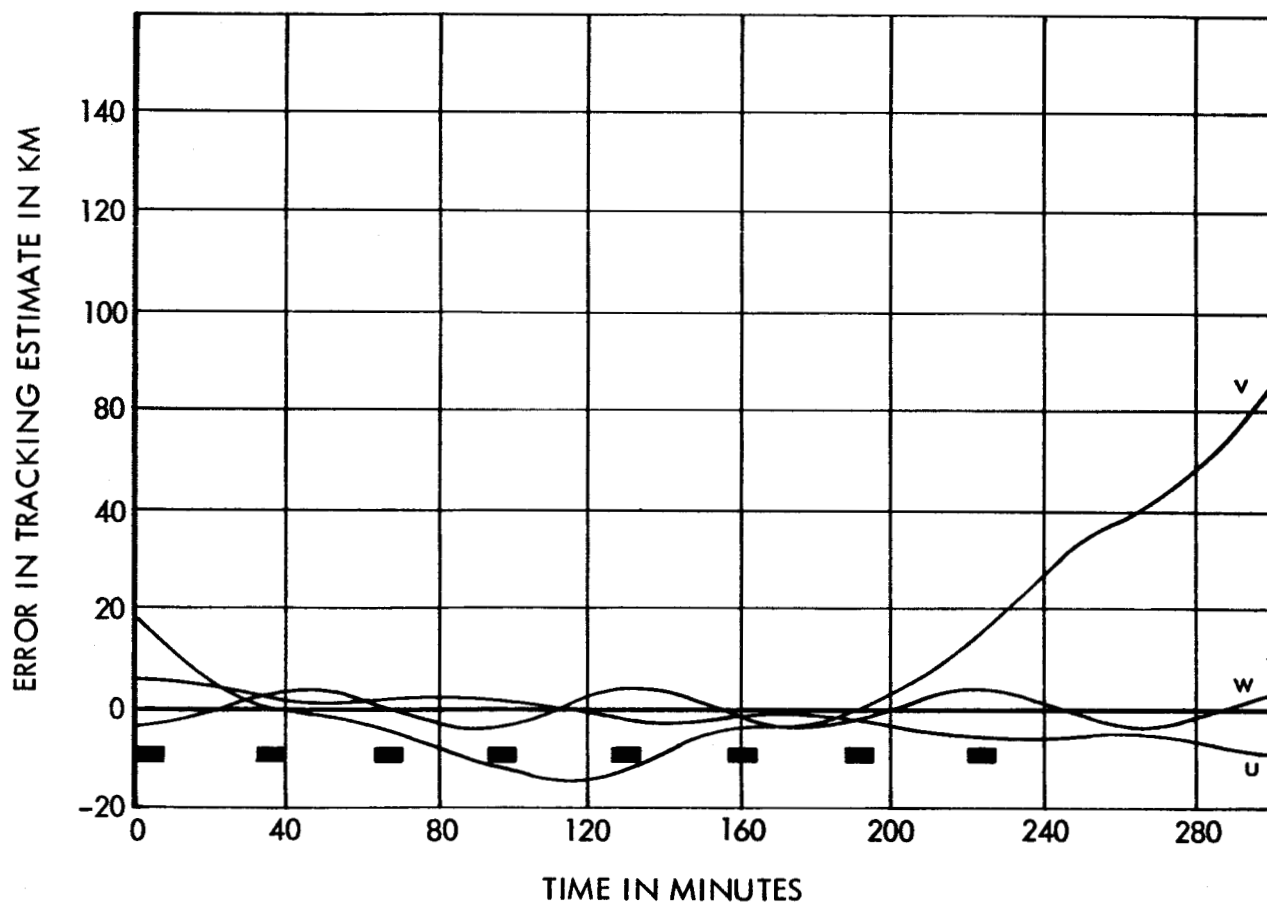


Figure 2.2.2-6. u, v, w Tracking Effect of v Thrust, 50-Minute Periodic, 200 km Circular Orbit, 8 Passes

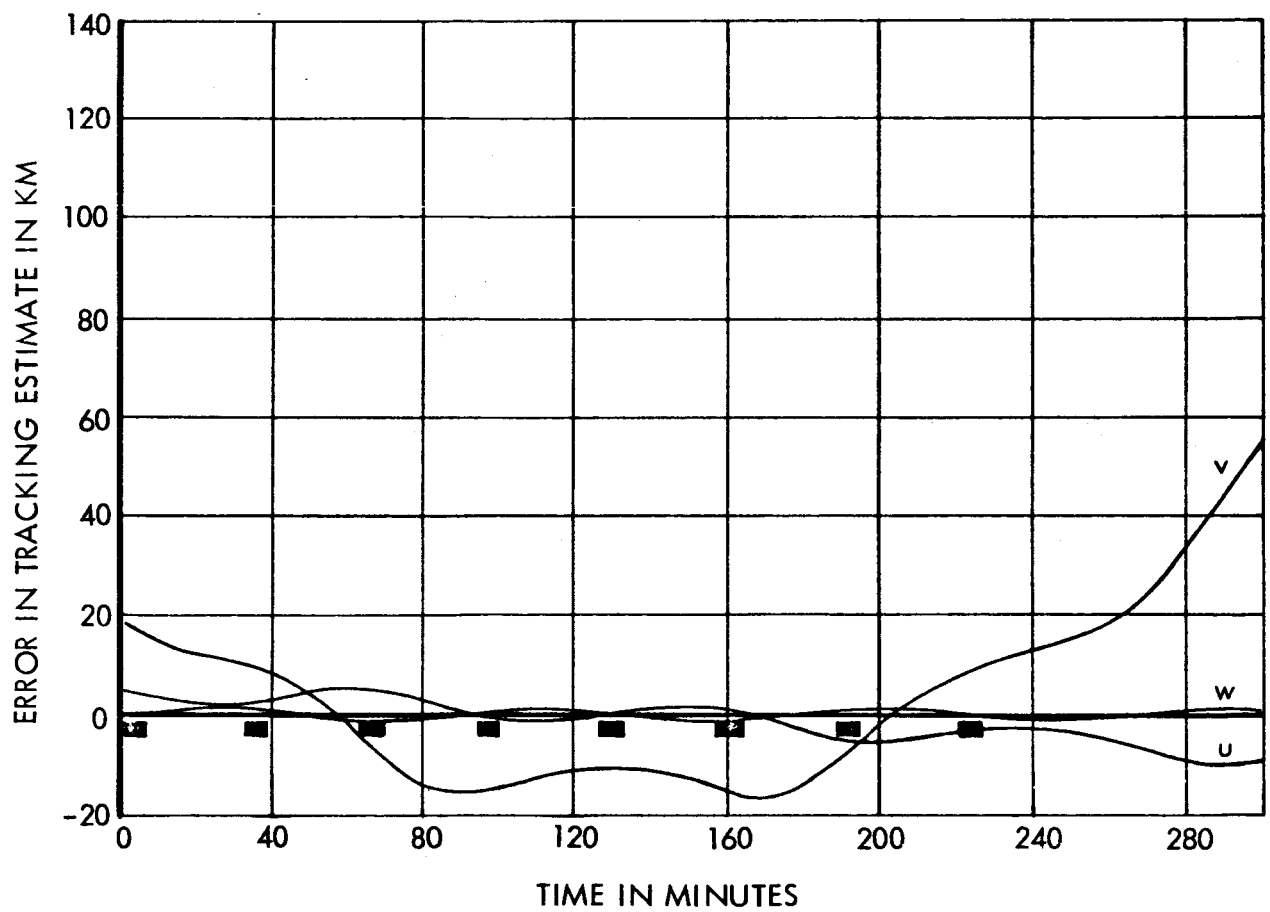


Figure 2.2.2-7. u, v, w Tracking Effects of v Thrust, 50-Minute Periodic, 200 km Circular Orbit, 9 Passes

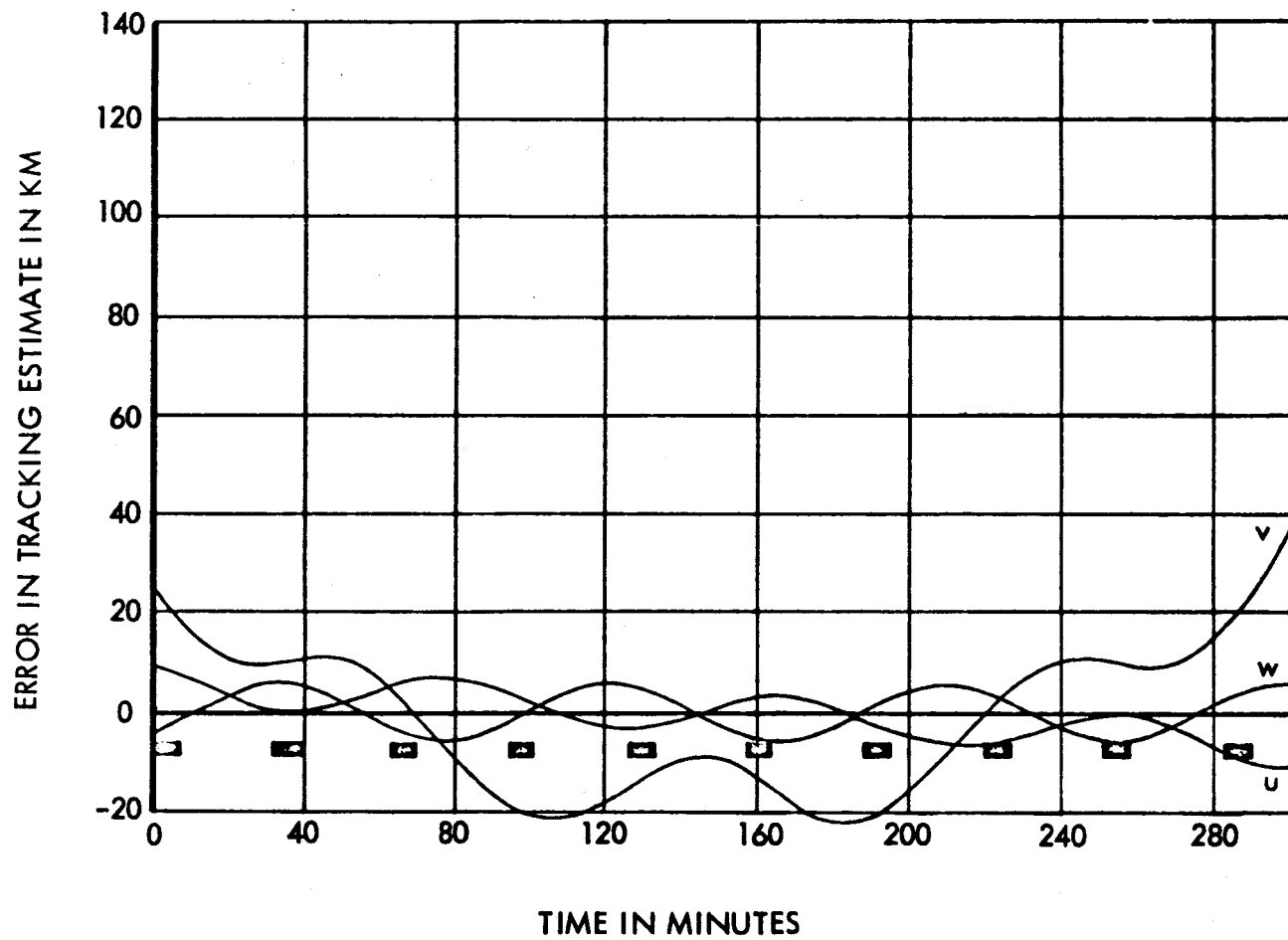


Figure 2.2.2-8. u, v, w Tracking Effects of v Thrust, 50-Minute Periodic, 200 km Circular Orbit, 10 Passes

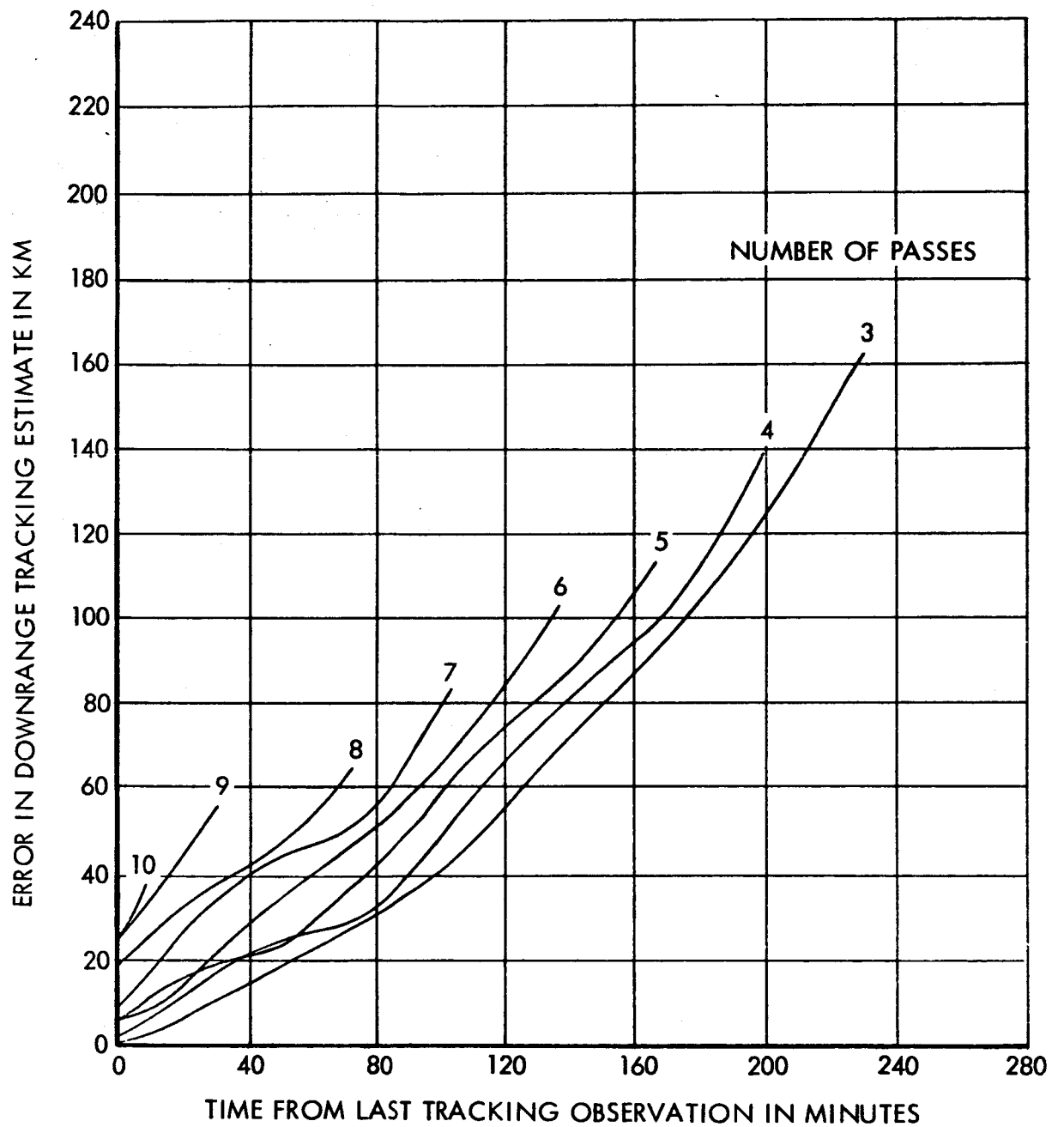


Figure 2.2.2-9. Tracking Prediction Error from 50-Minute Downrange Venting

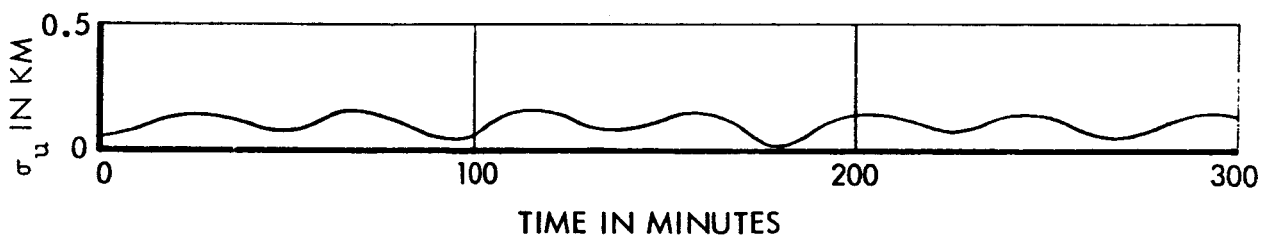
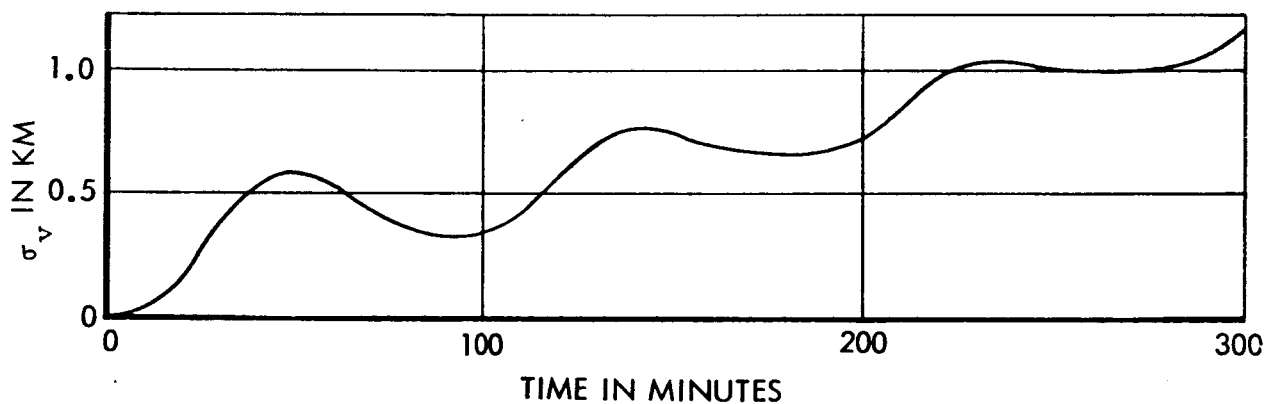
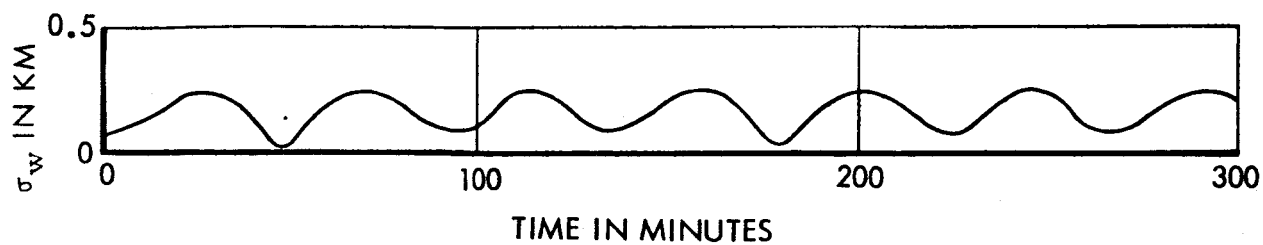


Figure 2.2.2-10. Tracking Prediction Errors from Random Data Noise for 1 Pass

2.2.3 Uncertainty Effects of Intermittent Venting

The uncertainty in the effects of venting stems from the fact that the heat input and the state of agitation of the hydrogen cannot be predicted precisely. As a result, the length of time required for each venting and the interval between ventings are not accurately known. If the venting is controlled by a valve which opens and closes at specified pressures, however, the average thrust during each vent can be predicted more accurately than the venting schedule. Therefore, it would be desirable to measure and telemeter the time of opening the vent valve and the length of time that it is kept open. These times along with the estimated average thrust could then be used in the trajectory calculation to lead to an improved trajectory prediction. The errors in the times and the thrust level would lead to uncertainties considerably smaller than would be obtained if venting were entirely neglected.

In order to evaluate the errors, the approximate formulation given in Section 2.2.1 can be used in a more general form.

$$\begin{bmatrix} u(t) \\ v(t) \\ w(t) \end{bmatrix} = B(t - t_i - \frac{\tau_i}{2}) \begin{bmatrix} \tau_i a_u \\ \tau_i a_v \\ \tau_i a_w \end{bmatrix}$$

The parameters which cause error are

- t_i = the time of initiation of the i^{th} vent
- a_u = the duration of the i^{th} vent
- a_v = the acceleration in the v direction
- a_w = the acceleration in the w direction

The total error is

$$\begin{bmatrix} \delta u(t) \\ \delta v(t) \\ \delta w(t) \end{bmatrix} = G \delta t_i + H \delta t_i + K \begin{bmatrix} \delta a_u \\ \delta a_v \\ \delta a_w \end{bmatrix}$$

where

$$G = \frac{\partial B}{\partial \tau_i} (t - t_i - \frac{\tau_i}{2}) \begin{bmatrix} \tau_i a_u \\ \tau_i a_v \\ \tau_i a_w \end{bmatrix}$$

$$H = \frac{\partial B}{\partial \tau_i} (t - t_i - \frac{\tau_i}{2}) \begin{bmatrix} \tau_i a_u \\ \tau_i a_v \\ \tau_i a_w \end{bmatrix} + B(t - t_i - \frac{\tau_i}{2}) \begin{bmatrix} a_u \\ a_v \\ a_w \end{bmatrix}$$

$$K = B(t - t_i - \frac{\tau_i}{2}) \begin{bmatrix} \tau_i & 0 & 0 \\ 0 & \tau_i & 0 \\ 0 & 0 & \tau_i \end{bmatrix}$$

$$\frac{\partial B}{\partial t_i} = - \frac{dB}{dt}$$

$$\frac{\partial B}{\partial \tau_i} = - \frac{1}{2} \frac{dB}{dt}$$

The elements of matrices B and dB/dt are given in Section 2.1.1.

The covariance matrix of position uncertainty is given by

$$\Lambda_R = G\sigma_t^2 G^T + H\sigma_\tau^2 H^T + K\Lambda_A K^T$$

assuming that the timing errors are independent of each other and of the acceleration errors. This would be the case if separate timers were used to measure t_i and τ_i . The use of separate timers is desirable, since the result is more sensitive to σ_τ than σ_t . A more accurate clock should be used to measure the short time τ_i than the long time t_i .

The uncertainties in the components of acceleration arise from the error in predicting the magnitude of the acceleration and from the errors in the knowledge of the orientation of the vehicle at the time of venting.

2.3 USE OF VENTING THRUSTS FOR CONTROL OF EARTH ORBITS

Since venting perturbs the trajectory in a way that is to some extent controllable, the possibility of making use of the venting to improve the orbit exists. At first it appears that the venting thrust could be used to counteract drag or other natural perturbations and produce an orbit which is better in some sense. Some of the possibilities and complications involved in this procedure are discussed in this section.

2.3.1 Possible Control Schemes

In order to eliminate the effects of natural perturbations at all times along the orbit, the venting thrust must produce an acceleration equal and opposite to the total perturbing acceleration. Since the venting is subject to some randomness, this total elimination of the effects of natural perturbations is impossible. Some less difficult goal, therefore, must be set.

The correction of in-plane position and velocity at some time is possible if two venting pulses occur long enough before the time in question. This is accomplished by adjusting the attitude of the vehicle and in-plane velocity in addition appropriately at the two venting times. The excess velocity available at each time is eliminated by orienting the thrust vector sufficiently out of the orbit plane. Since the out-of-plane components of velocity are random, out-of-plane errors are generated. The sensitivity of the orbit to out-of-plane thrusts is small, however, and these effects are negligible. In addition, the out-of-plane thrust direction can be chosen (from the two possibilities) to have its effect opposite to the natural perturbation effect.

The control of any two in-plane quantities can be accomplished with only one venting pulse. For example, downrange position and radial velocity can be controlled at the expense of possibly increasing radial position and downrange velocity errors. Once again, out-of-plane venting required to reduce the in-plane venting to the desired level causes small out-of-plane errors.

With one venting pulse it is also possible to minimize an arbitrary quadratic function of the position and velocity error components at the time of interest. For example, the position error (squared) or the velocity error (squared)

could be minimized. This procedure involves doing a weighted least-squares fit with the constraint that the magnitude of the venting impulse is fixed.

Two methods of venting which do not precisely control any variables, but offer the advantages of simplicity, consist of either always venting downrange to make maximum use of the energy available or always venting crossrange to minimize the total venting effects. Downrange venting normally would more than cancel atmospheric drag, while crossrange venting would essentially eliminate the need to consider the effects of venting.

2.3.2 Difficulties Involved

Orbit control with venting thrust requires control of the orientation of the venting thrust. If the desired thrust direction is fixed in orbit-plane coordinates or in inertial coordinates, no particular difficulties arise. The vehicle can simply be held in the desired orientation at all times. If, however, the orientation of the venting thrust must change with time, then two possibilities exist -- the thrust direction may be fixed relative to the vehicle, or the thrust direction may be variable relative to the vehicle. If it is fixed, the entire vehicle must be reoriented for each venting pulse. If the thrust is to be variable in direction relative to the vehicle, a more complicated system of ullage must be used in order to avoid venting liquid in addition to the gas. One way to accomplish this is to provide ullage and venting equipment in both directions along three axes. Venting in an arbitrary direction could then be approximated by venting sequentially with the proper components along the three axes.

The problems involved in controlling the directions of venting make crossrange venting attractive, since the crossrange direction is fixed in both inertial and orbit-plane coordinates. Therefore, the vehicle attitude could be held fixed in either system and crossrange venting could be accomplished. Since the total effects of crossrange venting are small, it would not even be necessary to vent in both directions.

2.4 EFFECTS OF CONTINUOUS LOW THRUST ON TRANSLUNAR TRAJECTORIES

The sensitivity of a translunar trajectory to a continuous low thrust depends on the particular trajectory and on the direction of the thrust. Consideration of possible combinations of trajectories and thrusts could lead to a large and expensive parametric study. Fortunately, a good estimate of the effect of a small continuous acceleration applied over the whole trajectory is given by the simple relationship

$$\delta b = \frac{1}{2} a t_f^2$$

where

δb = the change in impact parameter caused by the acceleration

a = the perturbing acceleration

t_f = the time of flight

In order to make acceleration due to gas leakage negligible, it would have to be kept to less than $10^{-8}g$. If this can not be done, it may be necessary to solve for the thrust from tracking data so that its effect can be included in the calculation of midcourse corrections. The analysis of the accuracy attainable, however, is beyond the scope of this study.

2.5 EFFECTS OF INTERMITTENT VENTING ON TRANSLUNAR TRAJECTORIES

As for continuous thrust, a large parametric study of the effects of intermittent venting could be made. However, useful results may be obtained by considering a sample. For a particular 72-hour trajectory the maximum sensitivity of impact-parameter miss to velocity at injection is about 600 km per m/sec. At four hours after injection it is about 300 km per m/sec. A typical venting impulse of 1.5 m/sec in this interval would give from 450 km to 900 km miss, if no midcourse corrections were made subsequently. The midcourse correction velocity required to eliminate the venting effect depends on the time of making the correction. During the first four hours the midcourse sensitivity drops by about a factor of two. After that time it is roughly proportional to the time remaining before lunar arrival. If a correction were made as late as the halfway time, the midcourse velocity required could only be about four times as large as the venting impulse.

The effects of venting can be minimized by orienting the venting thrust in the least sensitive direction. If only impact parameter miss (two-dimensional) is important, the effect can be eliminated nominally, but if a three-dimensional miss is used, the effect can only be reduced.

The time of initiation and the duration of each venting can be telemetered and used to reduce the error in the tracking estimate just as for earth orbits. Of course, this does not reduce the amount of midcourse velocity required to remove the venting effect, but it does allow it to be commanded more accurately.

3. EFFECTS OF NATURAL PERTURBATIONS

Perturbing accelerations and physical model uncertainties in parking orbits and lunar transit trajectories are analyzed. Perturbations considered result from the following sources:

1. Point mass Moon, Sun, Jupiter
2. Aspherical Earth ($J_2, J_3, J_4, J_{2,2}$)
3. Aspherical Moon (A, B, C)
4. Earth atmosphere
5. Solar radiation

Uncertainties in the following physical constants are considered as they affect the accuracy of prediction of the vehicle's trajectory:

1. Gravitational constant of the Earth (μ)
2. Coefficients of zonal harmonics of Earth (J_2, J_3, J_4)
3. Mass ratio of Moon to Earth (M)
4. Atmospheric density and/or drag parameter ($\rho_A, W/C_d A$)
5. Aspherical Moon (A, B, C)

Notation, nominal values of constants, and uncertainties are detailed in Section 11.

A preliminary analytic study is made in Section 2 of the limiting magnitude of the perturbing accelerations, both in laboratory units (km, sec) and in ratios to central acceleration. The results of this portion of the study may be used for a rough general analysis of perturbation magnitudes for any satellite or cislunar trajectory. These numerical results allow the elimination of several perturbation sources and/or uncertainties from the physical models for parking and transit trajectories in Section 3.

Several variant trajectories are integrated in Section 3 to predict errors resulting from neglect or uncertainty of perturbing accelerations. Resulting error in position and velocity vectors is computed for the parking orbit and error in miss parameters for the transit trajectory. The following specific trajectories are considered, where h is altitude above spheroid and $a, e, M_0, i, \Omega, \omega$ are classical elements.

a. Nearly circular parking orbit

$$\begin{aligned} a &= 6561 \text{ km} & i &= 28^{\circ}.5 \\ e &= 0.00039 & \Omega &= 193^{\circ} \\ M_o &= 330^{\circ} & \omega &= 142^{\circ} \\ t_o &= 1967 \text{ Jan } 7 & 178 < h < 185 \text{ km} \end{aligned}$$

b. Elliptic parking orbit

$$\begin{aligned} a &= 6803 \text{ km} & i &= 28^{\circ}.5 \\ e &= 0.0404 & \Omega &= 193^{\circ} \\ M_o &= 330^{\circ} & \omega &= 250^{\circ} \\ t_o &= 1967 \text{ Jan } 7 & 150 < h < 700 \text{ km} \end{aligned}$$

c. 72 hours transit, Sun and Moon aligned

d. 72 hours transit, Sun 80° from Moon

e. 92 hours transit, Sun 90° from Moon

In Section 4 the results of the analytic and numerical studies are used to recommend which perturbations should be included in the parking and transit trajectory models, and which uncertainties will produce detectable prediction errors.

3.1 NOMINAL VALUES

The following nominal values and probable errors will be used for the physical constants of the problem:*

$$\begin{aligned} \mu &= 3.986032 \times 10^5 \text{ km}^3/\text{sec}^2 && \text{gravitational constant for Earth (=GE)} \\ &\pm 0.000010 \times 10^5 \text{ km}^3/\text{sec} \\ a_e &= 6378.165 \text{ km} && \text{equatorial radius of Earth} \\ &\pm 0.006 \text{ km} \\ J_2 &= 1082.30 \times 10^{-6} && \text{Earth zonal harmonic coefficients} \\ &\pm 0.13 \times 10^{-6} && (J_2 = 2/3 J, \quad J_3 = 2/5 H, \quad J_4 = 35/8 D \\ &&& \text{in Jeffreys' notation}) \end{aligned}$$

* Nominal values are those for APOLLO (Reference 1) and probable errors are those of References 2 and 3. Probable error (pe) is the deviation from a simple mean of a distribution corresponding to a 50% probability of the true mean lying within 1 pe.

$$J_3 = \begin{array}{l} -2.30 \times 10^{-6} \\ \pm 0.05 \times 10^{-6} \end{array}$$

$$J_4 = \begin{array}{l} -1.8 \times 10^{-6} \\ \pm 0.3 \times 10^{-6} \end{array}$$

$$S = \begin{array}{l} 332,951.3 \\ \pm 5.0 \end{array}$$

mass of Sun/mass of Earth

$$J = \begin{array}{l} 317.88 \\ \pm 0.03 \end{array}$$

mass of Jupiter/mass of Earth

$$M = 1/(81.3015 \pm 0.0010)$$

mass of Moon/mass of Earth

$$R = \begin{array}{l} 1738.09 \text{ km} \\ \pm 0.12 \text{ km} \end{array}$$

mean radius of Moon

coefficients of lunar potential:

$$\frac{3C}{2MR^2} = g = \begin{array}{l} 0.60 \\ \pm 0.10 \end{array}$$

$$A = 8.8782 \times 10^{28} \text{ kg-km}^2$$

$$\frac{B-A}{C} = \gamma = +0.000203$$

$$B = 8.8800 \times 10^{28} \text{ kg-km}^2$$

$$\frac{C-A}{C} = \beta = +0.000619$$

$$C = 8.8837 \times 10^{28} \text{ kg-km}^2$$

The above values for the lunar potential correspond to

$$J = 0.0003109$$

$$L = 0.0000608$$

in the APOLLO recommended form of the lunar potential.

The potential functions actually used for the Earth and Moon are as follows:

$$\begin{aligned} \Phi_E = \frac{\mu}{r} & \left[1 + \frac{1}{2} J_2 \left(\frac{a_e}{r} \right)^2 (1 - 3 \sin^2 \delta) + \frac{1}{2} J_3 \left(\frac{a_e}{r} \right)^3 (3 \sin \delta - 5 \sin^3 \delta) \right. \\ & \left. - \frac{1}{8} J_4 \left(\frac{a_e}{r} \right)^4 (3 - 30 \sin^2 \delta + 35 \sin^4 \delta) \right] \end{aligned}$$

$$\begin{aligned}\Phi_M &= \frac{\mu M}{r} \left[1 + \frac{g}{3} \left(\frac{R}{r} \right)^2 \left\{ \gamma \left(1 - 3 \left(\frac{y}{r} \right)^2 \right) + \beta \left(1 - 3 \left(\frac{z}{r} \right)^2 \right) \right\} \right] \\ &= \frac{\mu M}{r} \left[1 + \frac{C}{2MR^2} \left(\frac{R}{r} \right)^2 \left\{ \frac{B-A}{C} \left(1 - 3 \left(\frac{y}{r} \right)^2 \right) + \frac{C-A}{C} \left(1 - 3 \left(\frac{z}{r} \right)^2 \right) \right\} \right]\end{aligned}$$

The above form of Φ_M is exactly equivalent to the APOLLO recommended form. For the Earth's atmosphere, the ARDC 1959 Standard Atmosphere is used. More accurate models, both static and dynamic, are available. This model is that used by the Interplanetary Search Program and is sufficiently accurate to indicate the gross magnitude of errors due to uncertainty in density.

3.2 ANALYTIC APPROXIMATIONS TO MAXIMUM PERTURBING ACCELERATIONS

To determine when certain of the perturbing accelerations on a vehicle may be ignored, it is necessary to set an upper limit on their magnitudes for various positions of the vehicle. For most of the perturbations, such a limit may be expressed as a function of distances from the central and disturbing bodies only. For perturbations due to asphericity of the Earth and Moon, the angular orientation to the equators also pertains.

3.2.1 Point Mass Moon, Sun, and Jupiter

During the geocentric phase these accelerations may be approximated by an expression in terms of

$$\begin{aligned}r &= \text{distance from vehicle to geocenter} \\ r_j &= \text{distance from } m_j \text{ to geocenter} \\ r_{2j} &= \text{distance from vehicle to } m_j\end{aligned}$$

(see Figure 3.2-1). The limiting case is taken for which geocenter, vehicle, and m_j are in a straight line. The acceleration a_j on the vehicle by object j is then

$$a_j = \mu m_j \left(\frac{1}{r_{2j}^2} - \frac{1}{r_j^2} \right) = \frac{\mu m_j}{r_j^2} \left(\frac{r_j^2}{r_{2j}^2} - 1 \right) \quad (2.1)$$

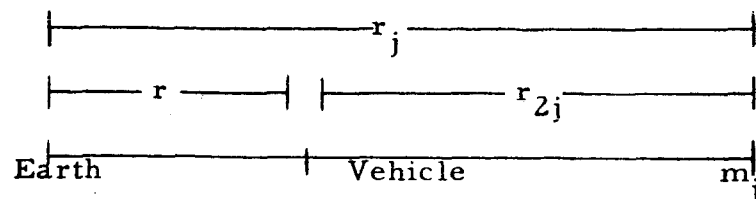


Figure 3.2-1. Perturbing Point Mass

Noting that $r_j = r + r_{2j}$, Equation (2.1) reduces to

$$a_j = \frac{\mu m_j}{r_j^2} \left[\frac{2r}{r_{2j}} + \left(\frac{r}{r_{2j}} \right)^2 \right] \quad (2.2)$$

For $r_{2j} \gg r$, the second term disappears, leaving

$$a_j = \frac{\mu m_j}{r_j^2} \left(\frac{2r}{r_{2j}} \right) \quad (2.3)$$

For r in km the following expressions yield maximum geocentric perturbing accelerations of Moon, Sun, and Jupiter in km/sec^2 :

$$a_M = 0.334 \times 10^{-7} \left[\frac{2r}{r_{2M}} + \left(\frac{r}{r_{2M}} \right)^2 \right]$$

$$a_S = 0.802 \times 10^{-13} r$$

$$a_J = 1.02 \times 10^{-18} r$$

Table 3.2-1 indicates the importance of the perturbing accelerations of Moon, Sun, and Jupiter relative to the central attraction of the Earth for the minimum distance of the disturbing body. It is apparent that the effect of Jupiter will be

negligible for any cislunar trajectory. Only for a high Earth satellite such as a synchronous would the cumulative effect amount to a significant perturbation, and special care would be required to prevent loss of the effect in roundoff in the integration.

Table 3.2-1. Geocentric n-Body Accelerations *

Geocentric Distance r (radii)	Altitude $h = r - 6378$ (km)	Central Acceleration a_o km/sec^2	Lunar Acceleration a_M km/sec^2	Solar Acceleration a_S km/sec^2	Jupiter Acceleration a_J km/sec^2
1.0	0	9.8×10^{-3}	1.14×10^{-9}	5.1×10^{-10}	6.5×10^{-15}
1.025	159	9.3×10^{-3}	1.17×10^{-9}	5.2×10^{-10}	6.7×10^{-15}
1.05	319	8.9×10^{-3}	1.19×10^{-9}	5.4×10^{-10}	6.8×10^{-15}
1.075	478	8.5×10^{-3}	1.22×10^{-9}	5.5×10^{-10}	7.0×10^{-15}
1.1	638	8.1×10^{-3}	1.25×10^{-9}	5.6×10^{-10}	7.1×10^{-15}
1.125	797	7.7×10^{-3}	1.28×10^{-9}	5.8×10^{-10}	7.3×10^{-15}
5.	-	3.9×10^{-4}	6.35×10^{-9}	2.6×10^{-9}	3.2×10^{-14}
10.	-	9.8×10^{-5}	1.47×10^{-8}	5.1×10^{-9}	6.5×10^{-14}
50.	-	3.9×10^{-6}	1.17×10^{-6}	2.6×10^{-8}	3.2×10^{-13}
60.	-	2.7×10^{-6}	-	3.1×10^{-8}	3.9×10^{-13}

* cf Figure 3.2-2

3.2.2 Earth Asphericity

The perturbing accelerations due to an aspherical Earth including zonal harmonics J_2 through J_4 are as follows (note that \underline{r} and δ are geocentric position vector and declination referred to true equator and equinox of date):

$$\frac{d^2 \underline{r}}{dt^2} = \nabla \Phi_2 + \nabla \Phi_3 + \nabla \Phi_4$$

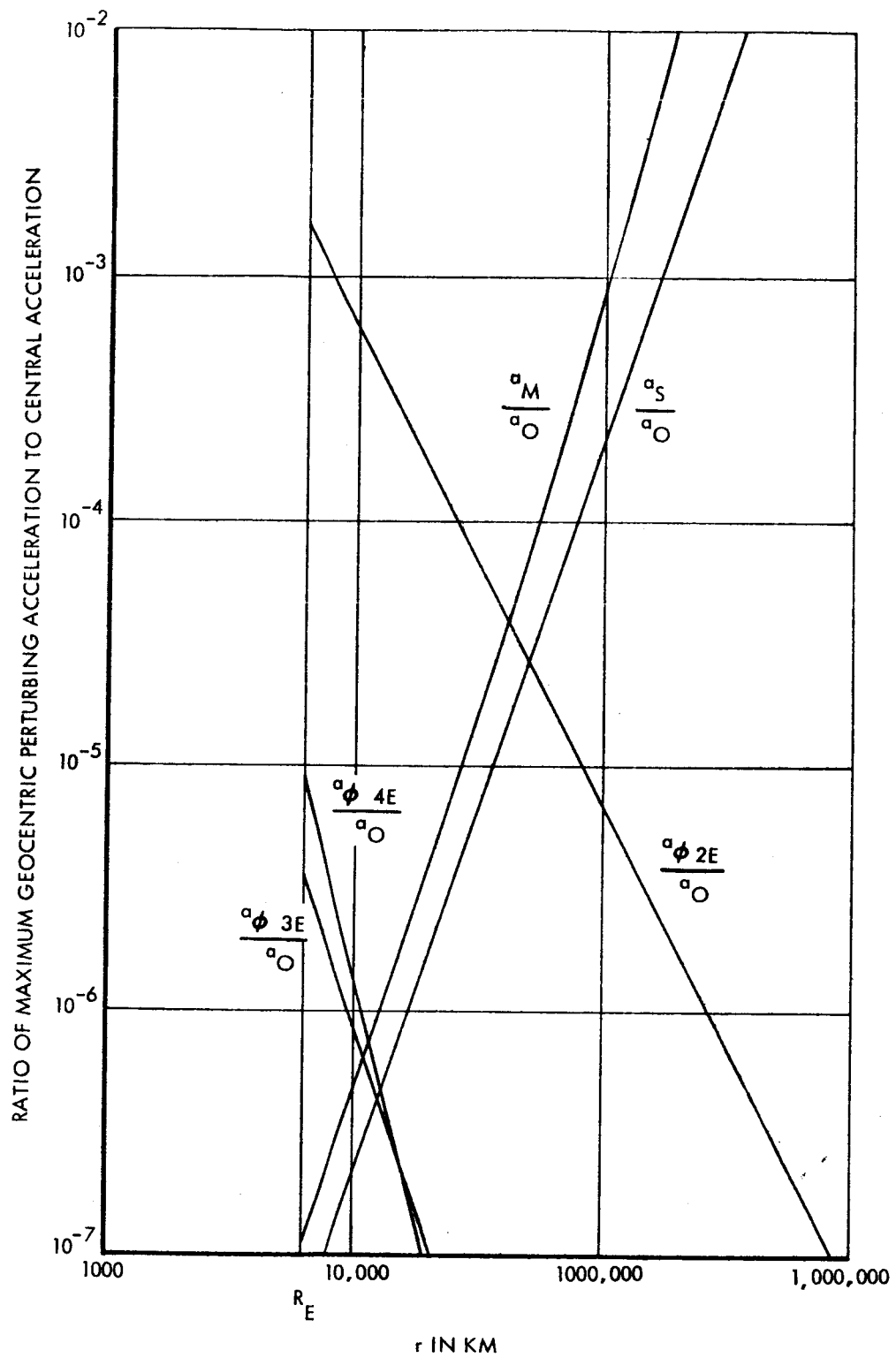


Figure 3.2-2. Maximum Geocentric Perturbing Accelerations versus Geocentric Distance

where

$$\nabla\Phi_2 = -\frac{\mu}{r^2} \left(\frac{3}{2}\right) J_2 \left(\frac{a_e}{r}\right)^2 \left[(1 - 5 \sin^2 \delta) \frac{r}{r} + 2 \sin \delta \underline{K} \right]$$

$$\nabla\Phi_3 = -\frac{\mu}{r^2} \left(\frac{1}{2}\right) J_3 \left(\frac{a_e}{r}\right)^3 \left[(15 \sin \delta - 35 \sin^3 \delta) \frac{r}{r} + (-3 + 15 \sin^2 \delta) \underline{K} \right]$$

$$\nabla\Phi_4 = -\frac{\mu}{r^2} \left(-\frac{5}{8}\right) J_4 \left(\frac{a_e}{r}\right)^4 \left[(3 - 42 \sin^2 \delta + 63 \sin^4 \delta) \frac{r}{r} + (12 \sin \delta - 28 \sin^3 \delta) \underline{K} \right]$$

The magnitudes of each of the above accelerations have been derived and may be written as follows:

$$a_{\Phi_2} = |\nabla\Phi_2| = \frac{\mu}{r^2} \left(\frac{3}{2}\right) J_2 \left(\frac{a_e}{r}\right)^2 \left[1 - 2 \sin^2 \delta + 9 \sin^4 \delta \right]^{\frac{1}{2}}$$

$$a_{\Phi_3} = |\nabla\Phi_3| = \frac{\mu}{r^2} \left(-\frac{1}{2}\right) J_3 \left(\frac{a_e}{r}\right)^3 \left[9 + 90 \sin^2 \delta - 495 \sin^4 \delta + 700 \sin^6 \delta \right]^{\frac{1}{2}}$$

$$a_{\Phi_4} = |\nabla\Phi_4| = \frac{\mu}{r^2} \left(-\frac{5}{8}\right) J_4 \left(\frac{a_e}{r}\right)^4 \left[9 - 36 \sin^2 \delta + 1194 \sin^4 \delta - 644 \sin^6 \delta + 441 \sin^8 \delta \right]^{\frac{1}{2}}$$

To obtain a quantitative feeling for the magnitude of these accelerations for the initial phases of a lunar mission, the following table has been computed assuming $\sin \delta = 1/2$, which would be approximately the maximum value for an orbit in or near the lunar orbit plane.

Table 3.2-2. Limiting Values for Aspherical Earth
Perturbations ($\sin \delta = 1/2$)*

Geocentric Distance r (radii)	Altitude ($r-6378$) (km)	Central Acceleration a_o km/sec ²	Relative Potential Accelerations		
			$\frac{a_{\Phi 2}}{a_o}$	$\frac{a_{\Phi 3}}{a_o}$	$\frac{a_{\Phi 4}}{a_o}$
1.0	0	9.8×10^{-3}	1.82×10^{-3}	3.89×10^{-6}	9.36×10^{-6}
1.025	159	9.3×10^{-3}	1.74×10^{-3}	3.61×10^{-6}	8.48×10^{-6}
1.05	319	8.9×10^{-3}	1.65×10^{-3}	3.45×10^{-6}	7.70×10^{-6}
1.10	638	8.1×10^{-3}	1.51×10^{-3}	2.92×10^{-6}	6.39×10^{-6}
1.125	797	7.7×10^{-3}	1.44×10^{-3}	2.73×10^{-6}	5.85×10^{-6}
5	-	3.9×10^{-4}	7.29×10^{-5}	3.11×10^{-8}	1.50×10^{-8}
10	-	9.8×10^{-5}	1.82×10^{-5}	3.89×10^{-9}	9.36×10^{-10}
50	-	3.9×10^{-6}	7.29×10^{-7}	3.11×10^{-11}	1.50×10^{-12}
60	-	2.7×10^{-6}	5.07×10^{-7}	1.80×10^{-11}	7.22×10^{-13}

* cf Figure 3.2-2

3.2.3 Lunar Asphericity and Selenocentric n-Body Accelerations

The acceleration on a lunar transit vehicle due to the lunar asphericity may be expressed as

$$\nabla \Phi_{2M} = \frac{\mu M}{r^2} \left(\frac{R}{r} \right)^2 g \left[\frac{\underline{r}}{r} \left\{ \gamma \left(1 - 5 \left(\frac{y}{r} \right)^2 \right) + \beta \left(1 - 5 \left(\frac{z}{r} \right)^2 \right) \right\} + 2 \gamma \underline{J} + 2 \beta \underline{K} \right]$$

where \underline{r} is position vector referred to the center of the Moon, R is lunar radius, and \underline{J} , \underline{K} are unit vectors along the y , z -axes. The relative magnitude of Φ_{2M} to the central attraction of the Moon would then be

$$\frac{a_{\Phi 2M}}{a_o} = \left(\frac{R}{r} \right)^2 g \beta S$$

where $S < 1.8$ from the following rough analysis, letting $z/r = 1$ (the worst case); and $\gamma/\beta = 0.33$ (cf Paragraph 1)

$$\underline{S} = \underline{K} \left[\frac{\gamma}{\beta} (1 - 0) + (1 - 5) \right] + 2 \frac{\gamma}{\beta} \underline{J} + 2 \underline{K}$$

$$S = |\underline{S}| = (-2 + \frac{\gamma}{\beta}) \underline{K} + 2 \frac{\gamma}{\beta} \underline{J}$$

$$S = \sqrt{4 - 4 \frac{\gamma}{\beta} + 5 \left(\frac{\gamma}{\beta} \right)^2}$$

$$S < 1.8$$

Hence

$$\frac{a_{\Phi 2M}}{a_o} < 1.8 g \beta \left(\frac{R}{r} \right)^2 = 0.00068 \left(\frac{R}{r} \right)^2$$

Expressions for point mass accelerations of Sun and Earth (a_S , a_E) are similar to those for the geocentric case (3.2.1) except r and r_j are measured from the Moon.

Table 3.2-3. Perturbations in Selenocentric Phase*

Seleno- centric Distance r	Altitude $h=r-1700$	Central Acceleration a_o	Earth Acceleration a_E	Solar Acceleration a_S	Relative Aspherical Moon Accel $\frac{a_{\Phi 2M}}{a_o}$	Aspherical Moon Acceleration $\frac{a_{\Phi 2M}}{a_o}$
(km)	(km)	km/sec ²	km/sec ²	km/sec ²		km/sec ²
1,700	0	1.7×10^{-3}	2.4×10^{-8}	1.4×10^{-10}	6.8×10^{-4}	1.2×10^{-6}
1,800	100	1.5×10^{-3}	2.5×10^{-8}	1.4×10^{-10}	6.3×10^{-4}	9.5×10^{-7}
1,900	200	1.3×10^{-3}	2.7×10^{-8}	1.5×10^{-10}	5.5×10^{-4}	7.2×10^{-7}
3,200	1,500	4.8×10^{-4}	4.6×10^{-8}	2.6×10^{-10}	2.0×10^{-4}	9.6×10^{-8}
6,400	4,700	1.2×10^{-4}	9.1×10^{-8}	5.1×10^{-10}	5.0×10^{-5}	6.0×10^{-9}
32,000	-	4.8×10^{-6}	4.5×10^{-7}	2.6×10^{-9}	2.0×10^{-6}	9.6×10^{-12}
64,000	-	1.2×10^{-6}	9.1×10^{-7}	5.1×10^{-9}	5.0×10^{-7}	6.0×10^{-13}

* cf Figure 3.2-3

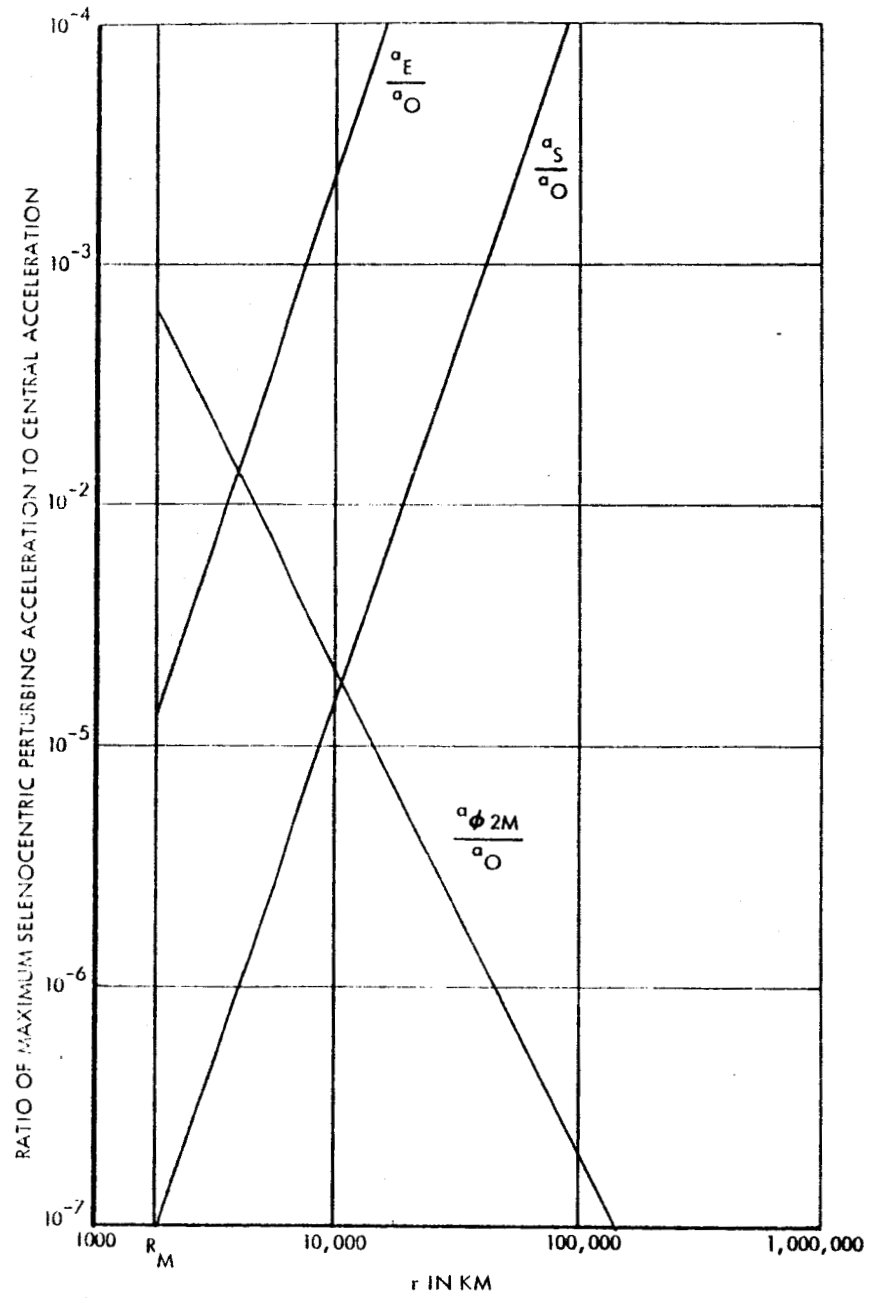


Figure 3.2-3. Maximum Selenocentric Perturbing Accelerations versus Selenocentric Distance

3.2.4 Earth Atmosphere

The acceleration due to the atmosphere of the Earth may be expressed as

$$a = \frac{\rho V^2 g_o}{2 W/C_d A}$$

where ρ is atmospheric density, V is velocity, g_o is acceleration of gravity at surface, and $W/C_d A$ is drag parameter. For the APOLLO parking orbit (1) and transit orbit (2) respectively

$$\frac{W_1}{C_d A} = 441 \frac{\text{lb}}{\text{ft}^2} = 5.51 \times 10^5 g_o \frac{\text{g}}{\text{m}^2}$$

$$\frac{W_2}{C_d A} = 113 \frac{\text{lb}}{\text{ft}^2} = 2.6 \times 10^6 g_o \frac{\text{g}}{\text{m}^2}$$

Hence for ρ in g/m^3 and V in km/s

$$a_1 = \frac{V^2 \rho}{4.32 \times 10^3} \frac{\text{km}}{\text{sec}^2}$$

$$a_2 = \frac{V^2 \rho}{1.012 \times 10^3} \frac{\text{km}}{\text{sec}^2}$$

To characterize the range of accelerations due to drag at various altitudes, the circular and parabolic velocities are used. The circular velocity is used to approximate the case for the parking orbit and the parabolic escape velocity approximates the early stages of the transit orbit.

Table 3.2-4. Atmospheric Perturbations

Geocentric Distance r (km)	Altitude h (km)	Density ρ g/m ²	Acceleration in Parking Orbit a ₁ km/sec ²	Acceleration in Transit a ₂ km/sec ²
6528	150	1.835 x 10 ⁻⁶	2.6 x 10 ⁻⁸	2.2 x 10 ⁻⁷
6538	160	2.258 x 10 ⁻⁶	1.6 x 10 ⁻⁸	1.4 x 10 ⁻⁷
6548	170	8.033 x 10 ⁻⁷	1.1 x 10 ⁻⁸	9.7 x 10 ⁻⁸
6568	190	4.345 x 10 ⁻⁷	6.1 x 10 ⁻⁹	5.2 x 10 ⁻⁸
6608	230	1.563 x 10 ⁻⁷	2.2 x 10 ⁻⁹	1.8 x 10 ⁻⁸
6678	300	3.583 x 10 ⁻⁸	5.0 x 10 ⁻¹⁰	4.2 x 10 ⁻⁹
6778	400	6.494 x 10 ⁻⁹	8.8 x 10 ⁻¹¹	7.5 x 10 ⁻¹⁰
6878	500	1.576 x 10 ⁻⁹	2.1 x 10 ⁻¹¹	1.8 x 10 ⁻¹⁰
6978	600	4.636 x 10 ⁻¹⁰	6.1 x 10 ⁻¹²	5.2 x 10 ⁻¹¹
7078	700	1.536 x 10 ⁻¹⁰	2.0 x 10 ⁻¹²	1.7 x 10 ⁻¹⁰

3.2.5 Solar Radiation

The acceleration due to radiation pressure* may be expressed as

$$a = \frac{A}{m} \frac{L_o}{4\pi r_o^2 c}$$

where at 1 au, the solar constant

$$\begin{aligned} \frac{L_o}{4\pi r_o^2} &= 2.00 \frac{\text{cal}}{\text{cm}^2 \text{min}} \\ &= 1.37 \times 10^6 \frac{\text{g}}{\text{sec}^3} \end{aligned}$$

and the velocity of light

$$c = 3.00 \times 10^5 \text{ km/sec}$$

* non-relativistic

For the parking orbit (1) and transit orbit (2) the area to weight ratios are

$$\frac{A}{W_1} = 1.053 \times 10^{-3} \frac{\text{ft}^2}{\text{lb}}$$

$$\frac{A}{W_2} = 4.10 \times 10^{-3} \frac{\text{ft}^2}{\text{lb}}$$

and area to mass ratios are

$$\frac{A}{m_1} = 2.31 \times 10^{-13} \frac{\text{km}^2}{\text{g}}$$

$$\frac{A}{m_2} = 9.00 \times 10^{-13} \frac{\text{km}^2}{\text{g}}$$

The accelerations due to solar radiation pressure are hence

$$a_1 = 1.053 \times 10^{-12} \text{ km/sec}^2$$

$$a_2 = 4.11 \times 10^{-12} \text{ km/sec}^2$$

For a 300-minute parking orbit, solar radiation pressure would produce a 1/2 meter change in position; for a 90-hour transit it would produce a 0.2 m change in position. In either case, the effect would be lost in the noise of numerical integration because of the small magnitude of the acceleration.

3.3 COMPUTER SIMULATION OF PERTURBATIONS

The Interplanetary Search Program is utilized to integrate parking orbit and transit orbit with nominal and perturbed values of physical constants. The results of the runs indicate what the prediction error would be if the true model

differed from the prediction model either by exclusion of a perturbing force or by a difference of 1 pe in the value of a physical constant.

3.3.1 Parking Orbit Perturbations

Error due to the following sources is considered:

- a. Drag uncertainty
- b. Geocentric gravitational constant uncertainty
- c. Neglect of third and fourth harmonics
- d. Uncertainty in third and fourth harmonics
- e. Uncertainty in second harmonic
- f. Neglect of luni-solar perturbations

Two parking orbits are considered:

- a. Nearly circular, altitude 180 km
- b. Elliptical, perigee altitude 150 km, apogee altitude 700 km

Integrations are performed for 300 minutes (about 3 orbits).

Figures 3.3-1 through 3.3-4 indicate errors in position and velocity for the two parking orbits for all error sources indicated above. The errors were computed by differencing position and velocity vectors of the varied orbit and the nominal orbit.

$$\Delta \underline{r} = \sqrt{(x - x_0)^2 + (y - y_0)^2 + (z - z_0)^2}$$

$$\Delta \underline{V} = \sqrt{(\dot{x} - \dot{x}_0)^2 + (\dot{y} - \dot{y}_0)^2 + (\dot{z} - \dot{z}_0)^2}$$

The varied orbits were produced as follows:

- a. $W/C_d A$ increased by a factor of 1.5
- b. μ increased from 398,603.20 to 398,603.68 km³/sec²
- c. J_3 and J_4 set to zero
- d. J_3 increased from -2.30×10^{-6} to -2.35×10^{-6}
and J_4 increased from -1.8×10^{-6} to -2.1×10^{-6}

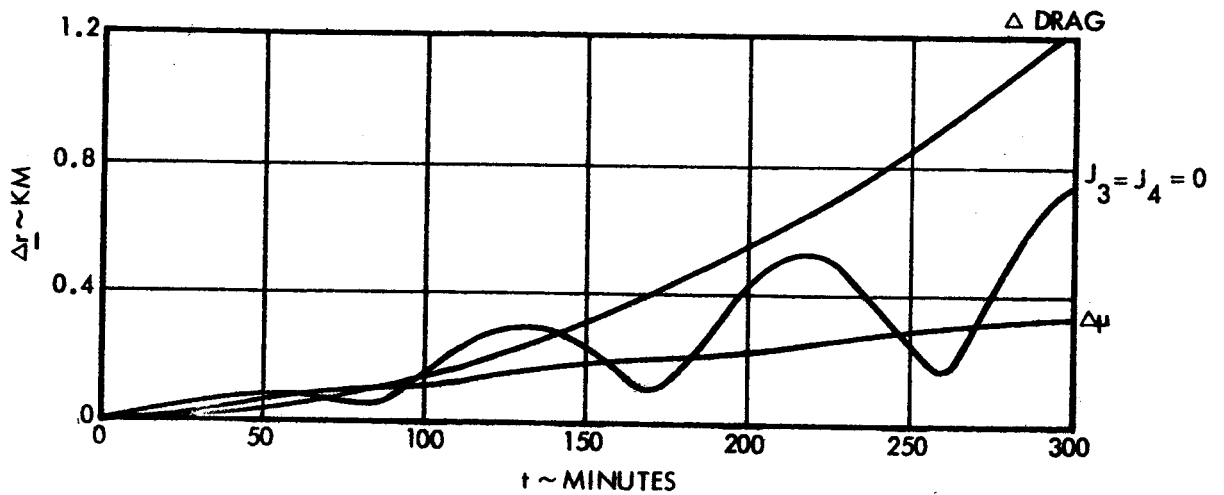
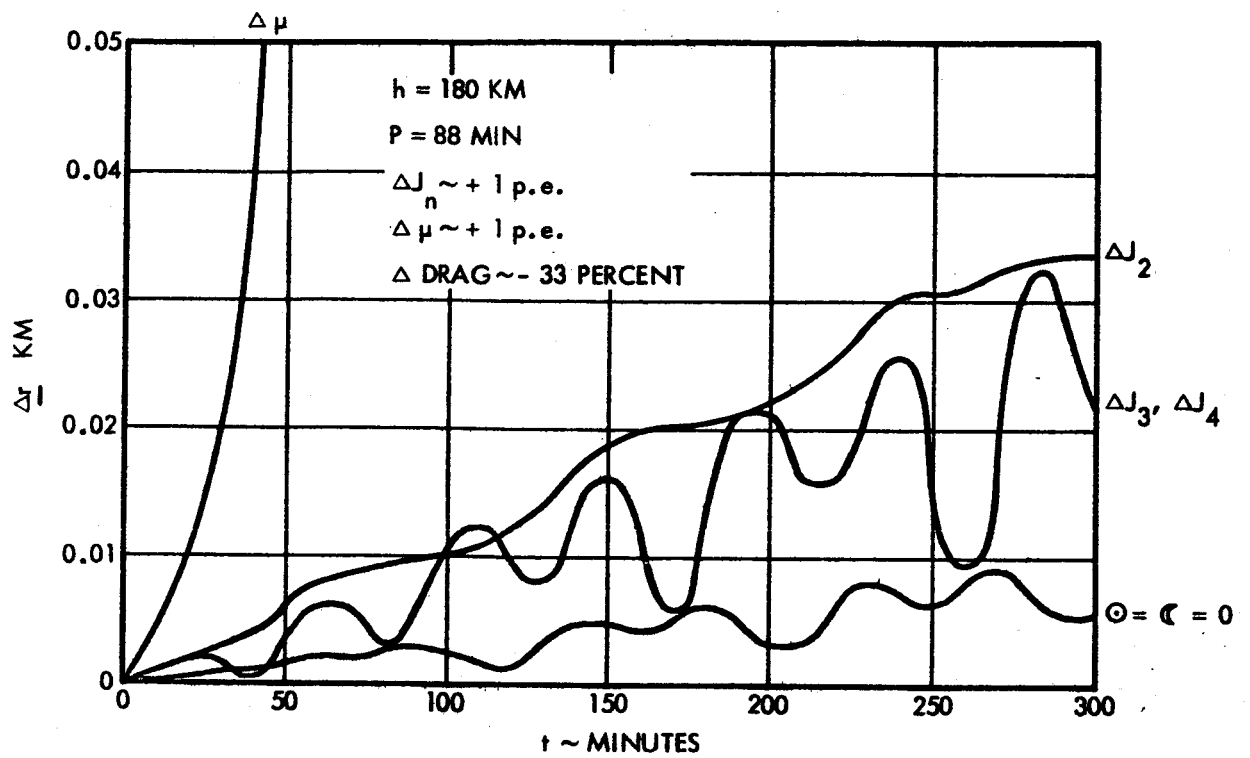


Figure 3.3-1. Circular Parking Orbit Position Prediction Error

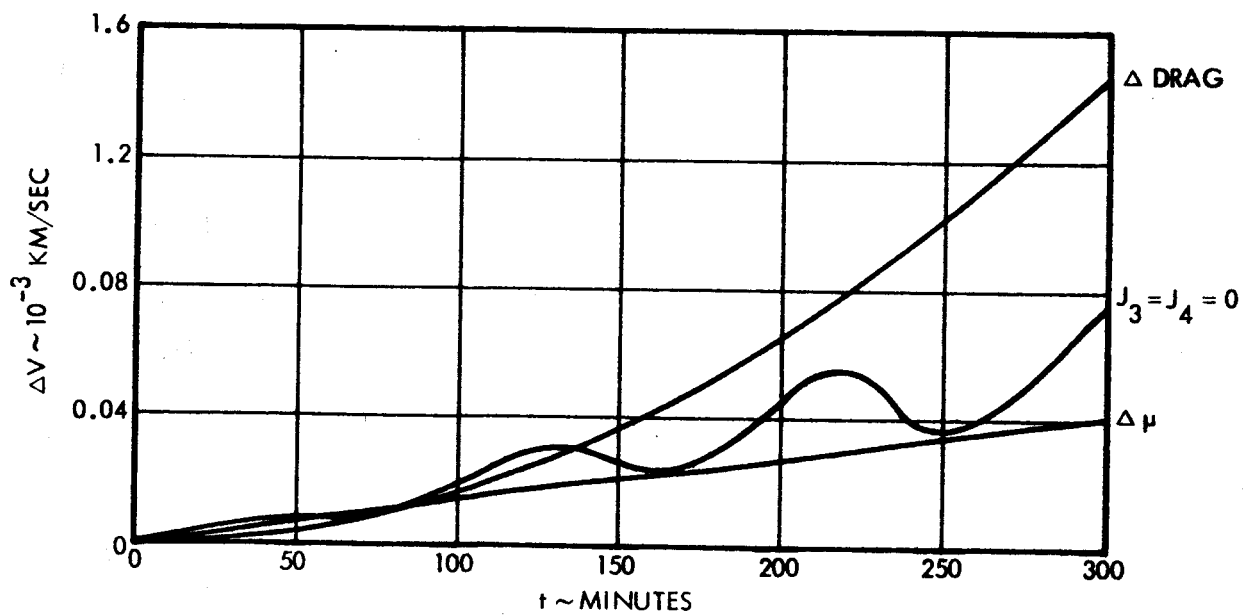
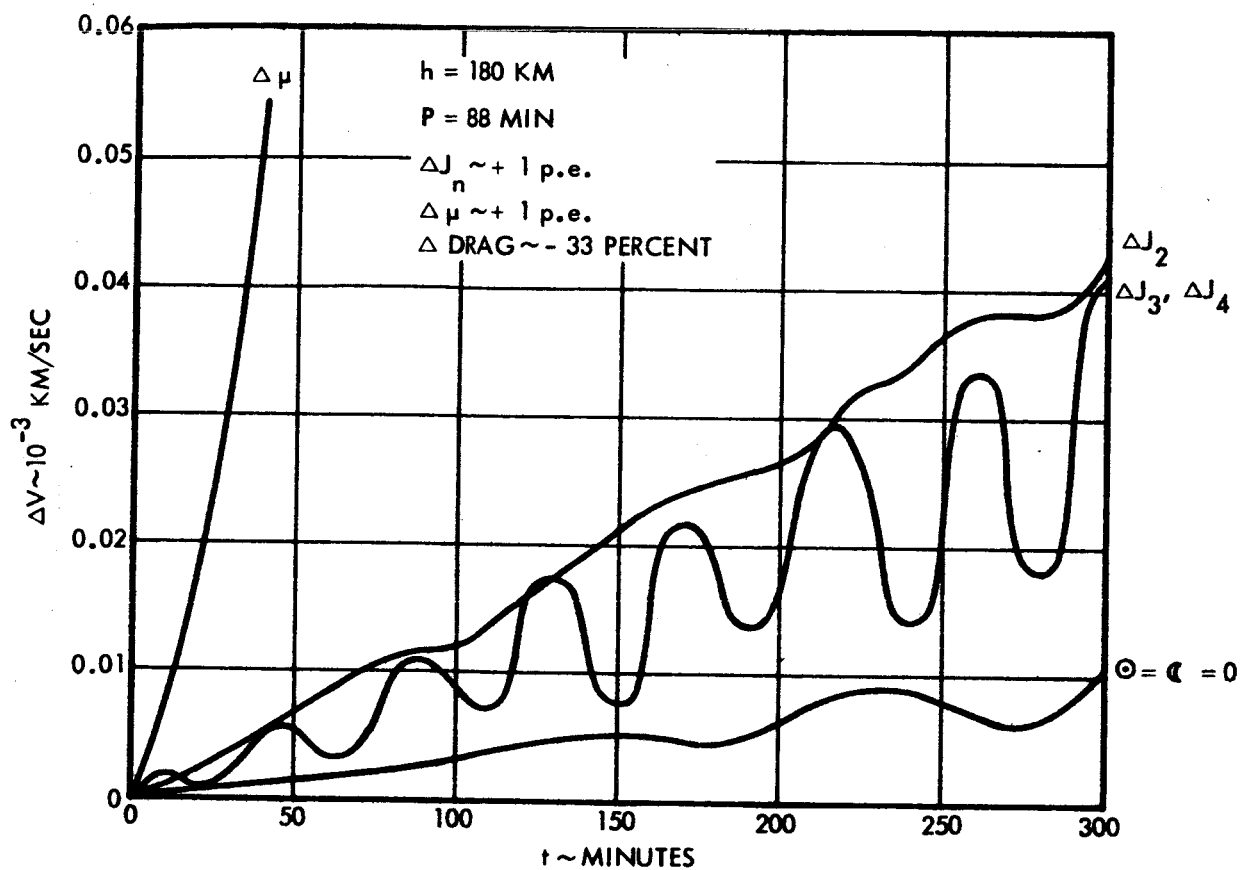


Figure 3.3-2. Circular Parking Orbit Velocity Prediction Error

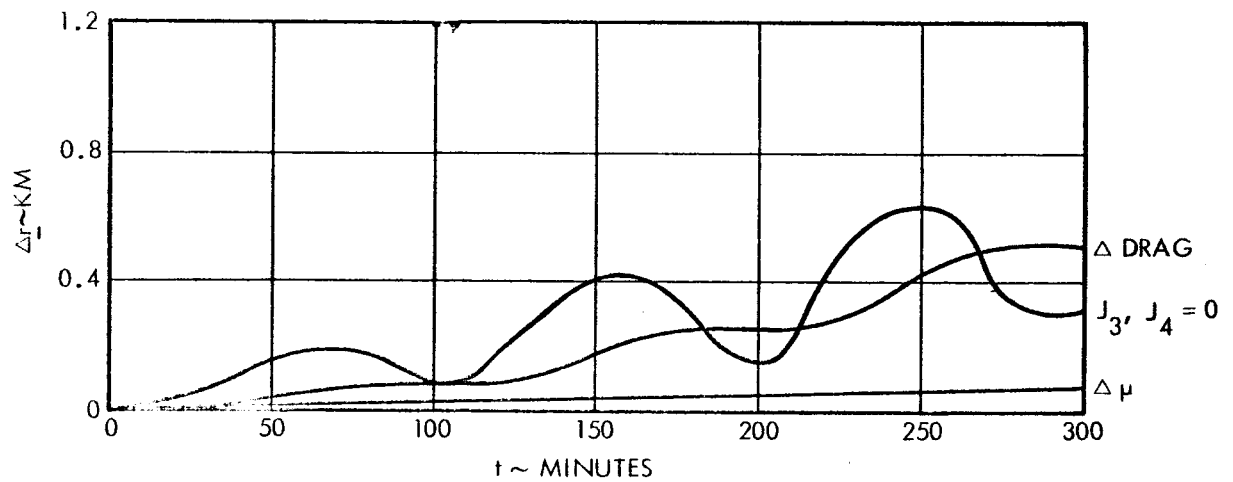
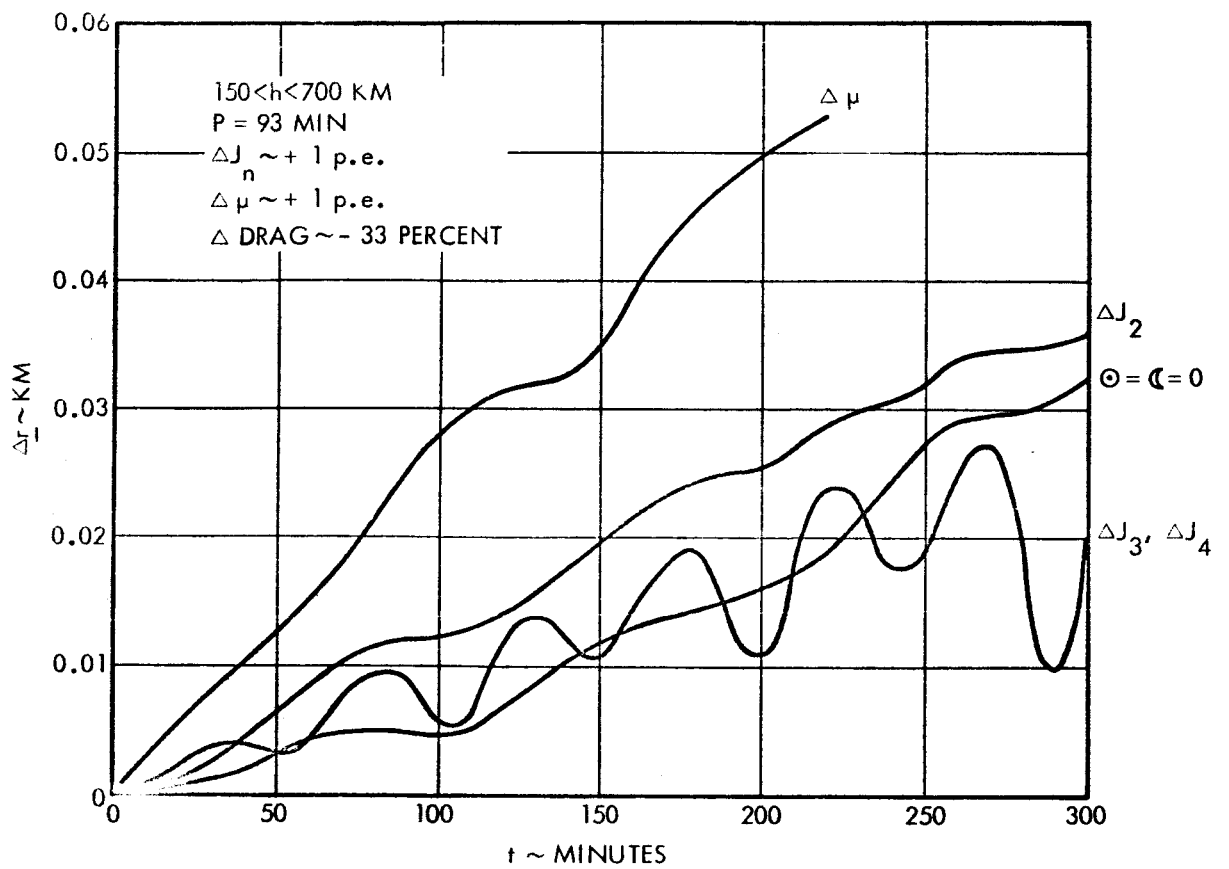


Figure 3.3-3. Elliptical Parking Orbit Position Prediction Error

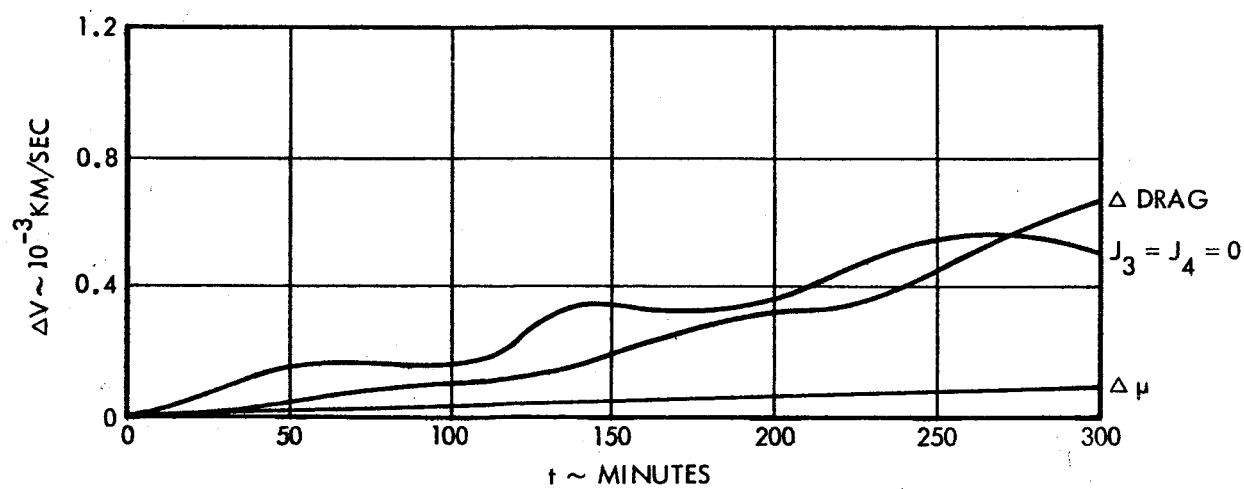
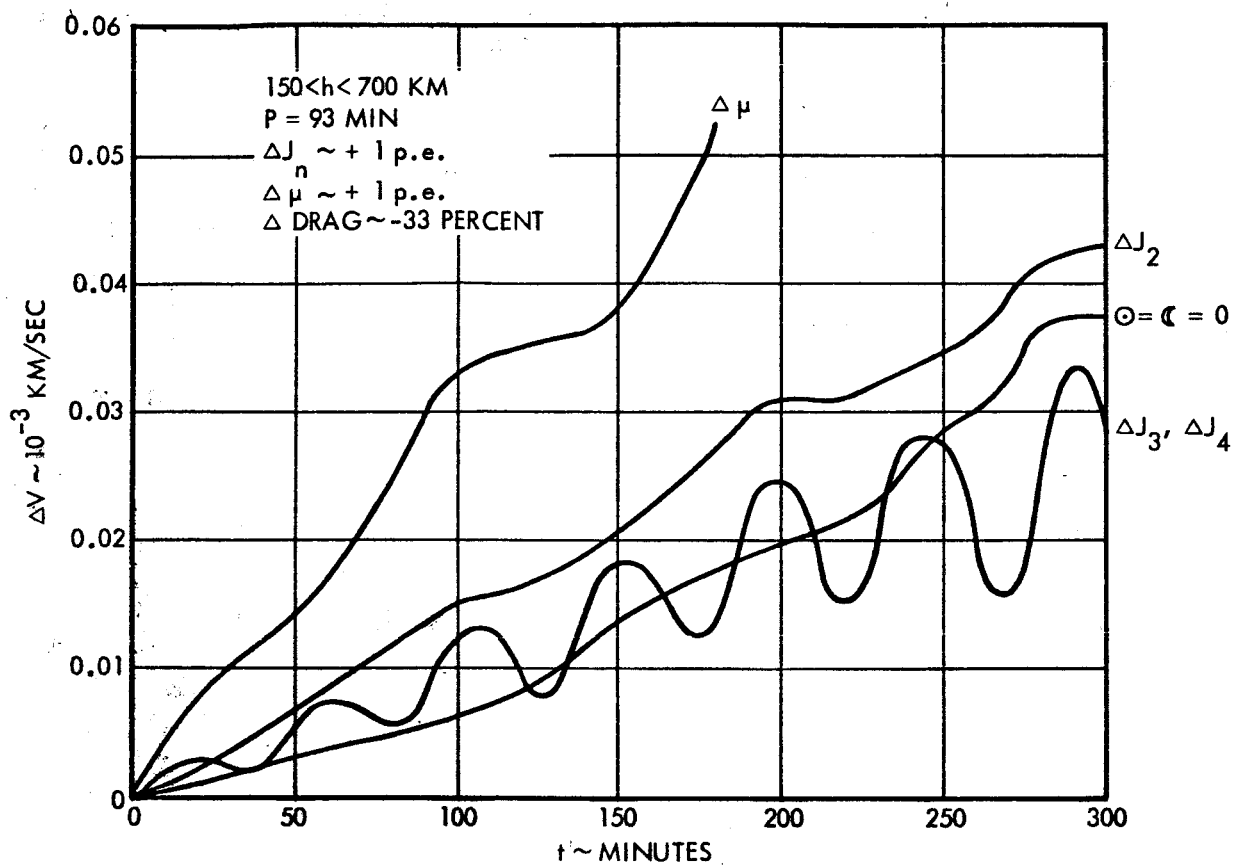


Figure 3.3-4. Elliptical Parking Orbit Velocity Prediction Error

- e. J_2 increased from 1082.30×10^{-6} to 1082.43×10^{-6}
- f. Luni-solar perturbation omitted

The changes described in (b), (d) and (e) correspond to increasing the perturbations by the amount of their probable error. For the perturbation due to uncertainty in atmospheric density (a), an arbitrary probable error is difficult to assign. Various models differ in accuracy depending upon whether seasonal and diurnal variations and solar flux variations are considered. For a non-time-variant atmosphere (which would be sufficiently accurate for a lunar transit) an error of one part in three in density has been simulated by the increase of $W/C_d A$ by 50 percent. This is equivalent to reducing ρ_A by one third. The effect may be scaled up or down according to the accuracy of the atmospheric model used. For the uncertainty in the central gravitational constant (b), only that uncertainty resulting from the equatorial acceleration of gravity, g_e , is applied, since error in the equatorial radius would be cancelled out by a corresponding change in that constant. Hence an increase of $0.45 \text{ km}^3/\text{sec}^2$ is made rather than the total probable error of $1.0 \text{ km}^3/\text{sec}^2$ (cf. Reference 1.0).

3.3.2 Transit Trajectory Perturbations

The following sources of error are considered for the transit trajectory:

- a. Drag uncertainty
- b. Geocentric gravitational constant uncertainty
- c. Neglect of third and fourth harmonics
- d. Uncertainty in J_2
- e. Neglect of J_2
- f. Neglect of solar perturbation
- g. Uncertainty in lunar mass
- h. Neglect of lunar asphericity
- i. Uncertainty in lunar asphericity

Three orbits are considered:

- a. 72-hour transit, with Sun and Moon aligned
- b. 72-hour transit, with Sun and Moon 80° out of phase
- c. 92-hour transit, with Sun and Moon 90° out of phase

For the second orbit, only neglect of the solar perturbation (f) is considered; for the third orbit, selected variations are omitted on the basis of conclusive results from the first orbit. The varied orbits are obtained by the following changes:

- a. $W/C_d A$ increased by a factor of 2, from 113 lb/ft² to 226 lb/ft²
- b. μ increased from 398,603.20 to 398,603.68 km³/sec²
- c. $J_3 = J_4 = 0$
- d. $J_2 = 1,082.30 \times 10^{-6}$ increased to $1,082.43 \times 10^{-6}$
- e. $J_2 = 0$
- f. Solar perturbation neglected
- g. $M = 1/81.3015$ increased to $1/81.2915$
- h. Lunar moments of inertia made equal, $A = B = C$; equivalent to setting $\beta = \gamma = 0$
- i. Lunar moments of inertia, A, B, C increased by a factor of 1.167

Again the perturbations are either omitted or increased by their uncertainty. The atmospheric density is effectively decreased by 50 percent here because of the great uncertainties at higher altitudes. Increasing the lunar moments of inertia by a factor 1.167 is equivalent to increasing g by its probable error (from 0.60 to 0.70) in the form of the lunar potential given in Section 1.0.

The controlling uncertainty is that associated with g' , the values for β and γ , the differences in ratios of moments of inertia, are known to two more orders of magnitude.

Prediction errors in impact and close approach parameters due to an uncertainty or omission in the physical model for transit trajectory are summarized in Table 3.3-1. The effect of tracking error reduction is not included.

The quantities b and V_∞ are parameters associated with the osculating two-body hyperbola at close approach (see Figure 3.3-5). The radius and velocity (r, V) at time of close approach were not differenced for the impact case in orbit (A) because a considerable part of the "error" would be due to the difference

Table 3.3-1. Prediction Errors in Lunar Miss and Impact Parameters

A. 72-hour, Sun and Moon aligned:		b (4601.387)	V_{∞} (1.022062)	r (1879.328)	V (2.502438)
	Δt	Δb	ΔV_{∞}	Δr	ΔV
a. ΔDrag	0 ^s	0.044	0.000000	0.033	-0.000018
b. $\Delta \mu$	+6 ^s	-6.199	-0.000051	-4.474	+0.002467
d. ΔJ_2	0 ^s	-0.136	+0.000001	-0.098	+0.000054
e. $J_2 = 0$	-28 ^m 14 ^s	+1305.267	+0.012758	1015.583	-0.391035
f. Sun = 0	-6 ^m 18 ^s	-502.781	-0.002814	- - -	- - - -
g. ΔM	(impact) -1 ^s	+0.041	-0.000003	-0.144	+0.000207
h. A = B = C ($\beta = \gamma = 0$)	0 ^s	+3.505	-0.000811	+0.363	-0.000510
i. $\Delta A, \Delta B, \Delta C$ ($\Delta g = 0.10$)	0 ^s	-2.674	+0.000600	-0.298	+0.000411
B. 72-hour transit Sun and Moon 80° apart:		(4483.8134)	(1.053677)	(1877.307)	(2.516632)
f. Sun = 0	-27 ^s	+275.6077	+0.001833	+204.155	-0.103128
C. 92-hour transit (impact):		(4430.275)	(0.886846)	_____	(2.535363)
b. $\Delta \mu$	-2 ^s	-11.855	-0.000035	- - - -	-0.000009
c. $J_3 = J_4 = 0$	-2 ^s	-8.791	-0.000025	- - - -	-0.000009
d. ΔJ_2	-1 ^s	-1.872	-0.000006	- - - -	-0.000002
g. ΔM	-2 ^s	-0.019	-0.000003	- - - -	+0.000136
h. A = B = C ($\beta = \gamma = 0$)	0 ^s	+4.301	-0.000868	- - - -	+0.000304

Δt change in time of closest approach or impact

Δb change in "effective radius" or "miss parameter"

ΔV_{∞} change in velocity at infinity relative to Moon

Δr change in radius of close approach

ΔV change in speed at close approach or impact

in time of impact from time of close approach. For case (c), where nominal and all varied trajectories ended in impact, only changes in velocity at impact were computed since r at impact is the radius of the Moon.

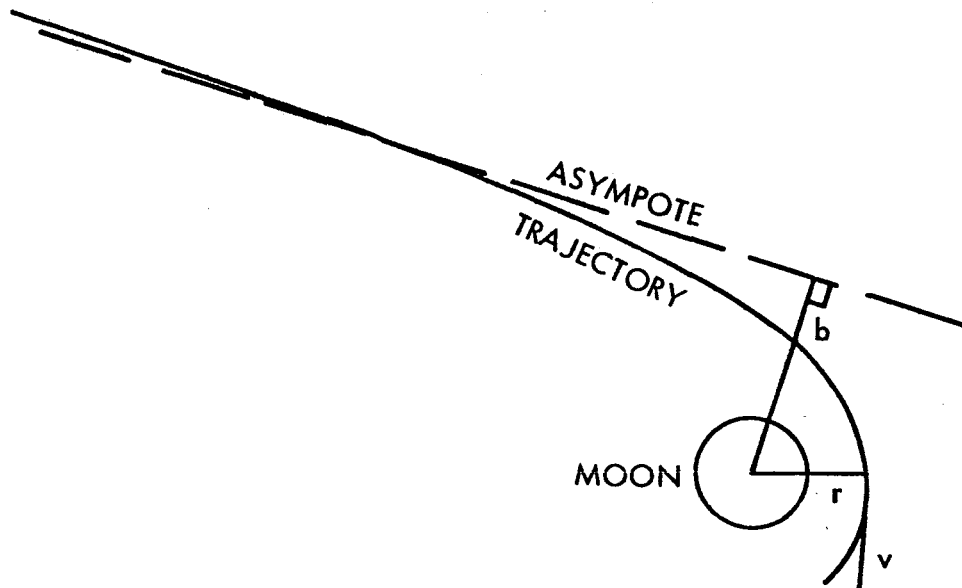


Figure 3.3-5. Selenocentric Hyperbola at Close Approach

3.4 RECOMMENDED MODELS AND ASSOCIATED PREDICTION ERRORS FOR PARKING AND LUNAR TRANSIT ORBITS

The numerical results of Sections 2 and 3 indicate that several of the perturbing forces will be so small as to be lost in the noise of the numerical integration. Hence, to include them in the force function would be wasteful. Uncertainties in several of the physical constants are also so small as to be negligible.

3.4.1 Parking Orbit Model

Figures 3.3-1, 3.3-2, 3.3-3, and 3.3-4 indicate the effects of omitting perturbing forces and of uncertainties in physical constants on prediction over three orbital revolutions. The Sun and Moon may be omitted from the parking orbit model on the basis that their omission produces less prediction error than do the uncertainties in the geopotential. The omission of J_3 and J_4 could produce about a 0.8 km error in position and 0.5 m/sec error in velocity; hence, they should be included in the parking orbit model. Newton's results from

Transit 2A and 4A (J. Geophysical Research, 67, pp 415-16; and Cook, Space Science Review, 2, pp 355-437) indicate as much as 0.8 km along track error occurring from neglect of $J_{2,2}$ - the ellipticity of the equator. This effect is periodic over a day and hence could produce its maximum error after 6 hours. Therefore, it is recommended that the ellipticity of the equator be included in the parking orbit model. The effects of solar radiation pressure and Jupiter were found to be negligible from consideration of analytic expressions in Section 3.2. To summarize,

<u>Parking Orbit Model</u>	
<u>Include</u>	<u>Omit</u>
Drag	Solar radiation
J_2, J_3, J_4	Jupiter, Sun, Moon
$J_{2,2}$	

Prediction error due to uncertainty in the model will be produced mainly by uncertainty in drag and in the gravitational parameter, μ . By use of a dynamic atmosphere the uncertainty in drag may be reduced considerably from that shown in Figures 3.3-3 through 3.3-6. The results of the Mariner 6 mission should reduce the probable error in μ . Each of these effects produce an error in the mean motion which may be corrected in large part by tracking. The uncertainties in J_2, J_3, J_4 are small compared to the drag uncertainty.

3.4.2 Transit Trajectory Model

Table 3.3-1 summarizes the effects of errors and omissions in the physical model on predicted lunar approach parameters, for transfers beginning at 275 km altitude. The effect of drag is negligible for this burnout altitude. A consideration of Table 3.2-4 indicates that drag effects for the interval from 150 to 300 km, (in which a transit vehicle would remain for about 15 sec) produce about a 1-cm change in position. Hence, drag may be omitted from the transit model. In Section 2.5 solar radiation pressure was shown to be negligible. From Table 3.3-1C it may be seen that the omission of J_3 and J_4 produces a small but significant error of about 9 km in miss parameter. Hence, J_3 and J_4

should be included in the near-Earth portion of the transit. J_2 should be included throughout, as it remains about 10^{-6} times the central acceleration even at the Moon's distance. Since its effect is included in the lunar ephemeris, it should be included in the terminal transit phase for consistency. The asphericity of the Moon ($A < B < C$) produces a small effect in miss parameter (≈ 4 km) and velocity (1 m/sec) and should probably be included in the near-Moon portion of the transit model. The Sun produces a large effect and should of course be included. Jupiter should be omitted as it never exceeds 10^{-7} the central acceleration and can at most produce only about 15 meters change in position in a 90-hour transit.

<u>Transit Trajectory Model</u>			
<u>Include Throughout</u>	<u>Near-Earth Only</u>	<u>Near-Moon Only</u>	<u>Omit</u>
Sun	J_3, J_4	A, B, C	Drag
J_2			Solar Radiation
Moon			Jupiter

Major sources of error in this model will be uncertainty in the gravitational parameter, μ , ($\Delta b \approx 10$ km, $\Delta V_\infty = 0.05$ m/sec) and uncertainty in lunar potential, A, B, C, ($\Delta b \approx 3$ km, $\Delta V_\infty = 0.6$ m/sec). Tracking data from Ranger 6 may reduce both these uncertainties. A minor source of uncertainty is J_2 for the Earth ($\Delta b \approx 2$ km, $\Delta V_\infty = 0.006$ m/sec); this effect may be removed by mid-course correction. The lunar mass may be considered well known ($\Delta b = 0.04$ km and $\Delta V_\infty = 0.006$ m/sec). All of the uncertainties were estimated by increasing the perturbing acceleration by its probable error in the integration.

4. CONCLUSIONS

The following paragraphs summarize the most significant findings of this study.

4.1 EFFECTS OF THRUSTS ON EARTH ORBITS

Analytic expressions can be used to analyze the effects of continuous or intermittent thrusts on earth orbits in the 150-700 km range considered in this study. Both total effects and the effects of uncertainties can be obtained.

Downrange thrust produces the largest in-plane effects which are downrange position and radial velocity. Crossrange thrust produces no in-plane effects and only a small periodic crossrange effect.

When a thrusting orbit is tracked and predictions are based on a non-thrusting orbit which best fits the data, only the last radar pass should be used. The use of earlier passes increases the prediction error. In order to improve the prediction, the capability of solving for the thrust in the tracking program must be developed.

The accuracy of predicting an orbit with intermittent venting from tracking data can be improved by telemetering the time of initiation and duration of each pulse and including this estimate of the pulse in the tracking fit.

Several methods of using venting pulses for orbit control are possible, but the difficulties involved in controlling the pulses and the resulting errors may make it more desirable to simply minimize the venting effect by venting crossrange.

4.2 EFFECTS OF THRUSTS ON TRANSLUNAR TRAJECTORIES

In order to produce a negligible miss, a gas leakage thrust must be kept down to about 10^{-8} g because of the long time period over which it acts. A larger thrust could be allowed if it were estimated from tracking data, but the accuracy with which this can be done has not been evaluated.

Intermittent venting in the early portion of a translunar trajectory can require midcourse correction velocities of something less than four times the total venting impulse. In order to improve the accuracy of the commanded

correction, the time of initiation and duration of each venting pulse should be telemetered and used in forming the tracking estimate of the trajectory.

4.3 EFFECTS OF NATURAL PERTURBATIONS ON EARTH ORBITS

It was found that some effects considered were smaller than the uncertainties in other effects, while some effects were so small that they would be lost in roundoff error if an attempt were made to include them. The recommended model based on this study can be summarized as follows:

<u>Include</u>	<u>Omit</u>
Drag	Solar radiation
J_2, J_3, J_4	Jupiter, Sun, Moon
$J_{2,2}$	

4.4 EFFECTS OF NATURAL PERTURBATIONS ON TRANSLUNAR TRAJECTORIES

Since different parameters are important in the near-earth and near-moon portions of the trajectory, the recommended model is slightly more complicated than for earth orbits. The model can be summarized as follows:

<u>Include Throughout</u>	<u>Include Near Earth Only</u>	<u>Include Near Moon Only</u>	<u>Omit Throughout</u>
Sun	J_3, J_4	A, B, C	Drag
J_2			Solar radiation
Moon			Jupiter

APPENDIX

The following section presents the results of an attempt to determine the statistics of random downrange venting effects with as few assumptions as possible. The approach is slightly different from that used in Section 2, and leads to a more complicated expression.

STATISTICAL ASPECTS OF THE HYDROGEN VENTING PROBLEM THE PROBLEM

The problem studied was the following: consider an object in a circular orbit. A series of tangential thrusts is applied to the vehicle. These thrusts represent the only perturbations of the orbit and they are to be considered to be small perturbations. If there are statistical variations in the magnitude, duration, and interval between thrusts, what is the effect on the orbit to first-order?

In solving this problem we began with the analysis of H. J. Klein, "Effects of Drift Forces on Satellite Motion," 9861.11-1, 27 September 1962. The following first-order equations have been used:

$$\frac{d^2 \rho}{d\tau^2} - 3\rho - 2\lambda = 0 \quad (A-1)$$

$$\frac{2d\rho}{d\tau} + \frac{d\lambda}{d\tau} = \alpha(\tau) \quad (A-2)$$

These are Equations (8) and (9) of the document cited with the following changes:

- a. In the first equation, the right side equals 0, since we are not considering lift forces.
- b. We have replaced $\Delta\rho$ by ρ and $\Delta\lambda$ by λ .
- c. $\alpha(\tau)$ is the tangential thrust per unit weight. The quantities in this equation are defined as follows:
 - 1) ρ is the fractional change in radial distance.
 - 2) τ is equal to ωt , where t is the time and ω is the unperturbed angular velocity.
 - 3) λ is the fractional change in the angular velocity. Both ρ and λ are assumed to be small.

- 4) The fractional change in the angular position is
therefore $= \int_0^{\tau} \dot{\alpha} d\tau$.

Let us take the derivative of Equation A-1 and substitute in Equation A-2, using the prime notation to indicate derivatives with respect to τ . We find

$$\frac{1}{2}(\rho''' - 3\rho') = \lambda' \quad (\text{A-3})$$

$$\alpha - 2\rho' = \lambda' \quad (\text{A-4})$$

or

$$\rho''' + \rho' = 2\alpha \quad (\text{A-5})$$

Setting $\rho' = \sigma$, we find

$$\sigma'' + \sigma = 2\alpha \quad (\text{A-6})$$

Before discussing the solution of Equation A-6, it should be mentioned that a preliminary calculation was performed. This calculation involved the Fourier expansion of the forcing term in the equation of motion. The problem is, essentially, that of a forced harmonic oscillator with periodic driving force. The solution is obtained with ease. However, such a solution is of little value in handling the statistical aspect of the venting problem.

SOLUTION

The form of the quantity, α , in Equation A-6 was a series of square waves. Each square wave began at "time" τ_n and lasted to $\tau_n + \Delta_n$. The magnitude of each pulse was equal to α_n . At first the problem was solved assuming that all Δ_n and α_n and $\tau_{n+1} - \tau_n$ were the same for each impulse. However, it is possible to obtain a solution in the general case, where these quantities may be different for each pulse applied to the vehicle. It is necessary to obtain the solution in this case, if we are to be able to include statistical effects later on in the study.

We write down the solutions of Equation A-6 for a time between thrusts, i.e., in the region

$$\tau_n + \Delta_n \leq \tau \leq \tau_{n+1}$$

The solution is

$$\begin{aligned} \sigma(\tau) = 4\alpha_n \sin\left(\tau - \tau_n - \frac{\Delta_n}{2}\right) \sin\left(\frac{\Delta_n}{2}\right) + \sigma_{n-1} \cos(\tau - \tau_n) \\ + \sigma'_{n-1} \sin(\tau - \tau_n) \end{aligned} \quad (\text{A-7})$$

$$\begin{aligned} \sigma'(\tau) = 4\alpha_n \cos\left(\tau - \tau_n - \frac{\Delta_n}{2}\right) \sin\left(\frac{\Delta_n}{2}\right) - \sigma_{n-1} \sin(\tau - \tau_n) \\ + \sigma'_{n-1} \cos(\tau - \tau_n) \end{aligned} \quad (\text{A-8})$$

In the region where a thrust is applied

$$\tau_n \leq \tau \leq \tau_n + \Delta_n$$

the solution is

$$\begin{aligned} \sigma(\tau) = 4\alpha_n \sin^2\left(\frac{\tau - \tau_n}{2}\right) + \sigma_{n-1} \cos(\tau - \tau_n) \\ + \sigma'_{n-1} \sin(\tau - \tau_n) \end{aligned} \quad (\text{A-9})$$

$$\begin{aligned} \sigma'(\tau) = 4\alpha_n \sin\left(\frac{\tau - \tau_n}{2}\right) \cos\left(\frac{\tau - \tau_n}{2}\right) - \sigma_{n-1} \sin(\tau - \tau_n) \\ + \sigma'_{n-1} \cos(\tau - \tau_n) \end{aligned} \quad (\text{A-10})$$

Let us set $\tau = \tau_{n+1}$ and substitute in Equations A-7 and A-8. We will then find σ_n and σ'_n . These will be the initial conditions, just as the n^{th} pulse is to be applied. We find

$$\sigma_n = 4\alpha_n \sin\left(\theta_n - \frac{\Delta_n}{2}\right) \sin\left(\frac{\Delta_n}{2}\right) + \sigma_{n-1} \cos \theta_n + \sigma'_{n-1} \sin \theta_n \quad (\text{A-11})$$

$$\sigma'_n = 4\alpha_n \cos\left(\theta_n - \frac{\Delta_n}{2}\right) \sin\left(\frac{\Delta_n}{2}\right) - \sigma_{n-1} \sin\theta_n + \sigma'_{n-1} \cos\theta_n \quad (\text{A-12})$$

where $\theta_n = \tau_{n+1} - \tau_n$.

MATRIX TECHNIQUE

A useful technique for solving the problem is the matrix technique, which will be outlined in this section. Such a procedure is related to the matrix methods used in solving the betatron oscillation problem for nuclear accelerators. However, in the latter case, the equation is always homogeneous, i.e., Equation A-6, with α equal to zero. The technique shown here extends the procedure to non-homogeneous equations.

Let us consider σ_n and σ'_n as components of a vector, Σ_n . Then Equation A-6 becomes

$$\Sigma_n = L_n + R_n \Sigma_{n-1} \quad (\text{A-13})$$

where

$$\Sigma_n = \begin{pmatrix} \sigma_n \\ \sigma'_n \end{pmatrix} \quad (\text{A-14})$$

$$L_n = \begin{pmatrix} J_n \\ K_n \end{pmatrix} \quad (\text{A-15})$$

$$L_n = 4\alpha_n \sin\left(\frac{\Delta_n}{2}\right) \begin{pmatrix} \sin\left(\theta_n - \frac{\Delta_n}{2}\right) \\ \cos\left(\theta_n - \frac{\Delta_n}{2}\right) \end{pmatrix} \quad (\text{A-16})$$

$$R_n = \begin{pmatrix} \cos\theta_n & \sin\theta_n \\ -\sin\theta_n & \cos\theta_n \end{pmatrix} \quad (\text{A-17})$$

Note that R_n is just the rotation operator. Therefore, we can say that, if we examine the vector, Σ , just before the n^{th} thrust and compare it to the value it has just before the $n+1^{\text{st}}$ thrust, then in the two-dimensional coordinate space (σ, σ') it has been subjected to two effects. It has been translated by L_n and has been operated upon by the rotation operator R_n .

Equation A-13 tells us that

$$\Sigma_{n-1} = L_{n-1} + R_{n-1} \Sigma_{n-2} \quad (\text{A-18})$$

and we can substitute into Equation A-13. We then replace Σ_{n-2} by a similar expression. We repeat until we have reached Σ_0 . Finally, we find

$$\Sigma_n = \sum_{s=1}^n \left(\prod_{j=s+1}^n R_j \right) L_s + \left(\prod_{j=1}^n R_j \right) \Sigma_0 \quad (\text{A-19})$$

Please note that Σ_n , L_s and Σ_0 are vectors.

(A-20)

$$T_{s+1}(n) = R_n R_{n-1} \dots R_{s+1} = \begin{pmatrix} \cos(\tau_{n+1} - \tau_{s+1}) & \sin(\tau_{n+1} - \tau_{s+1}) \\ -\sin(\tau_{n+1} - \tau_{s+1}) & \cos(\tau_{n+1} - \tau_{s+1}) \end{pmatrix}$$

$$L_s = 4\alpha_s \sin\left(\frac{\Delta_s}{2}\right) \begin{pmatrix} \sin\left(\tau_{s+1} - \tau_s - \frac{\Delta_s}{2}\right) \\ \cos\left(\tau_{s+1} - \tau_s - \frac{\Delta_s}{2}\right) \end{pmatrix} \quad (\text{A-21})$$

Therefore,

$$T_{s+1}(n)L_s = 4\alpha_s \sin\left(\frac{\Delta_s}{2}\right) \begin{pmatrix} \sin\left(\tau_{n+1} - \tau_s - \frac{\Delta_s}{2}\right) \\ \cos\left(\tau_{n+1} - \tau_s - \frac{\Delta_s}{2}\right) \end{pmatrix} \quad (\text{A-22})$$

And

$$\sum_{s=1}^n T_{s+1}(n) L_s = 4 \begin{pmatrix} \sum_{s=1}^n \alpha_s \sin\left(\frac{\Delta_s}{2}\right) \sin\left(\tau_{n+1} - \tau_s - \frac{\Delta_s}{2}\right) \\ \sum_{s=1}^n \alpha_s \sin\left(\frac{\Delta_s}{2}\right) \cos\left(\tau_{n+1} - \tau_s - \frac{\Delta_s}{2}\right) \end{pmatrix} \quad (A-23)$$

However, since σ_0 and σ'_0 are equal to zero for our problem, $\Sigma_0 = 0$ and according to Equation A-19, Σ_n is given by Equation A-23.

CALCULATION OF ρ

We now return to the differential equation $\rho' = \sigma$. We have to integrate this equation as follows:

$$\rho(\tau) = \int_0^{\tau_1} \rho \, d\tau + \int_{\tau_1}^{\tau_1 + \Delta_1} \rho \, d\tau, \dots, \text{etc.}$$

We have to join the solutions at each region and use the result shown in Equation A-23. The procedure is straightforward and we will write down the result for $\rho(\tau)$ at τ equal to τ_{N+1} , i.e., just prior to applying the $N+1^{\text{st}}$ impulse. The result is

$$\begin{aligned} \rho(\tau_{N+1}) = & \sum_{n=1}^N \left\{ 4\alpha_n \left[\frac{\Delta_n}{2} - \sin\left(\frac{\Delta_n}{2}\right) \cos\left(\tau_{n+1} - \tau_n - \frac{\Delta_n}{2}\right) \right] \right. \\ & + 2\alpha_s \sum_{s=1}^{n-1} \alpha_s \left[(1 - \cos \Delta_s) \{ \sin(\tau_n - \tau_s) - \sin(\tau_{n+1} - \tau_s) \} \right. \\ & \left. \left. + \sin \Delta_s \{ \cos(\tau_n - \tau_s) - \cos(\tau_{n+1} - \tau_s) \} \right] \right\} \quad (A-24) \end{aligned}$$

Equation A-24 gives the fractional change in the radial distance following N thrusts of magnitude α_n , of duration Δ_n and of spacing $\tau_{n+1} - \tau_n$.

STATISTICAL PROBLEM

We now will include the effect of the statistical fluctuations on the three parameters α , Δ , and τ . We will make the following assumptions:

$$\alpha_n = \alpha_o + A_n \quad (A-25)$$

$$\Delta_n = \Delta_o + D_n \quad (A-26)$$

$$\tau_n = n\tau_o + B_n \quad (A-27)$$

$$\overline{A_n} = \overline{D_n} = \overline{B_n} = 0 \quad (A-28)$$

$$A_n, D_n \text{ and } B_n \text{ are independent.} \quad (A-29)$$

The bar over a quantity is the mean of that quantity over the assumed statistics.

We now proceed to calculate $\overline{\rho}$ and $\overline{(\rho - \overline{\rho})^2} = \overline{\rho^2} - \overline{\rho}^2$.

CALCULATION OF $\overline{\rho}$

The calculation of $\overline{\rho}$ is simple to carry out. The result of this calculation is given in the following equation:

$$\begin{aligned} \overline{\rho(\tau_{N+1})} = 2N\alpha_o & \left\{ \Delta_o - \left[\overline{\cos B}^2 + \overline{\sin B}^2 \right] \left[\overline{\sin D} \cos(\tau_o - \Delta_o) + \sin \tau_o \right. \right. \\ & \left. \left. - \overline{\cos D} \sin(\tau_o - \Delta_o) \right] \right\} + 2\alpha_o \left[\overline{\cos B}^2 + \overline{\sin B}^2 \right] \\ & \cdot \left\{ (\sin \Delta_o \overline{\cos D} + \cos \Delta_o \overline{\sin D}) G \right. \\ & \left. - (1 - \cos \Delta_o \overline{\cos D} + \sin \Delta_o \overline{\sin D}) H \right\} \quad (A-30) \end{aligned}$$

where

$$G = N \cos \tau_o - \frac{\sin\left(\frac{N\tau_o}{2}\right)}{\sin\left(\frac{\tau_o}{2}\right)} \cos\left[(N+1) \frac{\tau_o}{2}\right]$$

$$H = -N \sin \tau_o + \frac{\sin\left(\frac{N\tau_o}{2}\right)}{\sin\left(\frac{\tau_o}{2}\right)} \sin\left[(N+1) \frac{\tau_o}{2}\right]$$

Note that we have only to evaluate $\overline{\cos x}$ and $\overline{\sin x}$, where x is either B or D , in order to study statistical effects. These averages are easily evaluated in closed form for Gaussian, exponential, uniform or triangular distributions of the parameters. For these symmetric distributions $\overline{\sin x} = 0$. One feature of the solution to be noted is the occurrence of expressions of the form $\sin(N\tau_o/2)/\sin(\tau_o/2)$. This is similar to the expression for the amplitude of a wave passing through a diffraction grating. This is not surprising, since the problem we have solved is very similar to the optical problem.

CALCULATION OF $\overline{\rho^2} - \bar{\rho}^2$

The calculation of the mean square deviation from the average was also carried out. However, this was a gigantic computation. Since the formula for $\bar{\rho}$ in Equation A-24 involves a double sum and a single sum, the expression for $\overline{\rho^2} - \bar{\rho}^2$ involves a double, triple, and quadruple sum.

The calculation was carried out without specializing to any particular statistics except that A_n , D_n , and B_n are independent. In this problem the statistically varying parameters occur only in the following form: $\overline{\cos x}$ and $\overline{\sin x}$; $\overline{x \sin x}$ and $\overline{x \cos x}$; $\overline{\cos 2x}$ and $\overline{\sin 2x}$; and $\overline{x^2}$. In the final expression for $\overline{\rho^2} - \bar{\rho}^2$, it is assumed that we have a symmetric statistics. This means that terms of the forms $\overline{\sin x}$, $\overline{x \cos x}$ and $\overline{\sin 2x}$ are all zero. This was done to allow typing of the final result on 5, rather than 10 pages.

$$\begin{aligned}
\overline{\rho}^2 - \overline{p}^2 = & \frac{N}{4} \left[\Delta_o^2 \overline{A}^2 + \alpha_o^2 \overline{D}^2 + \overline{A}^2 \overline{D}^2 \right] - 8N \Delta_o \overline{A}^2 [\overline{\cos B}]^2 \left[\sin \tau_o - \overline{\cos D} \sin(\tau_o - \Delta_o) \right] \\
& - 8N(\alpha_o^2 + \overline{A}^2) \left[\overline{D} \sin \overline{D} \cos(\tau_o - \Delta_o) \right] - 2N(\alpha_o^2 + \overline{A}^2) [\overline{\cos 2B}]^2 \left\{ \cos 2\tau_o \right. \\
& - 2\cos(2\tau_o - \Delta_o) \overline{\cos D} + \cos 2(\tau_o - \Delta_o) \overline{\cos D} \left. \right\} + \left[2\alpha_o^2(3N - 2) \right. \\
& + 2N\overline{A}^2 \left. \right] [\overline{\cos B}]^2 \cdot \left\{ \cos 2\tau_o - 2\cos(2\tau_o - \Delta_o) \overline{\cos D} + \cos 2(\tau_o - \Delta_o) [\overline{\cos D}]^2 \right. \\
& + 2\cos \Delta_o \overline{\cos D} - [\overline{\cos D}]^2 - 1 \left. \right\} - 4\alpha_o^2(N - 1) [\overline{\cos B}]^2 \left\{ \cos 2\tau_o \right. \\
& - 2\cos(2\tau_o - \Delta_o) \overline{\cos D} + \cos 2(\tau_o - \Delta_o) \overline{\cos D}^2 \left. \right\} \\
& + 4\alpha_o^2(N - 1) [\overline{\cos 2B} \overline{\cos B}]^2 \left[2\cos \Delta_o \overline{\cos D} - \overline{\cos D}^2 - 1 \right] \\
& + 8N\overline{A}^2 \Delta_o [\overline{\cos B}]^2 \left\{ \sin \Delta_o \overline{\cos D} G + (1 - \cos \Delta_o \overline{\cos D}) \left[N \sin \tau_o \right. \right. \\
& - \frac{\sin \frac{N}{2} \tau_o}{\sin \frac{\tau_o}{2}} \sin(\frac{N+1}{2} \tau_o) \left. \right] \left. \right\} + 8N(\overline{A}^2 + \alpha_o^2) (\overline{\cos B})^2 \left\{ \cos \Delta_o \overline{D} \sin \overline{D} G \right. \\
& + \sin \Delta_o \overline{D} \sin \overline{D} \left[N \sin \tau_o - \frac{\sin \frac{N}{2} \tau_o}{\sin \frac{\tau_o}{2}} \sin(\frac{N+1}{2} \tau_o) \right] \left. \right\} + 4 \frac{\overline{\cos B}^4}{\sin \frac{\tau_o}{2}} \left\{ - N \sin \tau_o \right. \\
& + \frac{\sin \frac{N}{2} \tau_o}{\sin \frac{\tau_o}{2}} \sin(\frac{N+1}{2} \tau_o) \left. \right\} \left[(K_{2A} + 3K_{1A}) \sin \frac{\tau_o}{2} + (K_{2C} + 3K_{1C}) \cos \frac{\tau_o}{2} \right] \\
& + 8 \overline{\cos B}^4 \sin(\frac{N-1}{2} \tau_o) \left[-K_{1A} \cos(\frac{N+1}{2} \tau_o) + K_{1C} \sin(\frac{N+1}{2} \tau_o) \right] \\
& + 4(N - 1) \overline{\cos B}^4 \left[K_{2A} \sin \tau_o + K_{2C} \cos \tau_o \right]
\end{aligned}$$

$$\begin{aligned}
& + 2 \overline{\cos 2B} \overline{\cos B}^2 \left\{ \left[(3K_{1A} + K_{2A}) + (K_{2D} - K_{1D}) \right] \left[N \sin \tau_o \right. \right. \\
& - \frac{\sin \frac{N}{2} \tau_o}{\sin \frac{\tau_o}{2}} \sin \left(\frac{N+1}{2} \tau_o \right) + \left[(3K_{1c} + K_{2c}) + (K_{2B} - K_{1B}) \right] \left[N \cos \tau_o \right. \\
& - \frac{\sin \frac{N}{2} \tau_o}{\sin \frac{\tau_o}{2}} \cos \left(\frac{N+1}{2} \tau_o \right) \left. \right\} + 2(N-1) \overline{\cos 2B} \overline{\cos B}^2 \left[-(K_{2A} + K_{2D}) \sin \tau_o \right. \\
& - (K_{2B} + K_{2c}) \cos \tau_o \left. \right] + 4 \overline{\cos B}^2 \left[-N \sin \tau_o \right. \\
& + \frac{\sin \frac{N}{2} \tau_o}{\sin \frac{\tau_o}{2}} \sin \left(\frac{N+1}{2} \tau_o \right) \left. \right] \left[-(3K_{1A} + K_{2A}) + (K_{2B} - K_{1B}) \frac{\cos \frac{\tau_o}{2}}{\sin \frac{\tau_o}{2}} \right. \\
& + (K_{2c} + 3K_{1c}) \frac{\cos \frac{\tau_o}{2}}{\sin \frac{\tau_o}{2}} + (K_{2D} - K_{1D}) \left. \right] \\
& + 4 \overline{\cos B}^2 \sin \left(\frac{N-1}{2} \tau_o \right) \left[(K_{1A} + K_{1D}) \cos \left(\frac{N+1}{2} \tau_o \right) - (K_{1B} + K_{1c}) \sin \left(\frac{N+1}{2} \tau_o \right) \right] \\
& + 4 \overline{\cos 2B} \overline{\cos B}^2 \sin \left(\frac{N-1}{2} \tau_o \right) \left[(K_{1A} - K_{1D}) \cos \left(\frac{N+1}{2} \tau_o \right) \right. \\
& + (K_{1B} - K_{1c}) \sin \left(\frac{N+1}{2} \tau_o \right) \left. \right] + 2(N-1) \overline{\cos 2B}^2 \left[(K_{2A} + K_{2D}) \sin \tau_o \right. \\
& + (K_{2c} + K_{2B}) \cos \tau_o \left. \right] + 2(N-1) \left(1 - \overline{\cos B}^2 \right) \left[(K_{2A} - K_{2D}) \sin \tau_o \right. \\
& + (K_{2c} - K_{2B}) \cos \tau_o \left. \right]
\end{aligned}$$

$$\begin{aligned}
& + 2 \left[\overline{\cos 2B} - \overline{\cos B} \right]^2 \overline{\cos B}^2 \left[K_{c2} + K_{s2} \right] \left\{ (N-1) \cos 2\tau_o - \frac{\sin(N+\frac{1}{2})\tau_o}{\sin \frac{\tau_o}{2}} \right. \\
& + \frac{\sin(2N-1)\tau_o}{2\sin \tau_o} + \left(\cos \tau_o + 2\cos^2 \frac{\tau_o}{2} - \frac{1}{2} \right) \left. \right\} + 2K_2 \left\{ (N-1) \sin 2\tau_o \right. \\
& + \cos \frac{(N+\frac{1}{2})\tau_o}{\sin \frac{\tau_o}{2}} - \frac{\cos(2N-1)\tau_o}{2\sin \tau_o} + \left(\sin \tau_o - \cos \tau_o \frac{\cos \frac{\tau_o}{2}}{\sin \frac{\tau_o}{2}} + \frac{1}{2} \frac{\cos \tau_o}{\sin \tau_o} \right) \left. \right\} \\
& + 4 \frac{\overline{\cos B}^2 [1 - \overline{\cos B}^2]}{\sin \frac{\tau_o}{2}} \left[(K_{c1} + K_{s1}) \left\{ \frac{\sin \frac{N}{2} \tau_o}{\sin \frac{\tau_o}{2}} - N \cos(\frac{N-1}{2} \tau_o) \right\} \sin(\frac{N+2}{2} \tau_o) \right. \\
& + \left. \left\{ \frac{\sin(\frac{N-1}{2} \tau_o)}{\sin \frac{\tau_o}{2}} - (N-1) \cos(\frac{N-2}{2} \tau_o) \right\} \sin(\frac{N+3}{2} \tau_o) \right] \\
& - 2K_1 \left\{ \left[\frac{\sin \frac{N}{2} \tau_o}{\sin \frac{\tau_o}{2}} - N \cos(\frac{N-1}{2} \tau_o) \right] \cos(\frac{N+2}{2} \tau_o) \right. \\
& + \left. \left[\frac{\sin(\frac{N-1}{2} \tau_o)}{\sin \frac{\tau_o}{2}} - (N-1) \cos(\frac{N-2}{2} \tau_o) \right] \cos(\frac{N+3}{2} \tau_o) \right\} \\
& + 2 \overline{\cos B}^2 \left[\overline{\cos 2B} - \overline{\cos B} \right]^2 \left\{ \left[K_{c1} - K_{s1} \right] \left[(2N-3) - \frac{\sin(\frac{2N-3}{2} \tau_o)}{\sin \frac{\tau_o}{2}} \right] \right\} \\
& + 4 \overline{\cos B}^4 \left[\frac{K_{c1} + K_{s1}}{4\sin^2 \frac{\tau_o}{2}} \right] \left\{ \frac{\sin 2N\tau_o}{\sin \tau_o} + 1 - \frac{\sin(N+\frac{1}{2})\tau_o}{\sin \frac{\tau_o}{2}} + N \cos \tau_o \right\}
\end{aligned}$$

$$\begin{aligned}
& + \left[\frac{\sin(2N+2)\tau_o}{2\sin\tau_o} - \frac{\sin(N+\frac{5}{2})\tau_o}{\sin\frac{\tau_o}{2}} + N\cos 3\tau_o + \cos 2\tau_o - \cos\tau_o (1 - 4\cos^2\frac{\tau_o}{2}) \right] \\
& - \frac{2}{\sin\frac{\tau_o}{2}} \left[\frac{\sin[(N-2)\tau_o]\cos[(N+2)\tau_o]}{2\cos\frac{\tau_o}{2}} - 2\cos\frac{\tau_o}{2} \sin\left(\frac{N-2}{2}\tau_o\right)\cos\left(\frac{N+4}{2}\tau_o\right) \right. \\
& \quad \left. + \left(\frac{N-2}{2}\right)\sin 2\tau_o \right] \Bigg\} \\
& + 2\overline{\cos B}^2 \left[1 - \overline{\cos B}^2 \right] \left[\frac{(K_{c1} - K_{s1})}{\sin^2\frac{\tau_o}{2}} \left\{ \left(\frac{2N-1}{2}\right) - \frac{\sin(\frac{2N-1}{2}\tau_o)}{2\sin\frac{\tau_o}{2}} \right. \right. \\
& \quad \left. \left. - \frac{2}{\sin\frac{\tau_o}{2}} \left[2(N-2)\sin\tau_o - \sin\left(\frac{N-2}{2}\tau_o\right)\cos\frac{N\tau_o}{2} \right] \right\} \right] \\
& + 4\overline{\cos B}^4 \left[\frac{2K_1}{\sin^2\frac{\tau_o}{2}} \left\{ \left[\frac{1}{2\sin\tau_o} - \frac{\cos 2N\tau_o}{\sin\tau_o} + \cos\frac{(N+\frac{1}{2})\tau_o}{\sin\frac{\tau_o}{2}} + N\sin\tau_o - \frac{\cos\frac{\tau_o}{2}}{\sin\frac{\tau_o}{2}} \right. \right. \right. \\
& \quad \left. \left. + \left[-\frac{\cos(2N+2)\tau_o}{2\sin\tau_o} + \frac{\cos(N+\frac{5}{2})\tau_o}{\sin\frac{\tau_o}{2}} + N\sin 3\tau_o + \sin 2\tau_o - \frac{\cos 2\tau_o \cos\frac{\tau_o}{2}}{\sin\frac{\tau_o}{2}} \right] \right. \right. \\
& \quad \left. \left. - \frac{2}{\sin\frac{\tau_o}{2}} \left[\frac{\sin[(N-2)\tau_o]\sin[(N+2)\tau_o]}{2\cos\frac{\tau_o}{2}} - 2\cos\frac{\tau_o}{2} \sin\left(\frac{N-2}{2}\tau_o\right)\sin\left(\frac{N+4}{2}\tau_o\right) \right. \right. \right. \\
& \quad \left. \left. \left. - \left(\frac{N-2}{2}\right)\cos 2\tau_o \right] \right\} \right] + 2 \left[\overline{\cos B}^2 - \overline{\cos 2B} \right]^2 \left[\frac{(K_{c2} + K_{s2})}{2\sin^2\tau_o} \left\{ \left(\frac{1-N}{2}\right)(1 + \cos 2\tau_o) \right. \right. \right.
\end{aligned}$$

$$\begin{aligned}
& + \cos \tau_o \left[N \cos 3\tau_o - \cos(2N+1)\tau_o \right] \Bigg\} - \left[(N-1) \cos 4\tau_o - \cos 2N\tau_o \right. \\
& \left. - (N-2) \cos 2\tau_o \right] \Bigg\} + \frac{2K_2}{2\sin^2 \tau_o} \left\{ \left[\left(\frac{1-N}{2} \right) \sin 2\tau_o + \cos \tau_o \left[N \sin 3\tau_o \right. \right. \right. \\
& \left. \left. - \sin(2N+1)\tau_o \right] \right] - \left[(N-1) \sin 4\tau_o - \sin 2N\tau_o - (N-1) \sin 2\tau_o \right] \right\} \\
& + 2 \left[\overline{\cos B} - 1 \right]^2 \left[K_{c2} - K_{s2} \right] \left[N-1 \right] \left\{ N - (N-2) \cos^2 \tau_o \right\} \\
& + 2 \overline{\cos B}^2 \left[1 - \overline{\cos B}^2 \right] (K_{c2} - K_{s2}) \left\{ (2N-3) - \frac{\sin(\frac{2N-3}{2}\tau_o)}{\sin \frac{\tau_o}{2}} \right\} \\
& + 2 \left[\overline{\cos 2B} \overline{\cos B}^2 \right] \left[K_{c1} + K_{s1} \right] \left\{ \frac{\sin(2N+1)\tau_o}{2\sin \tau_o} - \frac{\sin(N+\frac{3}{2}\tau_o)}{\sin \frac{\tau_o}{2}} \right. \\
& \left. + N \cos 2\tau_o + \left(\cos \tau_o - \frac{1}{2} + \frac{\cos \frac{\tau_o}{2}}{\sin \frac{\tau_o}{2}} \sin \tau_o \right) \right\} \\
& + 2K_1 \left\{ - \frac{\cos(2N+1)\tau_o}{2\sin \tau_o} + \frac{\cos(N+\frac{3}{2}\tau_o)}{\sin \frac{\tau_o}{2}} + N \sin 2\tau_o \right. \\
& \left. + \left(\sin \tau_o + \frac{1}{2} \frac{\cos \tau_o}{\sin \tau_o} - \frac{\cos \frac{\tau_o}{2}}{\sin \frac{\tau_o}{2}} \cos \tau_o \right) \right\}
\end{aligned}$$

To use the above results, we need the following items:

For Pages 10 through 11

$$G = \left[N \cos \tau_o - \frac{\sin \frac{N}{2} \tau_o}{\sin \frac{\tau_o}{2}} \cos \left(\frac{N+1}{2} \tau_o \right) \right]$$

$$K_{1A} = 2\alpha_o^2 \left[\sin \tau_o - \sin(\tau_o - \Delta_o) \overline{\cos D} - \sin \tau_o \cos \Delta_o \overline{\cos D} \right. \\ \left. + \sin(\tau_o - \Delta_o) \cos \Delta_o \overline{\cos D}^2 \right]$$

$$K_{2A} = 2(\alpha_o^2 + A^2) \left[\frac{3}{2} \sin \tau_o - \sin(\tau_o - \Delta_o) \overline{\cos D} - \sin \tau_o \cos \Delta_o \overline{\cos D} \right. \\ \left. + \frac{1}{2} \sin(\tau_o - 2\Delta_o) \overline{\cos 2D} \right]$$

$$K_{1B} = -2\alpha_o^2 \left[\cos \tau_o - \cos(\tau_o - \Delta_o) \overline{\cos D} - \cos \tau_o \cos \Delta_o \overline{\cos D} \right. \\ \left. + \cos(\tau_o - \Delta_o) \cos \Delta_o \overline{\cos D}^2 \right]$$

$$K_{2B} = -2(\alpha_o^2 + A^2) \left[\frac{3}{2} \cos \tau_o - \cos(\tau_o - \Delta_o) \overline{\cos D} - \cos \tau_o \cos \Delta_o \overline{\cos D} \right. \\ \left. + \frac{1}{2} \cos(\tau_o - 2\Delta_o) \overline{\cos 2D} \right]$$

$$K_{1c} = 2\alpha_o^2 \left[\sin \tau_o \sin \Delta_o \overline{\cos D} - \sin(\tau_o - \Delta_o) \sin \Delta_o \overline{\cos D}^2 \right]$$

$$K_{2c} = 2(\alpha_o^2 + \overline{A}^2) \left[\sin \tau_o \sin \Delta_o \overline{\cos D} - \frac{1}{2} \cos(\tau_o - 2\Delta_o) \overline{\cos 2D} + \frac{1}{2} \cos \tau_o \right]$$

$$K_{1D} = 2\alpha_o^2 \left[\cos \tau_o \sin \Delta_o \overline{\cos D} - \cos(\tau_o - \Delta_o) \sin \Delta_o \overline{\cos D}^2 \right]$$

$$K_{2D} = 2(\alpha_o^2 + \overline{A}^2) \left[\cos \tau_o \sin \Delta_o \overline{\cos D} + \frac{1}{2} \sin(\tau_o - 2\Delta_o) \overline{\cos 2D} - \frac{1}{2} \sin \tau_o \right]$$

For Pages 12 through 14

$$K_{s1} + K_{c1} = \alpha_o^2 \left[-1 + 2 \cos \Delta_o \overline{\cos D} - \overline{\cos D}^2 \cos 2\Delta_o \right]$$

$$K_{s2} + K_{c2} = (\alpha_o^2 + \overline{A}^2) \left[-1 + 2 \cos \Delta_o \overline{\cos D} - \overline{\cos 2D} \cos 2\Delta_o \right]$$

$$K_{c1} - K_{s1} = \alpha_o^2 \left[1 - 2 \cos \Delta_o \overline{\cos D} + \overline{\cos D}^2 \right]$$

$$K_{c2} - K_{s2} = (\alpha_o^2 + \overline{A}^2) \left[2 - 2 \overline{\cos D} \cos \Delta_o \right]$$

$$K_1 = \alpha_o^2 \left[\sin \Delta_o \overline{\cos D} - \cos \Delta_o \sin \Delta_o \overline{\cos D}^2 \right]$$

$$K_2 = (\alpha_o^2 + \overline{A}^2) \left[\sin \Delta_o \overline{\cos D} - \cos \Delta_o \sin \Delta_o \overline{\cos 2D} \right]$$

For distributions of form

$$P(x) = \frac{e^{-x^2/w^2}}{\int_{-\infty}^{+\infty} e^{-x^2/w^2} dx}$$

$$\overline{\cos x} = e^{-w^2/4}$$

$$\overline{x \sin x} = \frac{w^2}{2} e^{-w^2/4}$$

$$\overline{\cos 2x} = e^{-w^2}$$

$$\overline{x^2} = \frac{\pi^{1/2}}{2} w^3$$

COMMENTS

The result for $\overline{\rho^2} - \bar{\rho}^2$ is a formidable one. However, in spite of this the expression can be very useful. For example, suppose we assume that A, B, and D have Gaussian distributions with widths W_A , W_B , and W_D . Then, once we have written a program to compute $\overline{\rho^2} - \bar{\rho}^2$, we can determine how the mean square deviation changes with the widths of each of the three statistical quantities. While the expression for the mean square deviation is very long, the terms are relatively simple.

While we have only obtained expressions for $\bar{\rho}$ and $\overline{\rho^2} - \bar{\rho}^2$, it is possible to use the same technique to find $\bar{\lambda}$ and $\overline{\lambda^2} - \bar{\lambda}^2$. The calculation of the latter would be even more imposing than the ρ calculation.

REFERENCES

1. Stableford, C.V., "APOLLO Project Astrodynamic Constants," STL Memo 9861.3-319, 5 August 1963.
2. Francis, M.P., "The Geocentric and Heliocentric Systems of Constants," Lockheed Report LR 17055, July 1963.
3. Makemson, M.W., "Selenocentric Constants," Lockheed Report LR 17060, July 1963.